

6688

NATIONAL LIBRARY
OTTAWA



BIBLIOTHÈQUE NATIONALE
OTTAWA

NAME OF AUTHOR..... *Richard Earl Berkley*

TITLE OF THESIS..... *Hydrogen Transfer*

..... *Reactions of Alkyl*

..... *Radicals*

UNIVERSITY..... *U. of Alberta*

DEGREE FOR WHICH THESIS WAS PRESENTED..... *Ph. D.*

YEAR THIS DEGREE GRANTED..... *1970*

Permission is hereby granted to THE NATIONAL LIBRARY
OF CANADA to microfilm this thesis and to lend or sell copies
of the film.

The author reserves other publication rights, and
neither the thesis nor extensive extracts from it may be
printed or otherwise reproduced without the author's
written permission.

(Signed)..... *Richard Berkley*

PERMANENT ADDRESS:

..... *2030 Highview*

..... *Port Moody, B.C.*

.....

DATED..... *October 20*, 1970

THE UNIVERSITY OF ALBERTA
HYDROGEN TRANSFER REACTIONS
OF ALKYL RADICALS

by



RICHARD EARL BERKLEY

A THESIS
SUBMITTED TO THE FACULTY OF GRADUATE STUDIES
IN PARTIAL FULFILLMENT OF THE REQUIREMENTS FOR THE DEGREE
OF DOCTOR OF PHILOSOPHY

DEPARTMENT OF CHEMISTRY

EDMONTON, ALBERTA

ABSTRACT

The reactions of ethyl radicals with azoethane were studied. In photolysis at 97°C the secondary products ethyl 2-butyl diimide, ethanal diethylhydrazone, and tetraethylhydrazine were found. In pyrolysis at 293°C ethyl 2-butyl diimide and ethanal diethylhydrazone were found, but tetraethylhydrazine was absent. The isomer of azoethane, ethanal ethylhydrazone, was found to arise from wall-catalyzed reaction of azoethane on fresh surfaces. Isomerization of azoethane on conditioned surfaces or by a free radical mechanism was found to be of minor importance. The equilibrium constant for isomerization of azoethane was determined as a function of temperature.

The reaction of n-propyl radicals with propane was studied, using photolysis of azo-n-propane as the free radical source. Reactions of radicals with the azo compound was found to be a serious complication. The Arrhenius parameters for the abstraction of hydrogen from propane by n-propyl radicals were determined.

The reactions of ethyl, n-propyl, and iso-propyl radicals with silane, silane-d₄, disilane, and disilane-d₆ were studied. The Arrhenius parameters for these reactions were found to be remarkably similar to those already determined for methyl radicals. The results of Bond Energy

Bond Order calculations for methyl, ethyl, n-propyl, and isopropyl radicals reacting with silane were contrasted with the experimental data. The kinetic isotope effects found experimentally were consistent with the other data obtained, and were similar to those found previously for methyl radicals.

The reactions of methyl radicals with methylsilane, dimethylsilane, trimethylsilane, tetramethylsilane, and methylsilane-d₃ were studied. The reactions of trideuteromethyl radicals with methylsilane-d₃, dimethylsilane-d₂, and trimethylsilane-d were also studied. The reaction of methyl radicals with the methyl groups in methylsilane-d₃ and dimethylsilane-d₂ was found to be negligible, while there was measurable reaction with the methyl groups of trimethylsilane-d. The kinetic isotope effects were found to be consistent with the other data. Methyl substitution of silane was found to result in an increase in activation energy for abstraction of hydrogen atoms bound to the silicon atom. This is contrary to the trend in the reported bond dissociation energies.

ACKNOWLEDGEMENTS

The author wishes to express his gratitude to Drs. H. E. Gunning and O. P. Strausz for their guidance and support during the course of this investigation.

Special thanks go to Drs. E. Jakubowski and H. S. Sandhu for valuable advice and criticism and for many hours of helpful discussion.

The author would like to thank Mr. J. Campbell, Mr. P. Young, Mr. P. Vitins, Dr. W. B. O'Callaghan, Dr. B. Woods, Dr. F. Garneau, Dr. T. DoMinh, Dr. J. Font, Mr. T. Pollock, Mr. G. Alexander, Dr. M. de Sorgo, Dr. R. Gosavi, and Dr. I. Safarik of the Photochemistry Group for their advice and assistance.

The advice and assistance of Mr. A. Clement, Mr. W. Duholke, and Mr. A. Jodhan are gratefully acknowledged. The help of the technical staff of the department is also much appreciated.

Special thanks are due Dr. E. Lown for her valuable advice and criticism during the preparation of this thesis.

The author would like to acknowledge the invaluable support given by Drs. R. Pertel and E. McElrath, whose encouragement was crucial to the undertaking of this work.

The author would like especially to acknowledge the devotion and co-operation of his wife Anne. The encouragement and support of the author's parents, Dr. & Mrs. E. E. Berkley were also of great importance.

The efforts of Mrs. Judy Kuhnert in typing this thesis are especially appreciated.

The financial assistance provided by the University of Alberta and the National Research Council of Canada during the course of this work is gratefully acknowledged.

TABLE OF CONTENTS

	<u>Page</u>
ABSTRACT.....	i
ACKNOWLEDGEMENTS.....	iii
LIST OF TABLES.....	ix
LIST OF ILLUSTRATIONS.....	xii
CHAPTER I INTRODUCTION.....	1
1) The Chemistry of Alkyl Radicals.	
2) The Chemistry of the Azoalkanes.	
3) The Reaction of n-Propyl Radicals with Propane.	
4) The Reactions of Alkyl Radicals with Silanes.	
CHAPTER II EXPERIMENTAL.....	26
1) Vacuum System.	
2) Photolysis System.	
3) Pyrolysis System.	
4) Analytical System.	
5) Auxiliary Systems.	
6) Experimental Procedures.	
CHAPTER III SECONDARY PRODUCTS IN THE PHOTOLYSIS AND PYROLYSIS OF AZOETHANE.....	47
RESULTS	
1) Isomerization of Azoethane to	

Ethanal Ethylhydrazone.

- 2) Photolysis of Azoethane.
- 3) Pyrolysis of Azcethane.
- 4) Product Identification.

DISCUSSION

- 1) Mechanism.
- 2) The Azo-alkyl Radical.
- 3) The Triethylhydrazyl Radical.
- 4) Ethanal Ethylhydrazone.
- 5) Summary.

CHAPTER IV	ARRHENIUS PARAMETERS FOR THE REACTION OF PROPYL RADICALS WITH PROPANE.....	64
------------	---	----

RESULTS

- 1) Photolysis of Azo-n-propane and
Azo-iso-propane.
- 2) Photolysis of Azo-n-propane in the
Presence of Propane.
- 3) Determination of the Radical
Disappearance Ratio.
- 4) Arrhenius Parameters.

DISCUSSION

- 1) Possible Consequences of the Mass
Balance Defect.
- 2) Conclusion.

CHAPTER V	THE REACTIONS OF HIGHER ALKYL RADICALS WITH SILANE AND DISILANE.....	95
-----------	---	----

RESULTS

- 1) Reaction of Methyl Radicals with Monosilane.
- 2) Reaction of Ethyl Radicals with Silane, Silane-d₄, Disilane, and Disilane-d₆.
- 3) Reaction of n-Propyl and iso-Propyl Radicals with Silane.
- 4) Determination of Relative Rates of Abstraction from Silane, Silane-d₄, Disilane, and Disilane-d₆ by n-Propyl and iso-Propyl Radicals.
- 5) Calculations.

DISCUSSION

- 1) Comparison of Arrhenius Parameters for Alkyl Radicals Reacting with Silanes and with Hydrocarbons.
- 2) Possible Reasons for the Lack of a Definite Trend in Activation Energies for a Series of Alkyl Radicals Reacting with Silane.
- 3) Kinetic Isotope Effect.
- 4) BEBO Calculations.

CHAPTER VI	THE REACTIONS OF METHYL RADICALS WITH METHYL SUBSTITUTED SILANE.....	147
------------	---	-----

RESULTS

- 1) Reaction of Methyl Radicals with
Tetramethylsilane and neo-Pentane.
- 2) Reaction of Methyl Radicals with
Methylsilane-d₃.
- 3) Reaction of Methyl-d₃ Radicals with
Deuterated Methylsilanes.
- 4) Reaction of Methyl Radicals with
Methylsilanes.

DISCUSSION

- 1) Comparison of Arrhenius Parameters
with Previous Values for Silanes and
for Hydrocarbons.
- 2) Kinetic Isotope Effect.
- 3) Correlation of Kinetic Data and
Magnetic Shielding.

BIBLIOGRAPHY.....	183
APPENDIX A.....	192
APPENDIX B.....	194

LIST OF TABLES

<u>Table</u>		<u>Page</u>
I	Comparison of Arrhenius Parameters for Methyl Reactions with Higher Alkyl Radical Reactions.....	19
II	G. L. C. Operating Conditions and Relative Retention Times.....	38
III	Materials Used.....	42
IV	Equilibrium Constant as a Function of Temperature for Isomerization of Azoethane.	50
V	Products of Photolysis and Pyrolysis of Azoethane.....	53
VI	Mass Spectral Data for Products of Azoethane Decomposition.....	55
VII	NMR Spectra for Products of Azoethane Decomposition.....	58
VIII	Determination of Disproportionation to Combination Ratios for Propyl Radicals.....	66
IX	Reaction of n-Propyl Radicals with Azo-n-propane.....	70
X	Reaction of iso-Propyl Radicals with Azo-iso-propane.....	71
XI	NMR Spectra for Products of Azo-n-propane Decomposition.....	74
XII	Mass Spectral Data for Products of Azo-n-propane Decomposition.....	76

<u>Table</u>	<u>Page</u>	
XIIII	Photolysis of n-Propane-azo-iso-propane with Added C_3F_8	85
XIV	Reaction of n-Propyl Radicals with Propane.	87
XV	Reaction of Methyl Radicals with Azomethane	98
XVI	Reaction of Methyl Radicals with Silane....	101
XVII	Reaction of Ethyl Radicals with Azoethane..	104
XVIII	Reaction of Ethyl Radicals with Silane	107
XIX	Reaction of Ethyl Radicals with Disilane...	109
XX	Reaction of Propyl Radicals with Silane....	113
XXI	Relative Rates of Reaction of n-Propyl Radicals with Deuterated and Nondeuterated Silanes.....	117
XXII	Relative Rates of Reaction of iso-Propyl Radicals with Deuterated and Nondeuterated Silanes.....	120
XXIII	Arrhenius Parameters for Relative Rates of Reaction of Propyl Radicals with Silanes...	125
XXIV	Arrhenius Parameters for Hydrogen Abstraction Reactions of Alkyl Radicals.....	127
XXV	Experimentally Determined Kinetic Isotope Effects at 300°K.....	133
XXVI	Input Parameters for BEBO Calculations....	134
XXVII	Potential Energies of Activation Calculated by the BEBO Method.....	136
XXVIII	Reaction of Methyl Radicals with Tetramethyl- silane and neo-Pentane.....	149

<u>Table</u>		<u>Page</u>
XXIX	Reaction of Methyl Radicals with Methyl- silane-d ₃	153
XXX	Reaction of Trideuteromethyl Radicals with Azomethane-d ₆	157
XXXI	Reactions of Trideuteromethyl Radicals with Deuterated Methyl Silanes.....	161
XXXII	Reaction of Methyl Radicals with Methyl Silanes.....	167
XXXIII	Arrhenius Parameters for Hydrogen Atom Abstraction by Methyl Radicals.....	172
XXXIV	Experimental Kinetic Isotope Effects for Methyl Radicals.....	177
XXXV	Comparison of Activation Energies for Methyl Radical Abstraction Reactions with NMR Chemical Shifts and with Quenching Cross- Sections for Hg6(³ P ₁) Atoms.....	179
XXXVI	Comparison of Activation Energies for Hydrogen Atom Abstraction by Methyl Radicals with Bond Dissociation Energies.....	181

LIST OF ILLUSTRATIONS

<u>Number</u>		<u>Page</u>
1)	Extinction Coefficients for Azomethane and Azoethane Vapor.....	13
2)	High Vacuum System.....	28
3)	Photolysis System.....	30
4)	Pyrolysis System.....	32
5)	Analytical System.....	34
6)	Auxiliary Vacuum System.....	35
7)	Plot of $\log K$ vs. $10^3/T^\circ K$ for Isomerization of Azoethane to Ethanal Ethylhydrazone.....	51
8)	NMR Spectrum of Ethyl 2-Butyl Diimide.....	60
9)	Arrhenius Plots for Reaction of Isopropyl Radicals with Azo-iso-propane and Reaction of n-Propyl Radicals with Azo-n-propane.....	72
10)	NMR Spectrum of Propanal Propylhydrazone.....	79
11)	NMR Spectrum of n-Propane-azo-iso-propane.....	80
12)	Determination of n-Propyl/iso-propyl Radical Disappearance Ratio q	86
13)	Arrhenius Plot for Reaction of n-Propyl Radicals with Propane.....	89
14)	Arrhenius Plot for Reaction of Methyl Radicals with Azomethane.....	99
15)	Arrhenius Plot for Reaction of Methyl Radicals with Silane.....	102

<u>Number</u>		<u>Page</u>
16)	Arrhenius Plot for Reaction of Ethyl Radicals with Azoethane.....	105
17)	Arrhenius Plots for Reaction of Ethyl Radicals with Silane, Silane-d ₄ , Disilane, and Disilane-d ₆	111
18)	Arrhenius Plots for Reaction of n-Propyl Radicals and iso-Propyl Radicals with Silane..	115
19)	Arrhenius Plots for Relative Rates of Reaction of n-Propyl-2,2-d ₂ Radicals with Mixtures of Silane with Silane-d ₄ , Silane with Disilane-d ₆ , and Disilane with Disilane-d ₆	123
20)	Arrhenius Plots for Relative Rates of Reaction of iso-Propyl Radicals with Mixtures of Silane and Silane-d ₄ , Silane and Disilane-d ₆ , and Disilane and Disilane-d ₆	124
21)	Kinetic Isotope Effect for Methyl Radicals Reacting with Methane, Ethane, Silane, and Disilane.....	129
22)	Kinetic Isotope Effect Calculated from Experimental Data for Ethyl Radicals Reacting with Silane and Disilane.....	130
23)	Kinetic Isotope Effect Calculated from Experimental Data for n-Propyl Radicals Reacting with Silane and Disilane.....	131

<u>Number</u>		<u>Page</u>
24)	Kinetic Isotope Effect Calculated from Experimental Data for iso-Propyl Radicals Reacting with Silane and Disilane.....	132
25)	Potential Energy vs. SiH ₃ -H Bond Order for Methyl Radicals and Ethyl Radicals Reacting with Silane.....	141
26)	Potential Energy vs. SiH ₃ -H Bond Order for n-Propyl Radicals and iso-Propyl Radicals Reacting with Silane.....	142
27)	Potential Energy vs. CH ₃ -H Bond Order for Methyl Radicals and Ethyl Radicals Reacting with Methane.....	143
28)	Arrhenius Plots for Reaction of Methyl Radicals with Tetramethylsilane and neo-Pentane.....	152
29)	Arrhenius Plot for Reaction of Methyl Radicals with Methylsilane-d ₃	154
30)	Arrhenius Plot for Reaction of Trideuteromethyl Radicals with Azomethane-d ₆	158
31)	Arrhenius Plots for Reaction of Trideuteromethyl Radicals with Methylsilane-d ₃ , Dimethylsilane-d ₂ , the Silyl Group of Trimethylsilane-d, and the Methyl Groups of Trimethylsilane-d.....	164
32)	Arrhenius Plots for Reaction of Methyl Radicals with Methylsilane, Dimethylsilane, and Trimethylsilane.....	170

<u>Number</u>		<u>Page</u>
33)	Kinetic Isotope Effect Calculated from Experimental Data for Methyl Radicals Reacting with Silane, Methylsilane, Dimethylsilane, and Trimethylsilane.....	175
34)	Kinetic Isotope Effect Calculated from Experimental Data for Methyl Radicals Reacting with Methane, Ethane, Propane, and iso-Butane.	176

HYDROGEN TRANSFER REACTIONS

OF ALKYL RADICALS

CHAPTER I

INTRODUCTION

- 1) The Chemistry of Alkyl Radicals.
- 2) The Chemistry of the Azoalkanes.
- 3) The Reaction of n-Propyl Radicals with Propane.
- 4) The Reactions of Alkyl Radicals with Silanes.

INTRODUCTION

The study of the chemistry of alkyl radicals is of considerable interest because of their frequent occurrence as intermediates in chemical processes. The relationship between the kinetic and thermochemical parameters for the reactions of alkyl radicals is often a valuable source of thermodynamic data (1-3), and there is a large, well established body of information about the kinetics and thermodynamics of their reactions with hydrocarbons. Comparison of these to reactions with other classes of molecules is a potentially fruitful source of new information. In making such comparisons, it is necessary to understand the essential features of alkyl radical structure and reactivity.

1) The Chemistry of Alkyl Radicals:

The ground state configuration of the carbon atom is $1s^2, 2s^2, 2p_x, 2p_y$, and it might be expected from this that carbon would be divalent. However, it is generally observed that carbon is tetravalent, due to hybridization of its s and p orbitals to form four orbitals among which

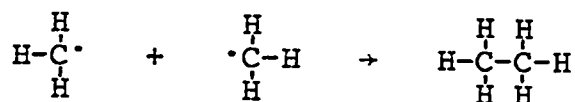
the four electrons are distributed so that each is available for bond formation. The energy necessary to promote the carbon atom from its $3P$ ground state configuration to its excited hybrid state is more than replaced by the two additional bonds which are eventually formed. A detailed discussion of hybridization has been given by Pauling (4).

Alkyl free radicals are alkane molecules in which one of the carbon atoms has a free valence with one unpaired electron. Radical formation can result from homolysis of any single bond, or of more than one bond in a molecule. However, the present discussion will be restricted to alkyl monoradicals.

The structures of alkyl radicals have been carefully investigated. Herzberg (5) has analyzed the ultraviolet absorption spectrum of the methyl radical. Analysis of evidence from vibrational and rotational intensity distribution showed that the molecule must be planar or very slightly pyramidal. Karplus (6,7) has investigated the electron spin resonance spectrum of methyl radicals, and he has been able to show from ^{13}C hyperfine interactions that the deviation from planarity is probably limited to about 5° . Although it is usually inferred that higher alkyl radicals are also planar at the radical site, it has not been possible to determine this unequivocally. Fessenden and Schuler (8) have studied the electron spin resonance spectra

of the lower alkyl radicals in the liquid phase. The coupling constants they found are consistent with planar structures but do not provide definite proof of planarity. Symons (9) has recently reviewed the evidence available from electron spin resonance studies in both liquid and solid phases and has concluded that it is very probable that alkyl radicals are planar. Non-planar alkyl radicals such as 1-apocamphyl, which are constrained to a pyramidal shape at the radical site by bridged, cyclic structures, are nevertheless easily formed (10).

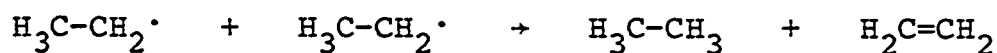
Though alkyl radicals are quite stable, they are also highly reactive, and, in the presence of a reactive substrate or of each other, they have very short lifetimes. The fastest reactions which they undergo are combination and disproportionation with each other. Combination takes place when the free electron associated with one radical pairs with the free electron of another radical so that a single bond is formed, uniting the two radicals to form a hydrocarbon molecule.



Radical combination appears to take place at a rate close to the collision frequency for lower alkyl radicals, and apparently does not require any activation energy (11-15), or, at most, a very small activation energy (16). Bond formation results in the release of a large quantity of

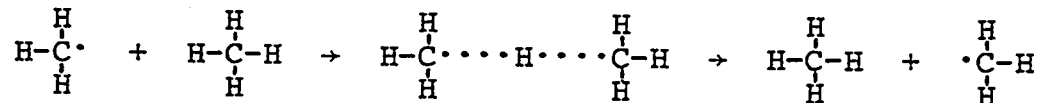
energy, which, if it remains in the newly formed molecule and is not dissipated, will result in its prompt decomposition. Collision with other gas molecules is a very effective means of stabilization, and the need for a third body in the gas phase combination of methyl radicals is met by a total pressure of at most 10 torr (17-21). There need be no concern about third body stabilization at ordinary pressures used in the gas phase study of the hydrogen atom abstraction reactions of free radicals.

Disproportionation involves abstraction of a hydrogen atom from a carbon atom adjacent to the one bearing the radical site.



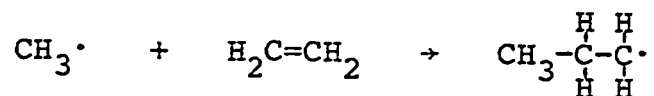
This abstraction is unique in that, like combination, it apparently has no activation energy (22), so there is a characteristic constant ratio of the rate constants for disproportionation and combination over a wide range of temperature (23). Because of this, there has been considerable discussion of whether or not disproportionation and combination occur through a common transition state (24-26).

Abstraction of an atom from another molecule is a common radical reaction.



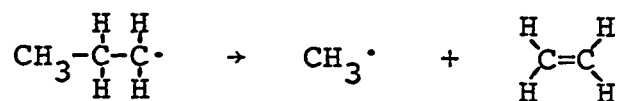
Apparently the radical simply displaces the remainder of the molecule from the atom under attack. The net result is homolytic formation of one bond and homolytic breakage of the other. This process is not as fast as disproportionation or combination, and it requires a measurable activation energy. The present work is concerned almost exclusively with the study of hydrogen atom abstraction reactions.

Addition to multiple bonds is a common and very important reaction of radicals.



It also requires an activation energy. When a radical adds to a multiple bond, its free electron pairs with one of the pi electrons to form a bond between the radical and one of the atoms involved in the multiple bond. This eliminates the pi bond and leaves an unpaired electron associated with the other atom which was involved in the double bond, so that a new radical is formed. This new radical may react with another double bond in the same manner. The eventual result of such a chain process is usually formation of polymer. Chain formation may be terminated by disproportionation, combination, or abstraction.

Finally, radicals may decompose.



The mode of decomposition may involve either radical or atom elimination to form a double bond. Decomposition is essentially the reverse of addition to a double bond. It generally requires a very large activation energy, and, within the temperature range used in the study of radical abstraction reactions, is usually negligible. Kerr and Lloyd (27) have recently reviewed these reactions, and they will not be considered further here.

There are several ways of producing alkyl radicals for study of gas phase reactions. Paneth in 1929 first demonstrated the existence of free radicals by pyrolysis of tetramethyl lead in a flow system (28,29). The radicals in the gas stream removed a previously deposited lead mirror from the wall of the glass flow tube. Free radicals may be produced in the thermal decomposition of almost any compound, but the classes of materials which may be pyrolyzed in a manner sufficiently orderly for use in mechanistic studies of alkyl radical reactions are limited. Thermal decomposition of most compounds takes place at such elevated temperatures that reaction systems are complicated by numerous processes which do not occur with measurable rates near room temperature. The alkyl and acyl peroxides are

among the few classes of compounds which decompose with sufficiently low activation energy to be used for radical production at low temperatures, but their primary decomposition forms oxygen containing radicals, and alkyl radicals only result from secondary decomposition of these peroxy radicals. In general thermolysis is not as suitable a method as photolysis for producing radicals for kinetic studies. Pryor has given a far more detailed description of radical sources, structure and reactivity than can be included here (30).

The great advantage of photolytic decomposition of molecules is that absorption of a single quantum of light increases the energy of a particular part of a molecule by a precise amount in a single, discrete step. From the resulting excited state the molecule will then react by the most favorable path. This may be fluorescence or phosphorescence, deactivation by collision, molecular elimination, homolysis of one or more bonds to form radicals, or, at high energies, ionization or dissociation into ionized fragments. Most of these paths would be unavailable to a molecule in thermal decomposition, since it would stand an excellent chance of being destroyed in some low energy process before it could accumulate sufficient energy at the right location by collisional activation to undergo a high energy process. Calvert and Pitts have written an excellent discussion of the details of photolytic

decomposition of molecules (31).

There are many kinds of compounds which may be photolyzed to produce alkyl radicals. Among the more important of these are the carbonyl compounds, the mercury dialkyls, and the azoalkanes.

Photodecomposition of aldehydes and ketones usually occurs by cleavage at the carbonyl group to form an alkyl radical and an acyl radical. At elevated temperatures the acyl radical decomposes to yield carbon monoxide and another alkyl radical. The 3130 Å photolysis of acetone at temperatures above 100°C, for example, is a very clean source of methyl radicals. However, aldehydes and ketones react with some substrates, and, in many cases, they have more than one primary mode of decomposition (31).

The principal advantage of the photolysis of dialkyl mercury compounds as sources of alkyl radicals is that there is only one primary process of decomposition to form two alkyl radicals and a mercury atom. However, the radicals are produced with some excess energy, and the higher homologs of dimethyl mercury are not very volatile.

In a number of ways the azoalkanes are the most suitable source for a homologous series of alkyl radicals for mechanistic studies. Their primary decomposition mode, while some doubt remains about details of its mechanism, dependably yields two thermally equilibrated alkyl radicals

and a nitrogen molecule. They are fairly volatile, and have been used in the production of all of the lower alkyl radicals for kinetic studies (32). Finally, they are inert toward a wide variety of substrate molecules. They have been used exclusively as alkyl radical sources throughout the present study, and a more detailed discussion of their chemistry is therefore warranted.

2) The Chemistry of the Azoalkanes:

The azoalkanes are volatile, light yellow liquids. The vapor pressure of azomethane is well above one atmosphere at room temperature, while the vapor pressures of the higher azoalkanes are all below one atmosphere. All of these compounds can be photolyzed by daylight at wavelengths where glass is transparent, so they must be stored in the dark, preferably at low temperature.

The first azo compound containing no aromatic groups was reported by Meyer and Constam (33) in 1882. The synthesis of azomethane was described by Thiele (34) in 1909. Leermakers (35) and Rice (36) independently reported mirror-removal experiments confirming the free-radical nature of azomethane decomposition in 1933, while Burton and co-workers (37) described the use of photolysis of azomethane as a source of free radicals for the study of radical molecule reactions in 1937. A variety of synthetic methods of preparation for azoalkanes are available,

including those described by Lochte, Noyes and Bailey (38), by Jahn (39), by Renaud and Leitch (40), by Ohme and Schmitz (41), and by Spialter and co-workers (42).

The ultraviolet absorption spectra of azomethane and azoethane are shown in Figure 1. They are characterized by a very intense band at wavelengths below 2700 Å. Absorption of light in this region leads to decomposition into highly excited radicals, and it will not be considered further here. There is a very weak absorption in the vicinity of 3600 Å which is generally thought to result in a singlet $n \rightarrow \pi^*$ transition. Intersystem crossing to the triplet state probably takes place, after which the excited molecule either undergoes collisional deactivation or cleavage of the C-N bond (43). Possibly cleavage of only one C-N bond occurs at first to form an alkyl radical and a RN_2 radical. If so, this must evidently be followed very rapidly by decomposition of the RN_2 radical, since it has never been detected (44). Fluorescence and phosphorescence have never been detected in the acyclic azoalkanes in the gas phase (45-49).

There are some minor differences between decomposition of azomethane and decomposition of the other azoalkanes. First of all, photolysis of azomethane at 3600 Å results in decomposition with a quantum yield of unity independent of pressure up to one atmosphere. The other azoalkanes all exhibit a pressure effect in 3600 Å

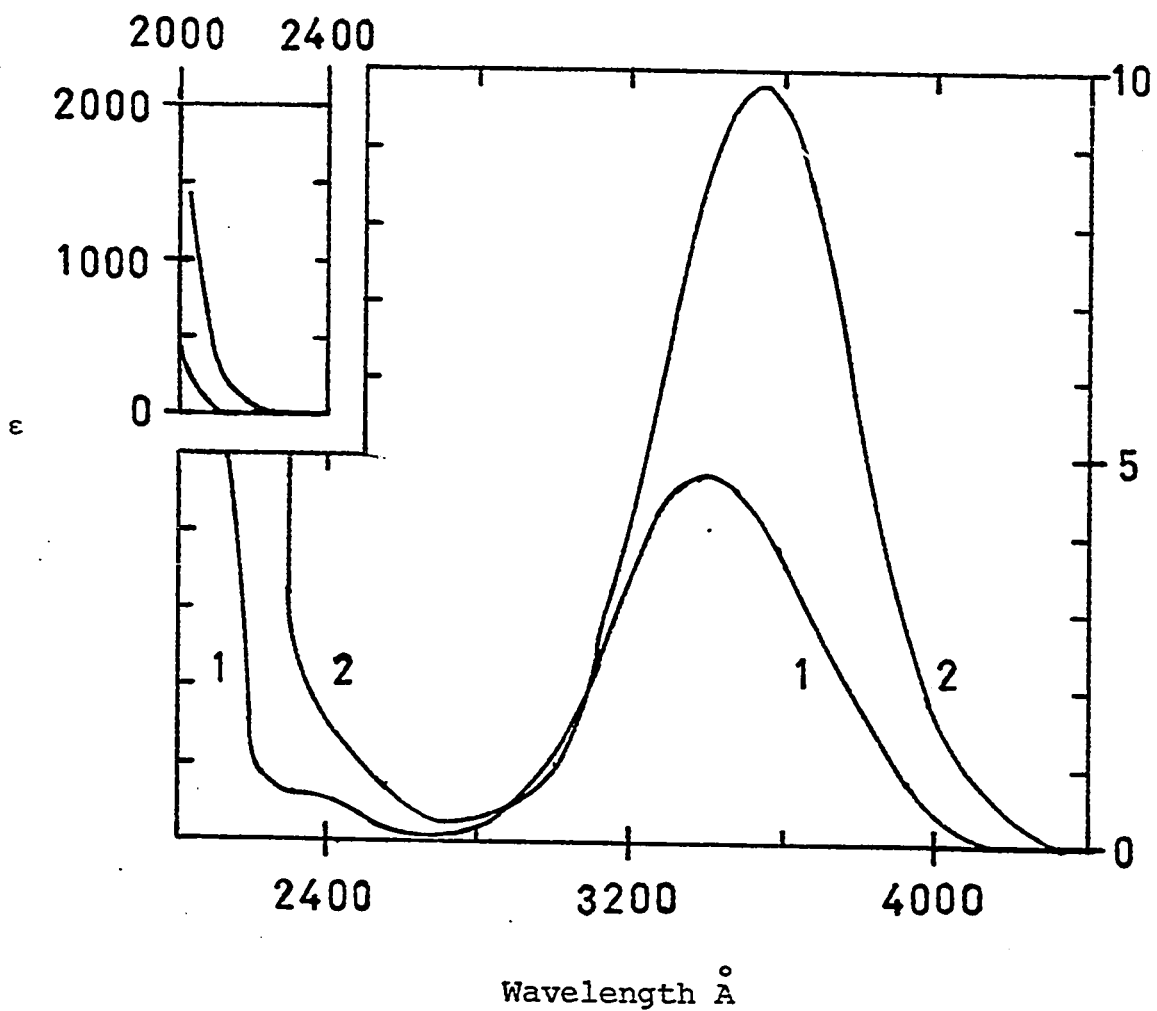


Figure 1. Extinction coefficients for azomethane vapor (curve 1) and azoethane vapor (curve 2) as a function of wavelength; $\epsilon = \log(I_0/I)/cl$ liter/mole-cm; data of V. McMillan (Reference 31).

photolysis, though pressure studies indicate unit quantum yield of decomposition at zero pressure (45,46,50-53). The activation energies for decomposition of the excited azo compound have been determined for a number of cases, and these are all on the order of two to five kcal/mole. Secondly, azomethane photolysis results in a small but detectable yield of intramolecular ethane formation. Several studies (54-57) of this process have established the quantum yield at 0.007. Such intramolecular elimination is insignificant for higher azoalkanes. Cis-trans isomerism of azomethane has been observed, conversion from one form to the other being effected by irradiation with ultraviolet light, and it has been proposed that the intramolecular elimination of ethane in azomethane photolysis may occur from the cis form of azomethane (54). However, cis-trans isomerism has recently been detected in the irradiation of higher azoalkanes as well (58,59), and it does not lead to significant molecular elimination.

When radicals are produced from photolysis of azoalkanes there are a number of possible ways in which they may react. In addition to combination or disproportionation with each other or abstraction from a substrate, they also react with the parent azo compound, either by abstraction of a hydrogen atom or by addition to the N=N double bond. The abstraction reaction produces the same hydrocarbon as does abstraction from the substrate, and this reaction must be

taken into account in calculating rate constants for reaction with the substrate. As a result, there have been numerous determinations of the Arrhenius parameters for this reaction for the various azoalkanes (45,46,51,60-66). On the other hand, addition to the double bond is not expected to lead to formation of any compound which might interfere in kinetic studies of radical-substrate reactions, so very little attention has been paid to this reaction, and there are few determinations of its Arrhenius parameters in the literature (45,67).

On the whole, surprisingly few of the products resulting from reactions of alkyl radicals with azoalkanes have been definitely identified. Gray and Thynne (61) have found tetramethylhydrazine and methyl ethyl diimide in the photolysis of azomethane. Wacks (68) has observed the formation of methyl amine in high temperature pyrolysis of azomethane and has suggested that heterogeneous isomerization of azomethane to formal methylhydrazone followed by decomposition of the hydrazone to HCN and methylamine may occur. Cohen and Zand (69) have reported spectroscopic evidence for the formation of acetone isopropylhydrazone in the pyrolysis of azo-iso-propane. Cerfontain and Kutschke (45) have determined the Arrhenius parameters for addition of ethyl radicals to the double bond in azoethane, and they have also proposed that decomposition of the radical formed by abstraction of hydrogen from the

azo compound may be an important process in the system. Sandhu (70) has also suggested this decomposition as part of a proposed mechanism for azoethane pyrolysis and has reported mass spectral evidence suggesting formation of ethyl amines in the pyrolysis of azoethane.

Because azoalkanes are such important and useful sources of alkyl radicals, and because so few of the products resulting from reactions of alkyl radicals with the parent azoalkane have been definitely characterized, an investigation of these reactions in both the photolysis and pyrolysis of azoethane has been undertaken.

3) The Reaction of n-Propyl Radicals with Propane:

Alkyl radicals have been reacted with a wide variety of alkane substrates. However, the overwhelming majority of this work has been done with methyl radicals. A few reactions of ethyl radicals with alkanes have been reported, but reactions of higher alkyl radicals with alkanes have not been reported.

The essential features of hydrogen abstraction reactions of methyl radicals with alkanes appear to be well understood. The activation energies vary in an orderly manner with the bond dissociation energy of the bond under attack, so that in general, the smaller the energy of the bond, the lower the activation energy required to break it, and the Polanyi Relation can be used to make an accurate

prediction of the activation energy, if the bond energy is known (71,72).

It must be accepted that during abstraction of a hydrogen atom some of the energy released in formation of the new bond is used to supply the energy necessary for breaking the old bond. If this were not true, then the activation energies for these reactions would be about equal to the energy of the bond under attack. In fact the activation energies are about an order of magnitude smaller than the bond energies. In view of this, it is reasonable to expect that the magnitude of the energy of the bond being formed must also have a significant effect on the activation energy for abstraction. Thus, if two different radicals react with bonds having the same energy, it would be expected that the radical which forms the bond having the higher energy should react with a lower activation energy. Since the C-H bond dissociation energies of methane and ethane are 104 and 98 kcal/mole, respectively, it would be expected that ethyl radicals would require a larger activation energy for abstraction of hydrogen from a given molecule. The few studies which have been done of the reactions of ethyl radicals with alkanes tend to bear this out (71,73-79). However, there has been much work done on the reactions of higher alkyl radicals with aldehydes, and, if the data can be relied upon, the higher alkyl radicals react with a substantially lower activation energy than do

methyl radicals, in spite of the trend in the energies of the bonds being formed (71,80-83). The Arrhenius parameters for methyl radical reactions and for higher alkyl radical reactions are contrasted in Table I.

The abstraction reactions of the higher alkyl radicals with alkanes are of importance in a variety of kinetic systems, particularly in mercury sensitization reactions, so determination of Arrhenius parameters for these reactions is of potentially great value. Accordingly, the determination of the Arrhenius parameters for the reaction of n-propyl radicals with propane has been carried out.

4) The Reactions of Alkyl Radicals with Silanes:

Since part of the value of any study of the abstraction of hydrogen from silanes must lie in the comparison that can be made with the analogous reactions of the alkanes, it will be useful to contrast the properties of silanes with those of alkanes.

Silicon is the next heavier element than carbon in Group IV of the periodic table. It has a lower electronegativity (1.8) than carbon (2.5) on the Pauling scale (4). The ground state distribution of its 14 electrons is $1s^2, 2s^2, 2p^6, 3s^2, 3p_x, 3p_y$, which is analogous to that of carbon. There are two important consequences of the fact that the valence electrons of carbon are in the second shell while

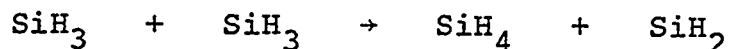
Table I

Comparison of Arrhenius Parameters for Methyl Radical
Abstraction Reactions with Arrhenius Parameters
for Higher Alkyl Radical Abstraction Reactions

Radical	Substrate	Log A	E kcal/mole	Refer- ence
CD ₃	n-C ₄ H ₁₀	11.92	9.6	77
C ₂ D ₅	n-C ₄ H ₁₀	11.33	10.4	74
CD ₃	iso-C ₄ H ₁₀	11.43	8.1	76
C ₂ D ₅	iso-C ₄ H ₁₀	10.92	8.9	74
CH ₃	neo-C ₅ H ₁₂	11.3	10.0	75
CH ₃	neo-C ₅ H ₁₂	12.3	12.0	73
C ₂ D ₅	neo-C ₅ H ₁₂	11.55	12.6	74
CH ₃	cyclo-C ₆ H ₁₂	12.47	9.5	78
C ₂ D ₅	cyclo-C ₆ H ₁₂	11.72	10.4	79
CH ₃	tert-C ₄ H ₉ CHO	13.0	10.2	80
tert-C ₄ H ₉	tert-C ₄ H ₉ CHO	10.5	4.3	80
CH ₃	sec-C ₄ H ₉ CHO	13.13	10.4	80
sec-C ₄ H ₉	sec-C ₄ H ₉ CHO	10.7	4.9	81
CH ₃	iso-C ₄ H ₉ CHO	12.3	8.4	80
iso-C ₄ H ₉	iso-C ₄ H ₉ CHO	11.7	6.5	82
CH ₃	n-C ₄ H ₉ CHO	12.1	8.0	80
n-C ₄ H ₉	n-C ₄ H ₉ CHO	10.9	5.4	83

those of silicon are in the third shell. The covalent radius (1) of silicon (1.17A) is larger than that of carbon (0.77A), and, in contrast to carbon, the valence shell of silicon contains empty d orbitals. These features are related to some striking chemical differences between the alkanes and the silanes. The valence electrons in silicon are hybridized in a manner analogous to those of carbon to form four equivalent sp^3 orbitals. It seems likely, however, that the d orbitals of the valence shell in silicon may be involved in the resonance hybrid as well. Silicon atoms do not participate in double bond formation as do carbon atoms, and this may be due in some way to d orbital involvement in hybridization, or it may be due simply to the greater covalent radius of silicon. It is clear that the d orbitals do tend to interact with p orbitals on neighboring atoms, since, for example, trisilylamine is planar, in striking contrast to pyramidal trimethylamine. They are also able to interact with nucleophilic ligands to form one or two dative bonds, in addition to the usual four covalent bonds. The empty d orbitals of silicon have often been invoked in explaining the many unique features of silicon chemistry, possibly more often than is justified.

Silyl radicals, in contrast to alkyl radicals, are pyramidal rather than planar (84-87). The bonds to hydrogen in the SiH_3 radical are evidently very weak (88,89), and disproportionation may be favored as a result.



Evidently disproportionation in which an alkyl radical acquires one of the hydrogen atoms of the silyl radical is not of sufficient importance to affect kinetic studies of alkyl radical abstraction reactions (60,90). Formation of silyl radicals is always associated with considerable solid polymer formation (91-93), and this may be the fate of most of the silyl radicals.

Carbon atoms can bond to each other to form highly stable chain compounds, but the stability of silane compounds decreases markedly with increasing length of the silicon chain. Although hydrocarbons have large heats of combustion, they are stable in the presence of oxygen at elevated temperatures. Silanes, on the other hand undergo spontaneous combustion in the presence of oxygen at room temperature. Relatively little is known about the bond dissociation energies of silanes in contrast to the very large body of information available on hydrocarbons, but what information is available strongly suggests that silanes (94-102) have smaller bond energies than alkanes (2,3). Aylett has published a comprehensive review of the chemistry of silicon hydrides (103), and the features of silane chemistry have also been reviewed by Eaborn (104), Stone (105), Ebsworth (106), and Van Dyke (107).

Compared with the vast body of knowledge about hydrocarbons, information about the kinetics of silane decomposition is relatively scant, although a number of studies of pyrolysis (91,108,109), mercury photosensitized decomposition (92,93), and photolysis (110-112) of silanes have been reported.

Kerr, Slater, and Young (60,113) first reported temperature studies for the reactions of methyl radicals with a number of substituted silanes. Some of the A factors they determined were about an order of magnitude higher than the A factors normally found in abstraction from alkanes, and they suggested this as the reason for the greater reactivity of silanes. However, subsequent work has established that A factors for these reactions are about the same as those for reactions with alkanes, and that lower activation energies are the cause of the greater reactivity of silanes (90,114-120).

Jakubowski and co-workers (115) have reported a study of the reaction of methyl radicals with silane and disilane. They calculated potential energies of activation and kinetic isotope effects for these reactions by the Bond Energy Bond Order method of Johnston (121) and obtained results which were in reasonable agreement with experiment, but which indicated that quantum mechanical tunneling was probably significant.

Chaudhry and Gowenlock (122) have studied the reactions of methyl radicals with the Group IV tetramethyls. Their results demonstrate a definite effect of the central Group IV atom on the reactivity of the hydrogen atoms attached to the methyl groups. Thynne has pointed out that recent studies of methyl radical reaction with tetramethylsilane show Arrhenius parameters very similar to those previously published for neopentane (75), and has suggested that there is no difference in the effect of carbon and silicon as central atom (118,123). However, Kerr and Timlin (73) have recently redetermined the Arrhenius parameters for neopentane, and have shown that in fact there is a pronounced effect due to substitution of silicon for carbon as the central atom.

Kerr, Stephens, and Young have reported reactions of tetramethylsilane (116) and trichlorosilane (117) with methyl, trifluoromethyl, and ethyl radicals. They have obtained results which refute the large A factors which they found earlier.

As a consequence of the lower electronegativity of silicon, it forms the positive end of a dipole with carbon in most compounds, and hydrogen attached to silicon has a much larger partial negative charge than hydrogen attached to carbon. Consequently, silicon compounds should be expected to display greater sensitivity to the polarity of an attacking radical. Cheng and Szwarc (124) have

investigated the reactions of trifluoromethyl radicals with a series of methylchlorosilanes, and Bell has also studied trifluoromethyl radical reactions with silane compounds (114,120). Jakubowski and co-workers (90) have reported a study of trifluoromethyl radical reactions with monosilane. The net effect of these studies is to suggest that polar effects are indeed important in the radical abstraction reactions of the silanes.

Morris and Thynne have reported studies of the reactions of silane, trimethylsilane, and tetramethylsilane with methyl radicals (118) and with trifluoromethyl radicals (119). The results show a difference in activation energy between the two radicals which is probably too great to explain in terms of the differences in energy of the bond being formed, and which suggests the effect of the polarity of the trifluoromethyl radical.

Although there is much current interest in radical abstraction reactions with silanes, there has been no work done involving higher alkyl radicals with the exception of the work recently reported by Kerr for the reaction of ethyl radicals with tetramethylsilane (116) and trichlorosilane (117). A study of the reactions of ethyl, n-propyl, and isopropyl radicals with monosilane and disilane has been undertaken, in order to learn more about higher alkyl radical reactions with silanes, and in hope of determining the extent to which the energy of the bond being formed in a

hydrogen abstraction reaction influences the activation energy.

There have been only a few studies of the reactions of methyl radicals with methyl substituted monosilane. Other than tetramethylsilane, which has been investigated many times, only trimethylsilane has been studied. The results which have been reported (activation energies of 7 and 7.8 kcal/mole) are in fairly close agreement (113,118), but, when compared with results for monosilane (115,118) (activation energies of 7 and 6.9 kcal/mole), tend to suggest a higher activation energy for abstraction of a hydrogen atom which is bound with less energy. Therefore it appeared to be desirable to undertake a thorough investigation of the reactions of methyl radicals with methyl substituted silanes with the aim of determining to what extent radicals react with the methyl groups, and whether the activation energy for abstraction from the Si-H bond in trimethylsilane is actually higher than for abstraction from monosilane. Also, it would be desirable to have a complete set of data for reactions of methyl radicals with all of the methyl substituted monosilanes, so that trends in reactivity could be observed. Accordingly, a study of methyl radical abstraction from silane, methylsilane, dimethylsilane, trimethylsilane, tetramethylsilane, and neo-pentane has been carried out.

CHAPTER II

EXPERIMENTAL

- 1) Vacuum System.
- 2) Photolysis System.
- 3) Pyrolysis System.
- 4) Analytical System.
- 5) Auxiliary Systems.
- 6) Experimental Procedures.

EXPERIMENTAL

The apparatus consisted of a photolysis system, a pyrolysis system, and an analytical system connected by a standard high vacuum apparatus.

1) Vacuum System:

The vacuum system was constructed of pyrex tubing and was evacuated to 10^{-6} torr with a mercury diffusion pump backed by a standard mechanical pump. High vacuum stopcocks, helium tested Hoke valves, Springham stopcocks with Viton A diaphragms, Teflon plug stopcocks, and Delmar mercury float valves were employed in the system. All calibrated volumes were kept grease free. A schematic diagram of the vacuum system is given in Figure 2.

Hydrocarbons were kept in pyrex bulbs, while azoalkanes and silanes were stored in glass fingers maintained at -196°C .

Pirani tubes (Consolidated Vacuum Co. Type GP-001), mercury manometers, and a McLeod gauge were used to measure pressures. A distillation system consisting of three U-traps, a spiral trap, a solid nitrogen trap, and a Toepler pump was used for purification of reactants and separation of products.

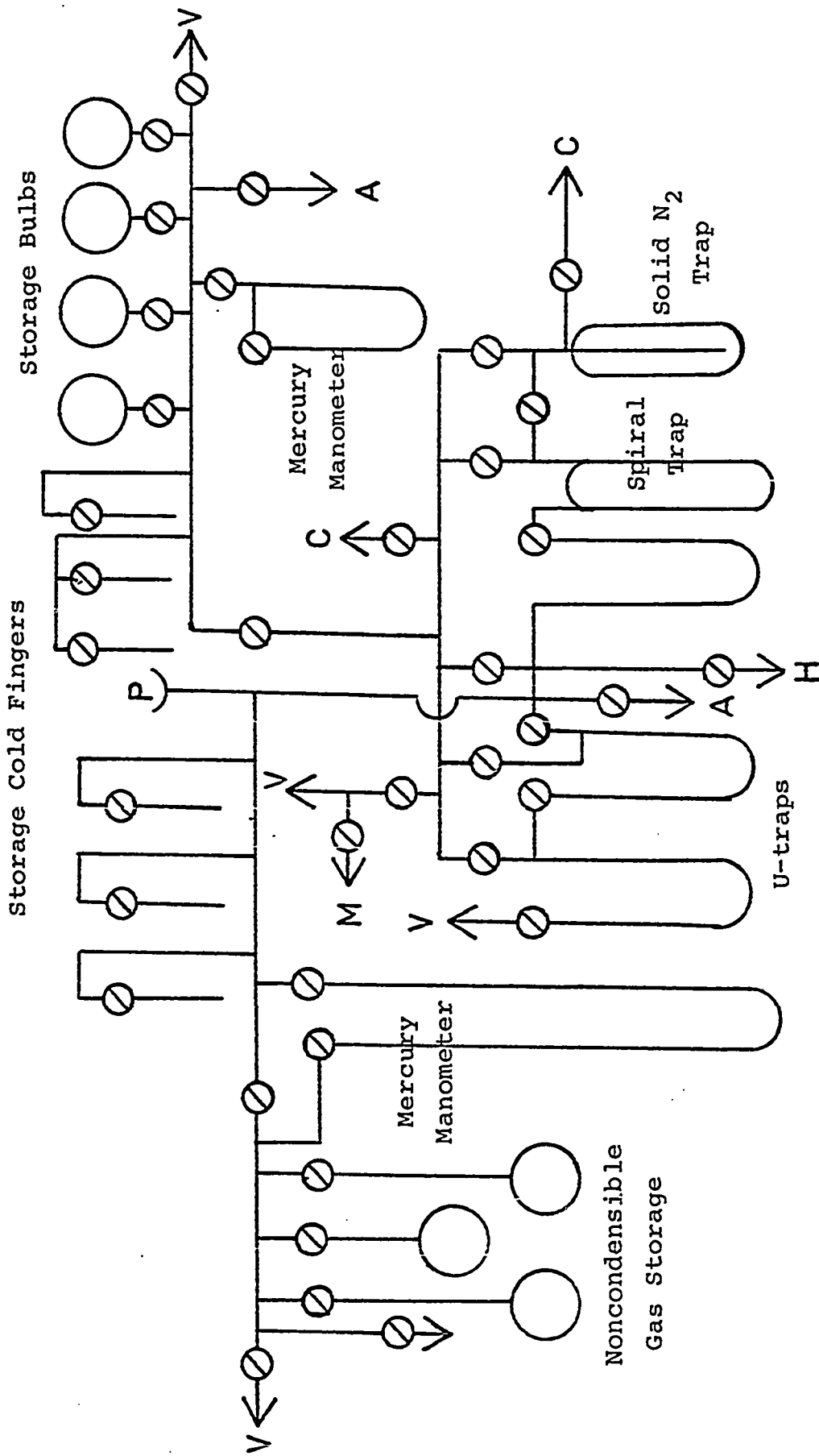


Figure 2. High vacuum system. A, to atmosphere; C, to analytical system; H, to photolysis or pyrolysis cell; M, to McLeod gauge; P, Pirani tube; V, to vacuum line.

2) Photolysis System:

The photolysis system consisted of a 54 mm. O.D. cylindrical quartz cell with an 11 mm. O.D. cold finger surrounded by a cylindrical aluminum block furnace 43 cm. in length. Different cell lengths were used from time to time. The ends of the furnace were covered with quartz windows, and additional quartz windows were mounted inside the furnace with brass snap rings to enhance temperature stability around the cell. The furnace was heated by eight Hotwatt pencil heaters (50 watt) to which power was supplied by two variacs. The outside of the furnace was covered with 2 cm. of glass wool insulation. The cold finger and exit tube could be heated to 80°C where necessary to prevent condensation of heavy compounds. A diagram of the photolysis system is given in Figure 3.

Temperature measurements were made with an Assembly Products pyrometer connected to several iron-constantan thermocouples through a selector switch. The pyrometer was checked periodically against ice, room temperature as measured by a calibrated mercury thermometer, and boiling water, and was found to be consistently accurate to $\pm 1^\circ$.

Light (3650-3663Å) was isolated from a medium pressure mercury arc (Hanovia Type 30620) by an Eastman Kodak Wratten 18A filter (50 x 50 x 5 mm.). In cases where higher light intensity was desired, window glass filters (78 x 80 x 2 mm.) were used. There was essentially no

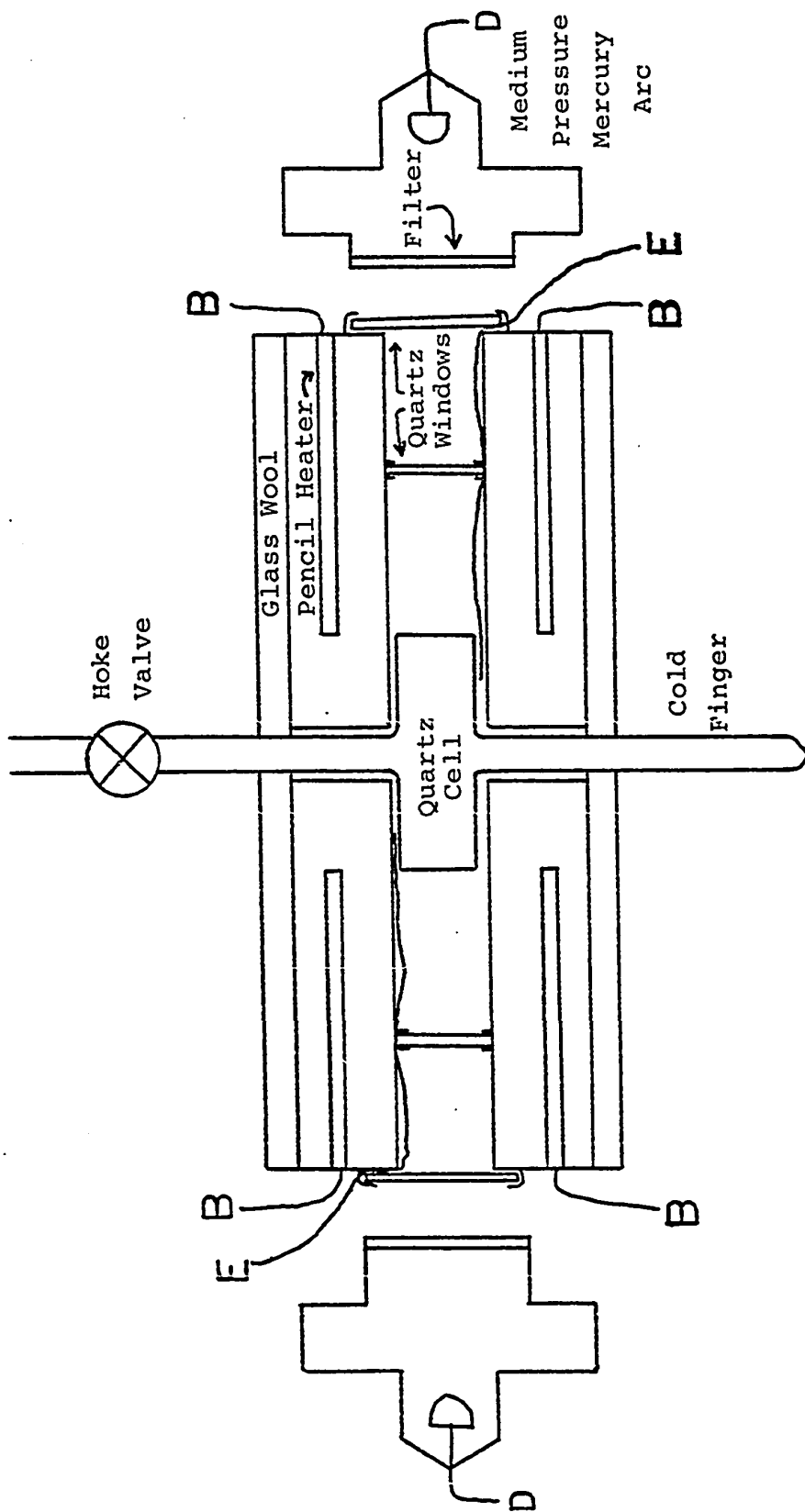


Figure 3. Photolysis system. B, from powerstat; D, from powerstat; E, to pyrometer.

difference in the short wavelength cutoff ($\sim 3200\text{\AA}$) between these two filters.

3) Pyrolysis System:

The pyrolysis system consisted of a cylindrical 125 ml. pyrex cell which was surrounded by an aluminum block furnace insulated with glass wool and heated by two 300 watt Chromalox pencil heaters. Temperature measurements were made using two iron-constantan thermocouples which were connected to the pyrometer. The entrance tube and valve were kept heated to 60 to 80°C with heating tape. The pyrolysis system is shown in Figure 4.

4) Analytical System:

The analytical system consisted of a gas burette and a gas chromatograph. The gas burette was fitted to the top of the Toepler pump at the end of the distillation system and connected to the injection loop of the gas chromatograph through another Toepler pump with a cold finger. Helium was used as the carrier gas. It was passed through drierite, ascarite, and then through an activated charcoal/molecular sieves trap which was kept at -196°C . Flow rates were determined by an oil manometer calibrated with a soap bubble flow meter. Provision was made for heating the flow lines to 60°C when necessary for analysis of heavy compounds. Glass spiral columns were used, and an aluminum cylinder wrapped with heating tape was used to maintain column

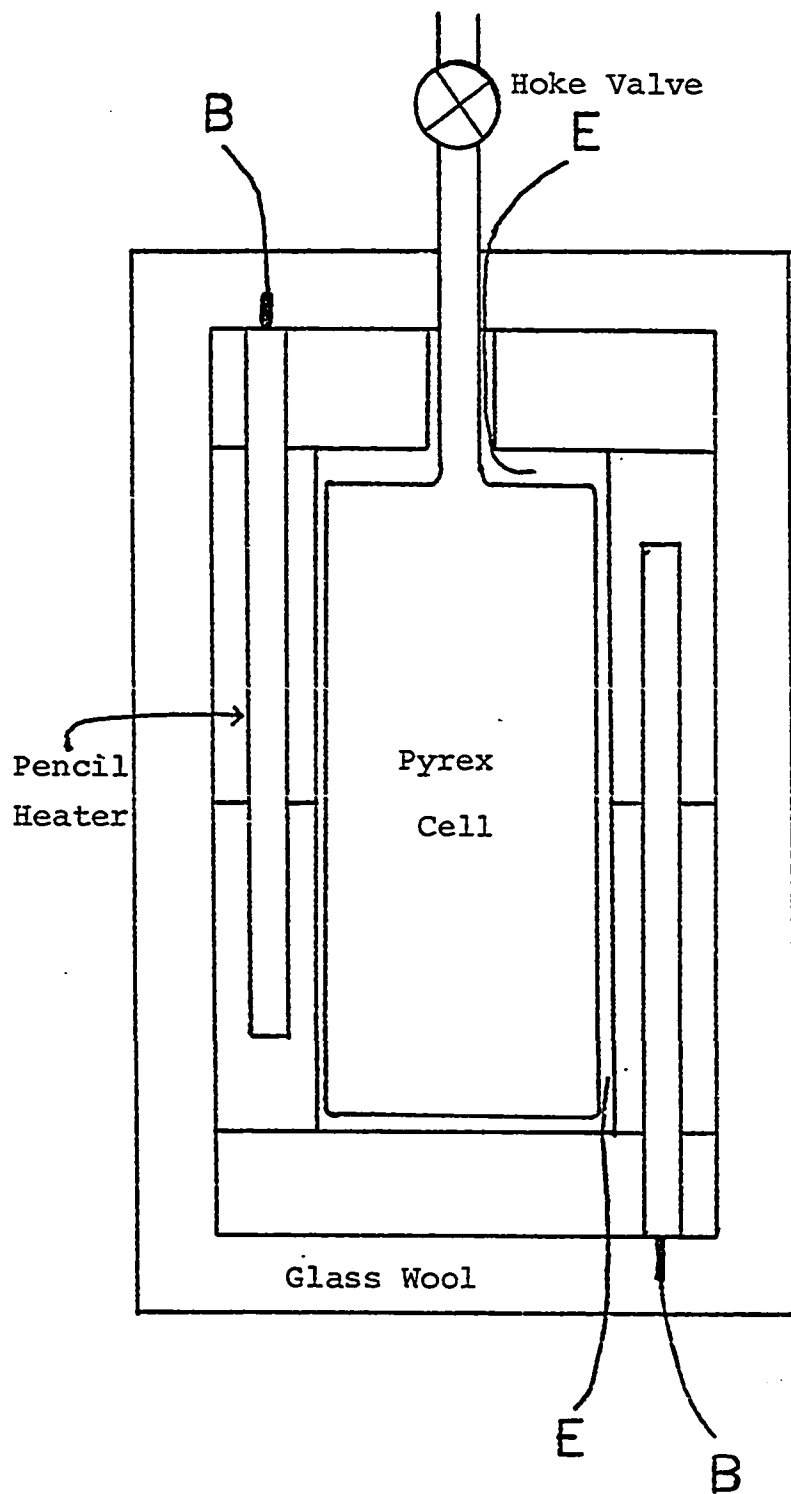


Figure 4. Pyrolysis system. B, from powerstat;
E, to pyrometer.

temperature. A schematic diagram of the analytical system is given in Figure 5.

The flow line was connected to the high vacuum system by a sample loop through which the helium flow could be diverted by means of three switch type Hoke valves. Condensable samples could be frozen into the sample loop, and noncondensable samples could be pumped in with the Toepler pump. Four spiral traps with fiberglass plugs were connected to the flow line downstream from the detector by four-way stopcocks, so that eluted materials could be selectively trapped. A thermal conductivity detector (Gow-Mac Model Tr II B), a power supply (Gow-Mac Model 9999 C) and a recorder (Sargent S-72180) were used. The thermal conductivity cell was maintained at 300°F, and the filament current was kept at 250 mA.

5) Auxiliary Systems:

A small vacuum system with a distillation line was used for purification of gases. A schematic diagram of this system is given in Figure 6. A small aluminum block furnace and photolysis cell were also attached and were used to carry out some of the photolyses. No provision for quantitative handling of noncondensable gases was included in this system.

Measurements of noncondensable gases and of isotopic ratios were carried out using an Associated Electrical

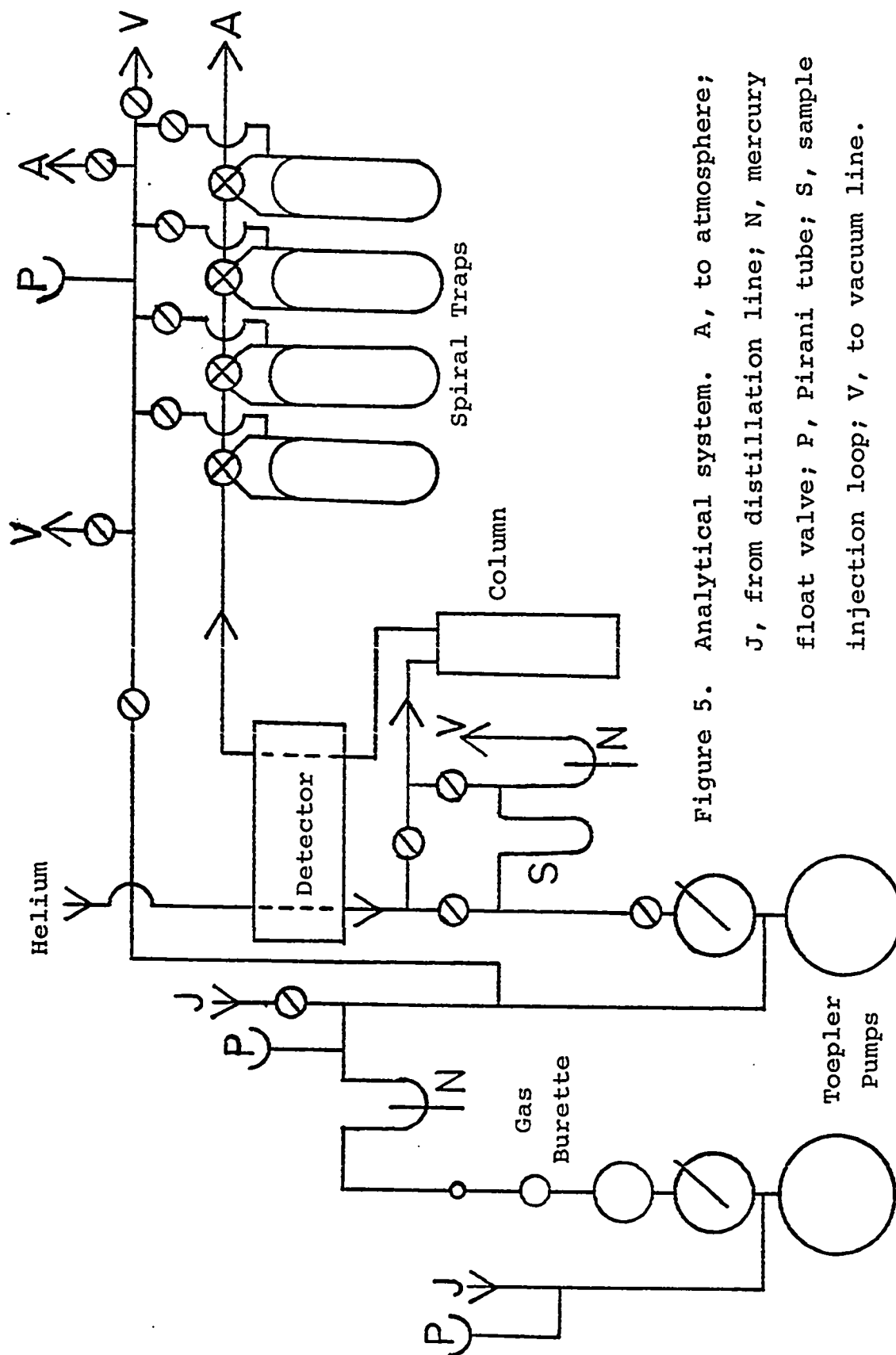


Figure 5. Analytical system. A, to atmosphere; J, from distillation line; N, mercury float valve; P, Pirani tube; S, sample injection loop; V, to vacuum line.

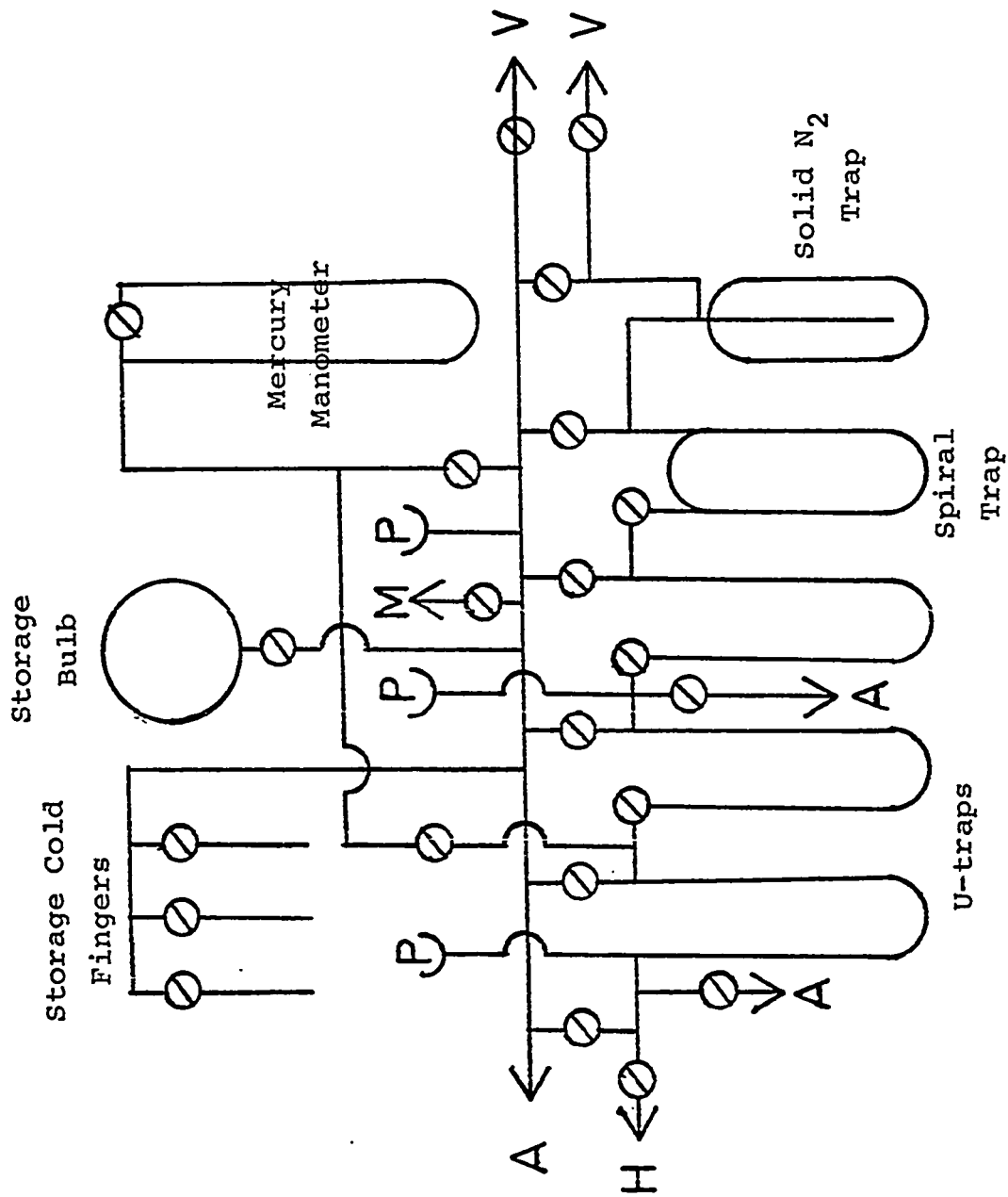


Figure 6. Auxiliary vacuum system. A, to atmosphere; H, to photolysis cell; M, to McLeod gauge; P, Pirani tube; V, to vacuum line.

Industries MS-10 mass spectrometer. All analyses were made using a trap current of 50 microamperes and an electron beam energy of 70 electron volts.

Mass spectra were also taken on AEI MS-2 and MS-9 instruments. The MS-9 was used for exact mass determinations in identification of unknown products.

Nuclear magnetic resonance spectra were taken using Varian 60 and 100 MHz spectrometers. Spin decoupling studies with the 100 MHz instrument were used in determining structures of unknown products.

6) Experimental Procedures:

The volume immediately adjacent to the photolysis system was calibrated by determining with the gas burette the quantity of N_2 necessary to create a given pressure in it. Gases used in photolysis runs were measured by determining temperature and pressure in this volume. They were then transferred to the cell by freezing into the cold finger. The lamps were allowed a warm-up period of about fifteen minutes prior to each run in order to reach operating intensity. Runs were initiated by removing a shutter between the lamp and the furnace window and simultaneously starting an electrical timer (Precision Scientific 69235). At the end of the run the products were separated by low temperature distillation into convenient fractions for analysis.

The gas chromatograph was calibrated in terms of peak area (in arbitrary units as measured with a planimeter) per micromole of standard. The mass spectrometer was similarly calibrated, using measured aliquots, in terms of peak height (mm.) per micromole. Cracking patterns were normalized against the sensitivity of the parent peak, and the cracking patterns of mixtures were resolved algebraically.

Operating conditions and retention times for the gas chromatograph system are summarized in Table II, and a list of the materials used in this study is given in Table III.

Table II
G.L.C. Operating Conditions and Relative Retention Times

Column	Length ft.	Tempera- ture °C	Flow cc min ⁻¹	Compounds Analyzed and Relative Retention Times
20% SE-30	20	100	74	2-methylpentane 0.43
Silicone Gum Rubber on Chromosorb W.A.W. 60/80 mesh				2,3-dimethylbutane 0.43 n-hexane 0.47 azo-n-propane <u>11.5 min.</u> 1.00 propanal propylhydrazone 2.37
20% SE-30	20	95	52	2-methylpentane 0.38
Silicone Gum Rubber on Chromosorb W.A.W. 60/80 mesh				2,3-dimethylbutane 0.38 n-hexane 0.43 Azo-iso-propane 0.58 n-propane-azo-iso-propane 0.80 Azo-n-propane <u>16.7 min.</u> 1.00

Table II (continued)

Column	Length ft.	Tempera- ture °C	Flow cc min ⁻¹	Compounds Analyzed and Relative Retention Times
Medium Activity	15	50	59	ethane 0.70
Silica Gel				ethylene 0.84
60/80 mesh				propane <u>8.1 min.</u> 1.00
				n-butane 2.32
				propylene 2.56
40% Isoquinoline on Chromosorb W.A.W.	20	27°C	72	2,3-dimethylbutane 0.61
60/80 mesh				2-methylpentane 0.68
				n-hexane <u>33.1 min.</u> 1.00
20% SE-30	20	100°C	70	azoethane <u>4.9 min.</u> 1.00
Silicone Gum Rubber				ethanal ethylhydrazone 1.90
on Chromosorb W.A.W.				ethyl 2-butyl diimide 1.90
60/80 mesh				ethanal diethylhydrazone 3.10
				tetraethylhydrazine 5.10

Table II (continued)

Column	Length ft.	Temperature °C	Flow cc min ⁻¹	Compounds Analyzed and Relative Retention Times	
13X Molecular Sieves, Crushed	10	0	33	hydrogen	0.29
				oxygen	0.64
				nitrogen	<u>1.00</u>
				methane	2.06
13X Molecular Sieves Crushed	10	27	60	nitrogen	<u>1.00</u>
				methane	1.68
Medium activity Silica Gel 60/80 mesh	15	27	60	ethane	<u>1.00</u>
				ethylene	1.56
				methylsilane	1.63
High activity Silica Gel 60/80 mesh	15	60	70	silane	0.56
				ethane	<u>1.00</u>
				ethylene	1.71

Table II (continued)

Column	Length ft.	Tempera- ture °C	Flow cc min ⁻¹	Compounds Analyzed and Relative Retention Times
20% SE-30	20	27	60	n-butane <u>6.3 min.</u>
Silicone Gum Rubber				<u>1.00</u>

Table III
Materials Used

Material	Source	Grade and Purity	Purification
Nitrogen	Airco	Assayed reagent	None
Helium	Canadian liquid air	Technical	Passed through charcoal-molecular sieves trap at -196°C
Methane	Phillips	Research 99.58 mole %	Degassed at -210°C
Methane-d ₂	Merck	Research 98% deuteration	Degassed at -210°C
Methane-d ₃	Merck	Research 98% deuteration	Degassed at -210°C
Methane-d ₄	Merck	Research 98% deuteration	Degassed at -210°C
Ethane-d ₆	Merck	Research 98% deuteration	Degassed at -210°C

Table III (continued)

Material	Source	Grade and Purity	Purification
Ethane	Phillips	Research 99.92 mole %	Degassed at -210°C
Ethylene	Phillips	Research 99.99 mole %	Degassed at -210°C
Propane	Phillips	Research 99.99 mole %	Degassed at -161°C
Propylene	Phillips	Research 99.70 mole %	Degassed at -161°C
n-butane	Phillips	Research 99.98 mole %	Degassed at -139°C
n-hexane	Phillips	Research 99.96 mole %	Degassed at -196°C
2-methylpentane	Matheson, Coleman & Bell	Technical	Preparative Gas Chromatography
2,3-dimethylbutane	Matheson, Coleman & Bell	Technical	Preparative Gas Chromatography
Monosilane	Merck	Research	Distilled at -161°C Collected at -196°C
Monosilane-d ₄	Merck	Research 97.5% deuterated	Distilled at -161°C Collected at -196°C

Table III (continued)

Material	Source	Grade and Purity	Purification
Disilane	Merck	Research	Distilled at -126°C
Disilane- d_6	Merck	Research 93.5% deuterated	Collected at -161°C Distilled at -126°C
Methylsilane	Merck	Research	Collected at -161°C Distilled at -139°C
Methylsilane- d_3	Merck	Research 97.5% deuterated	Collected at -196°C Distilled at -139°C
Dimethylsilane	Peninsular	Research	Collected at -196°C Distilled at -117°C
Dimethylsilane- d_2	Merck	Research 97.5% deuterated	Collected at -161°C Distilled at -117°C
Trimethylsilane	Peninsular	Research	Collected at -161°C Distilled at -84°C Collected at -139°C

Table III (continued)

Material	Source	Grade and Purity	Purification
Trimethylsilane-d	Merck	Research 97.5% deuterated	Distilled at -84°C Collected at -139°C
Tetramethylsilane	Merck	Research	Degassed at -196°C
Neo-pentane	Phillips	Research	Degassed at -139°C
Azo-methane	Merck	Research	Distilled at -98°C Collected at -131°C
Azo-methane-d ₆	Merck	Research 98% deuterated	Distilled at -98°C Collected at -131°C
Azo-ethane	Merck	Research	Preparative Gas Chromatography
Azo-n-propane	Merck	Research	Preparative Gas Chromatography
Azo-bis- (N-propane-2, 2-d ₂)	Merck	Research 93.7% deuterated	Preparative Gas Chromatography

Table III (continued)

Material	Source	Grade and Purity	Purification
Azo-iso-propane	Merck	Research	Preparative Gas Chromatography
n-propane-azo-iso-propane	Prepared by method of Spialter, et al		Preparative Gas Chromatography
	(42)		

CHAPTER III

SECONDARY PRODUCTS IN THE PHOTOLYSIS AND PYROLYSIS OF AZOETHANE (125)

RESULTS

- 1) Isomerization of Azoethane to Ethanal Ethylhydrazone.
- 2) Photolysis of Azoethane.
- 3) Pyrolysis of Azoethane.
- 4) Product Identification.

DISCUSSION

- 1) Mechanism.
- 2) The Azo-alkyl Radical.
- 3) The Triethylhydrazyl Radical.
- 4) Ethanal Ethylhydrazone.
- 5) Summary.

RESULTS

1) Isomerization of Azoethane to Ethanal Ethylhydrazone:

Isomerization of azo compounds to hydrazones is well known, having first been reported at the beginning of this century (126). There has been much recent interest in these reactions (127-133), and, since they might conceivably be of some importance in systems where azoalkanes are used as free radical sources, a preliminary study of the formation and properties of ethanal ethylhydrazone was made. Using the resulting analytical data, a careful search for this compound among the products of azoethane decomposition was made.

Isomerization of azoethane to ethanal ethylhydrazone was observed in pyrex reaction vessels at 150°C. The rate of isomerization was rapid at first, but decreased markedly as the walls of the vessel became conditioned. Ethanal ethylhydrazone was synthesized by condensation of ethylhydrazine and acetaldehyde. When exposed to fresh pyrex surfaces at 150°C it isomerized to azoethane. A temperature study of the equilibrium constant for this reaction was carried out, using a KOH lined pyrolysis cell to establish equilibrium rapidly. The cell was prepared by evaporating a methanol solution of KOH from it while it was turning on a rotary evaporator. It was then attached to the

high vacuum system, fitted with the pyrolysis furnace, and evacuated at 200°C for two days until evolution of gases ceased. Each experimental point was determined by starting with ethanal ethylhydrazone as well as with azoethane. After equilibrium had been achieved (as determined by trial runs to establish the necessary length of time) the cell was opened and the products were quickly cooled to -196°C, after which the cell was closed, and the products were transferred to the injection loop of the chromatograph. The data are summarized in Table IV and Figure 7. Least squares treatment gives $\Delta H = +0.19 \pm 0.08$ kcal/mole and $\Delta S = +2.72 \pm 0.22$ cal/mole deg for a 90% confidence level.

An attempt was made to determine the equilibrium constant (hydrazone/azo) for isomerization of azomethane, but the amount of formal methylhydrazone produced was extremely small and could not be accurately measured ($K = 0$). In contrast to this, $K = 3$ was found for isomerization of azoethane over a wide range of temperature. Ioffe and Stopskii (131,133) have reported studies of the isomerization of azopropanes at 100°C in which they found $K = 26.0$ for azo-n-propane and $K = 70.4$ for azo-iso-propane. They also found a value of $K = 82.3$ for n-propane-azo-iso-propane. This higher value arises from the fact that there are two possible hydrazone isomers and only one possible azo isomer. The equilibrium mixture reported was 90.8% acetone n-propylhydrazone, 8.0% propanal iso-propylhydrazone, and 1.2%

Table IV

Determination of Equilibrium Constant as a Function
of Temperature for Isomerization of
Azoethane to Ethanal Ethylhydrazone

Temp (°C)	Time (min)	Pressure (torr)	Ratio (hydrazone/azo)
145	60	8 ^a	3.12
144	45	4 ^b	3.15
173	30	8 ^a	3.11
173	45	8 ^b	3.26
95	105	9 ^a	2.96
95	120	6 ^b	2.99
72	255	5 ^a	2.87
71	240	5 ^b	2.89
39	245	6 ^a	2.92
39	253	5 ^b	2.99
52	240	6 ^a	2.94
124	60	5 ^a	2.98
124	60	4 ^b	2.98

^a Starting with azoethane.

^b Starting with ethanal ethylhydrazone.

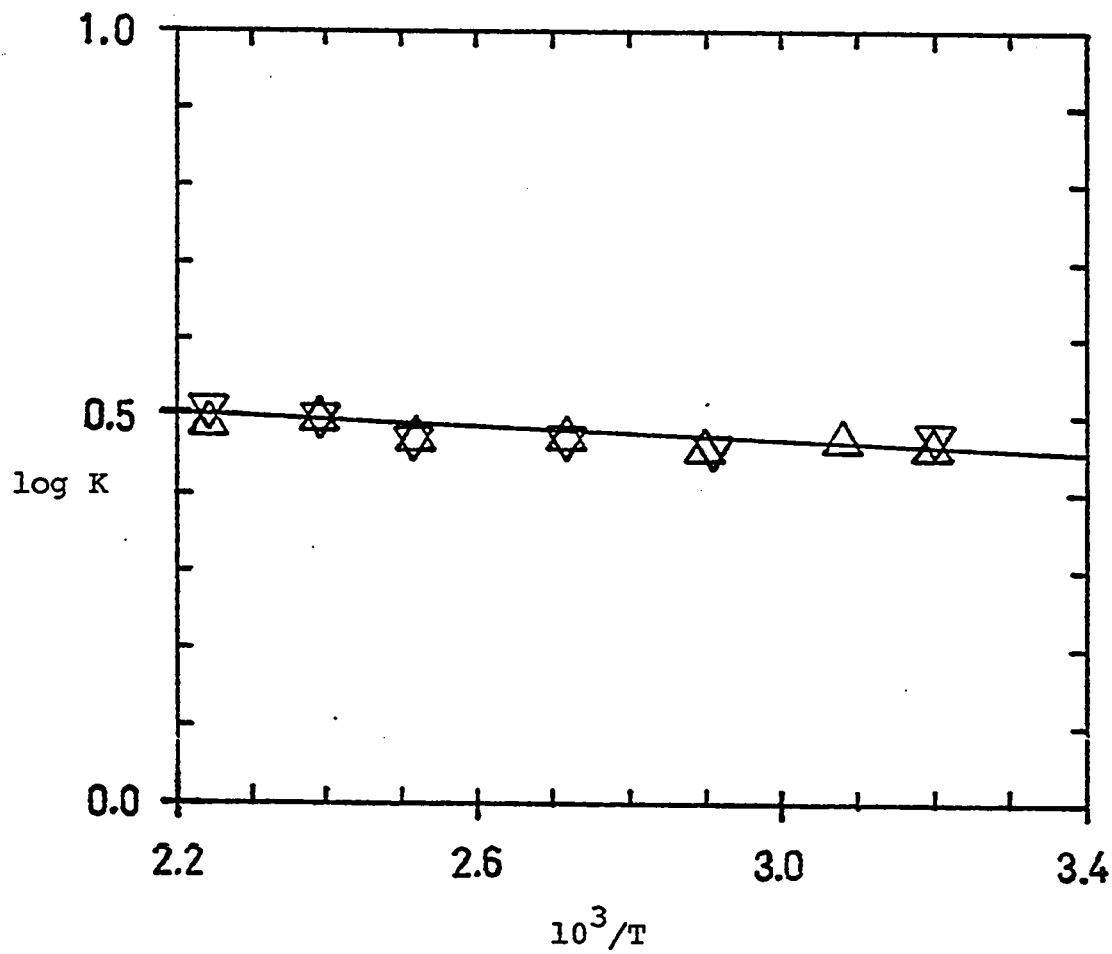


Figure 7. Plot of log of equilibrium constant vs. $10^3/T^\circ\text{K}$.
Runs starting with azoethane Δ , runs starting
with ethanal ethylhydrazone ∇ .

n-propane-azo-iso-propane.

The values for the equilibrium constant obtained in this study apparently form a consistent trend with those found by Ioffe and Stopskiĭ, and the stability of the hydrazone isomer is seen to increase with increasing substitution of the carbon atom which forms the double bond to nitrogen.

2) Photolysis of Azoethane:

A number of photolyses of azoethane were carried out at 100°C and 5 to 50 torr total pressure. In addition to the expected nitrogen, ethane, ethylene, and n-butane, three major heavy products were found. These were tetraethylhydrazine, ethanal diethylhydrazone, and ethyl 2-butyl diimide. Some other products were also formed in low yield. The yields of major products in photolysis are summarized in Table V. When photolysis was carried out in the presence of about 250 torr of propane, ethanal ethylhydrazone was formed in small yield. Photolysis with added nitric oxide was characterized by a complete suppression of the carbon-containing products except for a trace of ethanal ethylhydrazone which probably formed on the walls. The yield of nitrogen was not diminished.

3) Pyrolysis of Azoethane:

Pyrolysis in the temperature range 240-300°C yielded the expected nitrogen, ethane, ethylene, and n-butane and

Table V

Products of Photolysis and Pyrolysis of Azoethane

Compound	Amount μmoles
Photolysis of 34 torr azoethane at 97°C	
Unreacted azoethane	522
N ₂	20.5
C ₂ H ₄ + C ₂ H ₆	3.4
C ₄ H ₁₀	12.9
Tetraethylhydrazine*	2.5
Ethyl 2-butyl diimide*	1.7
Ethanal diethylhydrazone*	1.5
Ethyl not accounted for	0.7
Pyrolysis of 29 torr azoethane at 293°C	
Unreacted azoethane	130.5
N ₂	44.5
C ₂ H ₄ + C ₂ H ₆	22.2
C ₄ H ₁₀	14.5
Ethyl 2-butyl diimide*	5.5
Ethanal diethylhydrazone*	3.4
Ethyl not accounted for	9.8

*It was assumed that the chromatograph detector response was equal to that of azoethane.

more than a dozen other products, which appeared in quantities too small to permit identification. Since their peaks ran together on the chromatogram, they could not even be counted accurately. Evidently these products accounted for a significant fraction of the azoethane consumed.

The two major secondary products were ethanal diethylhydrazone and ethyl 2-butyl diimide. These were formed in approximately constant proportion to the azoethane concentration, independent of the length of the run, so they probably were being decomposed as well as formed in the system. When pyrolysis was carried out at 240°C where decomposition is fairly slow, with a pressure of about 500 torr of propane, ethanal ethylhydrazone was formed in low yield. Yields of major products in pyrolysis are summarized in Table V.

4) Product Identification:

Molecular structures of the heavy products were determined by mass spectrometry and nuclear magnetic resonance spectroscopy. Mass spectral data are summarized in Table VI, and NMR data are summarized in Table VII. Exact mass determinations of parent peaks were used in several cases to obtain molecular formulae. In NMR studies spin decoupling was used to confirm the apparent positions of the protons. The NMR spectrum of ethanal diethylhydrazone shows no evidence of cis-trans isomerism, and is

Table VI
Mass Spectral Data for Products of Azoethane Decomposition

Peak	m/e	Intensity
Azoethane		
Parent	86	
1	29	100
2	27	26
3	28	17
4	57	14
5	15	6
6	30	6
7	42	5
8	43	5
9	86	5
10	41	4
Ethanal Diethylhydrazone		
Parent	114	
1	99	100
2	29	67
3	28	59
4	30	51
5	42	43
6	56	38
7	114	37
8	44	34
9	71	32
10	27	32

Table VI (continued)

Peak	m/e	Intensity
Tetraethylhydrazine $C_8H_{20}N_2^*$		
Parent	144	
1	115	100
2	144	60
3	29	39
4	87	24
5	28	23
6	18	20
7	72	18
8	42	17
9	58	15
10	56	14
Ethanal Ethylhydrazone $C_4H_{10}N_2^*$		
Parent	86	
1	71	100
2	30	85
3	86	74
4	42	49
5	27	23
6	15	21
7	18	16
8	29	16
9	41	16
10	44	16

Table VI (continued)

Peak	m/e	Intensity
Ethyl 2-butyl diimide $C_6H_{14}N_2^*$		
Parent	114	
1	29	100
2	41	50
3	57	45
4	27	13
5	56	10
6	114	8
7	42	7
8	39	5
9	85	5
10	55	4

*Established by exact, high resolution mass determination on parent peak.

Table VII

NMR Spectra for Products of Azoethane Decomposition

Compound	Structure	τ	Splitting	J
Azoethane	CH_3^-	8.75	3	7
	$-\text{CH}_2-\text{N}$	6.28	4	7
Ethanal ethylhydrazone	CH_3^- (trans)	8.21	2	5
	CH_3^- (cis)	8.39	2	5
	$-\text{CH}=\text{N}$ (trans)	3.23	4	5
	$-\text{CH}=\text{N}$ (cis)	3.64	4	5
	$\text{N}-\text{NH}-\text{C}$	5.7	Broad	-
	$\text{N}-\text{CH}_2^-$	6.95	6	7
Ethanal-diethylhydrazone	$-\text{CH}_3$	8.91	3	7
	CH_3^-	8.15	2	5
	$-\text{CH}=\text{N}$	3.34	4	5
	$\text{N}-\text{CH}_2^-$	7.03	4	7
	$-\text{CH}_3$	8.97	3	7
Ethyl 2-butyl diimide	CH_3^-	8.75	3	7
	$-\text{CH}_2-\text{N}$	6.30	4	7
	$\text{N}-\text{C}-\text{H}$	6.79	Complex	-
	$\text{N}-\text{C}-\text{CH}_3$	8.83	3	7
	$\text{N}-\text{C}-\text{CH}_2^-$	8.31	Complex	-
	$\text{N}-\text{C}-\text{C}-\text{CH}_3$	9.17	3	7
Tetraethylhydrazine	CH_3^-	9.02	3	7
	$-\text{CH}_2-\text{N}$	7.61	4	7

consistent with the results of Stopskii (128) and co-workers. A sample of the ethyl 2-butyl diimide produced was photolyzed and yielded the expected hydrocarbon products. The NMR spectrum of ethyl 2-butyl diimide is shown in Figure 8. The NMR and mass spectral data for ethanal ethylhydrazone produced in isomerization of azoethane were identical to those for the synthesized sample, and the NMR spectrum is quite similar to that reported by Lemal and co-workers (134).

Detection of ethanal ethylhydrazone produced in photolysis and pyrolysis of azoethane was complicated by the fact that it had the same retention time on the silicone gum rubber column as ethyl 2-butyl diimide. The peaks at m/e 71 and 86 are quite small in the mass spectrum of ethyl 2-butyl diimide, but in runs where high pressures of propane and low decomposition rate would be expected to favor radical abstraction reactions there was some slight increase in the m/e 71 and 86 peaks relative to the spectrum of ethyl 2-butyl diimide, and this was presumed to be due to the presence of ethanal ethylhydrazone for which these peaks are the principal and the parent, respectively.

DISCUSSION

1) Mechanism:

As may be seen from the relative amounts of products formed, it is clear that formation of heavy products in

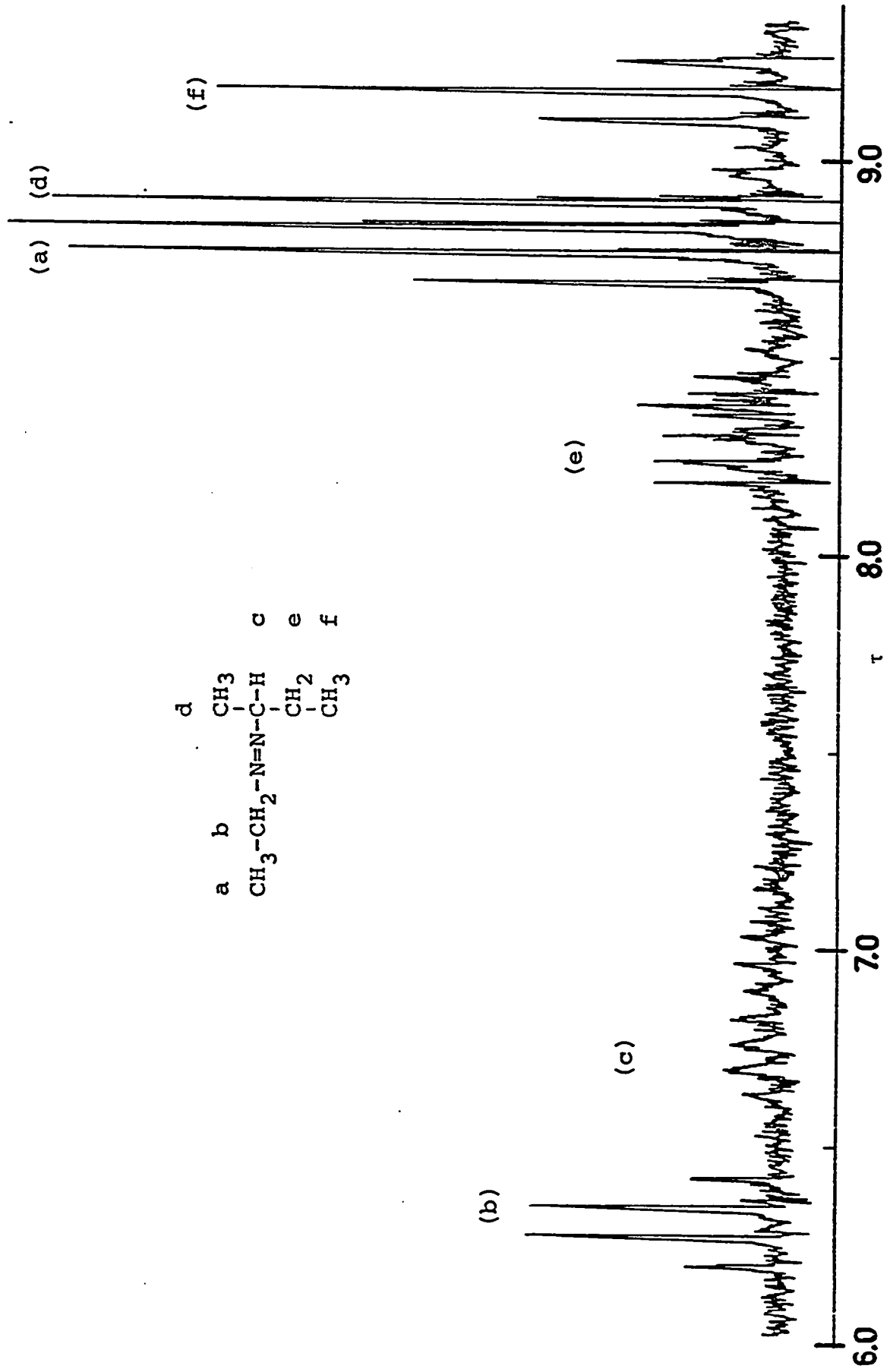
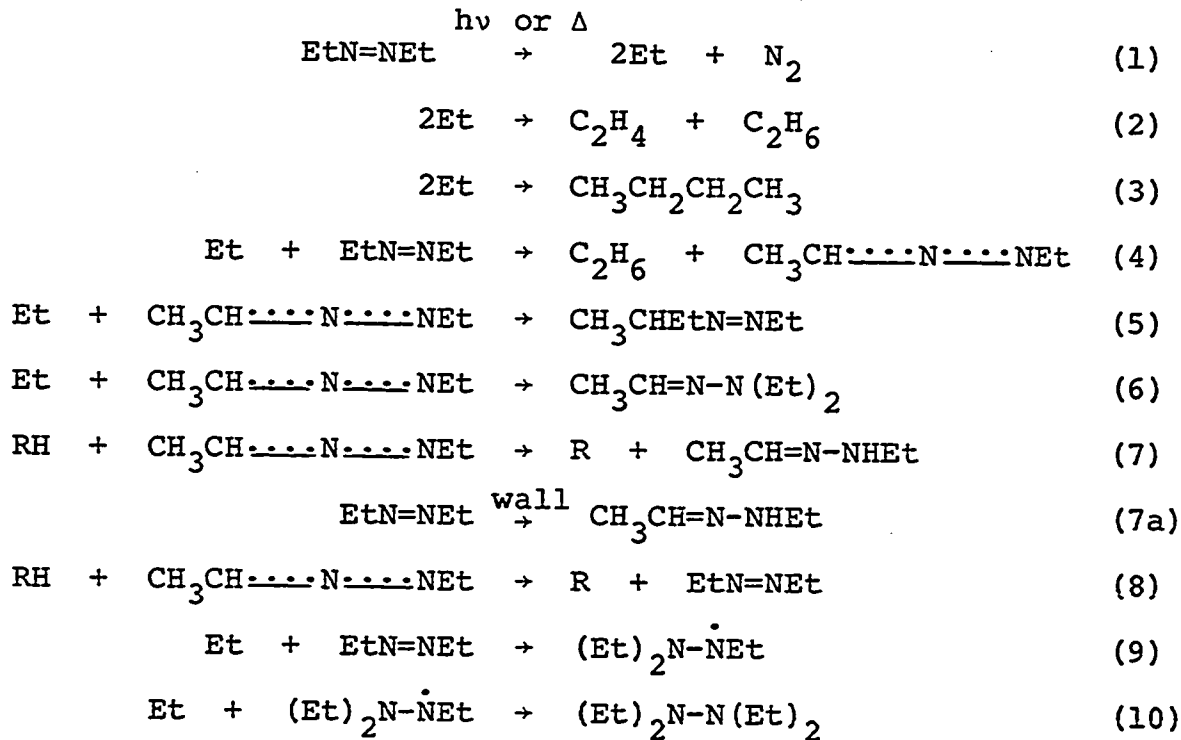


Figure 8. NMR spectrum of ethyl 2-butyl diimide.

secondary reactions initiated by radical abstraction from or addition to azoethane, though not dominant, is quite significant.

The products found suggest the following reaction scheme:



2) The Azo-alkyl Radical:

It has occasionally been suggested that the decomposition of the azoalkyl radical may be of possible significance in the photolysis and pyrolysis of azoalkanes at elevated temperatures (66,70). However, it was found in this work that abstraction of a hydrogen atom from azoethane to form an azoalkyl radical (Reaction 4) eventually results in a radical combination reaction either at the carbon atom where abstraction took place (Reaction 5) or else at the

nitrogen atom farthest from it (Reaction 6). This indicates that the radical must have an allylic structure, and it would be expected that such a radical would be quite stable. Since the products of combination of this radical with ethyl radicals are found in similar yields both in photolysis at 97°C and in pyrolysis at 293°C, it would seem unlikely that thermal instability of this radical could be important within the normal temperature range used in kinetic studies with azoalkanes.

3) The Triethylhydrazyl Radical:

In photolysis at 94°C tetraethylhydrazine was formed by addition of an ethyl radical to the double bond of azoethane (Reaction 9) followed by combination of the resulting triethylhydrazyl radical with another ethyl radical (Reaction 10). While tetraethylhydrazine was a very important secondary product at 97°C, there was no detectable yield of it in pyrolysis at 293°C. This could be due to thermal instability of the triethylhydrazyl radical or of tetraethylhydrazine itself.

4) Ethanal Ethylhydrazone:

It would appear that even the most perfunctory conditioning of cell walls should be sufficient to reduce wall-catalyzed formation of ethanal ethylhydrazone to relative insignificance. The evidence shown here tends to indicate that its formation in free radical processes by

disproportionation or abstraction reactions of the azoalkyl radical must also be slight, since, at best, only a trace of the compound was found in runs where a large concentration of hydrocarbon substrate and a slow rate of azoethane decomposition strongly favored its production by Reaction 7.

5) Summary:

The reaction scheme presented here differs from that suggested by Cerfontain and Kutschke (45) only in that formation of ethanal diethylhydrazone occurs parallel to formation of ethyl 2-butyl diimide. This could not affect the activation energies they determined for abstraction (8 kcal/mole) and addition (6 kcal/mole) reactions between ethyl radicals and azoethane. However, it would appear that the apparently high stability of the azoalkyl radical would cast serious doubt upon the validity of any proposed mechanism based on its thermal decomposition. On the other hand, much of the complexity of the pyrolysis of azoethane may be due to decomposition of ethanal diethylhydrazone and ethyl 2-butyl diimide.

The mechanism of alkyl radical reaction with the parent azo compound indicated by the results of this work is almost identical to that assumed by previous workers, and nothing found in this work offers any impediment to use of azoalkanes as free radical sources.

CHAPTER IV

ARRHENIUS PARAMETERS FOR THE REACTION OF PROPYL RADICALS WITH PROPANE (135)

RESULTS

- 1) Photolysis of Azo-n-propane and Azo-iso-propane.
- 2) Photolysis of Azo-n-propane in the Presence of Propane.
- 3) Determination of the Radical Disappearance Ratio.
- 4) Arrhenius Parameters.

DISCUSSION

- 1) Possible Consequences of the Mass Balance Defect.
- 2) Conclusion.

RESULTS

1) Photolysis of Azo-n-propane and Azo-iso-propane:

The photolysis of the azopropanes at room temperature yielded nitrogen, propane, propylene, and hexanes. The results are summarized in Table VIII. A disproportionation to combination ratio of 0.14 was found for n-propyl radicals and 0.55 for iso-propyl radicals. Kerr and Calvert (66) reported a value of 0.157 for n-propyl radicals, which is in close agreement with the result found here. In the course of a series of high intensity photolysis studies (136,137), Terry and Futrell found a value of 0.69 for iso-propyl radicals. However, values quite close to 0.55 have been determined by Riem and Kutschke (46) and by Durham and Steacie (65) under conditions similar to those of the present study. The values 0.15 for n-propyl radicals and 0.55 for iso-propyl radicals have been adopted for use in further study of propyl radicals in this work. Photolysis of a mixture of azo-n-propane and azo-iso-propane indicated a ratio of disproportionation to cross combination for n-propyl and iso-propyl radicals close to the mean value of 0.35, and this value has also been adopted here.

A temperature study of the photolysis of azo-n-propane was carried out to determine the Arrhenius parameters for abstraction of hydrogen from azo-n-propane by n-propyl

Table VIII

Determination of Ratio of Disproportionation to Combination
for Propyl Radicals Produced by Photolysis of Azopropanes

Temp (°C)	Time (min)	Nitrogen Propylene n-hexane	Products (μ mole)	2,3- butane	2- methyl- pentane	Δ (n-Pr, n-Pr)	Δ (i-Pr, i-Pr)	Δ (n-Pr, i-Pr)	k_d/k_c
(1) Photolysis of azo-n-propane									
29	60	6.63	0.71	5.62		0.13			
28	60	5.98	0.74	5.02		0.15			
27	59	5.12	0.57	4.12		0.14			
(2) Photolysis of azo-iso-propane									
26	1000	60.37	19.44	35.07					0.55
24	60	11.43	3.96	7.05					0.56
27	60	9.79	3.34	6.02					0.55
27	60	7.83	2.64	4.89					0.54

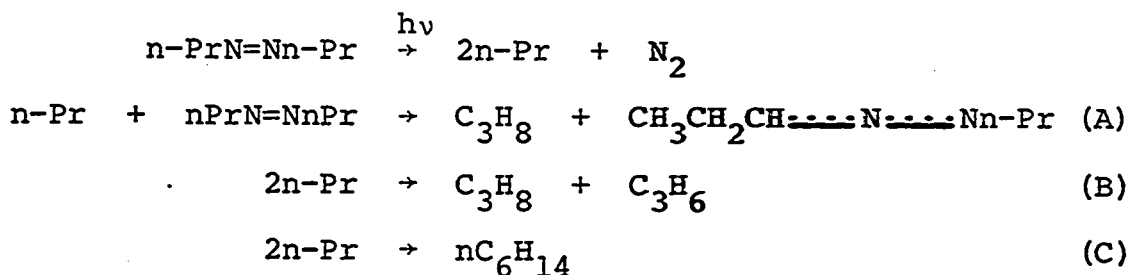
Table VIII (continued)

Temp (°C)	Time (min)	Nitrogen Propylene	Products (μ mole)		k_d/k_c		
			2,3- dimethyl- butane	2- methyl- pentane	Δ (n-Pr, n-Pr)	Δ (i-Pr, i-Pr)	
(3) Photolysis of a mixture of azo-n-propane and azo-iso-propane							
28	60	9.36	2.52	0.68	2.57	2.59	0.39 ^a
30	60	7.55	2.01	0.61	2.18	2.11	0.34 ^a
31	60	6.43	1.67	0.46	1.80	1.80	0.34 ^a

^a Δ (n-Pr, i-Pr) calculated from

$$[(\text{total propylene}) - 0.15(\text{n-hexane}) - 0.55(2,3\text{-dimethylbutane})]/(2\text{-methylpentane}).$$

radicals. The following mechanism was used



The vapor pressure of azo-n-propane is quite low, and, in the static system used in the present study, it was difficult to get sufficient conversion at the lower temperatures so that accurate rate constants could be measured. Least squares treatment of some of the points, mostly at high temperature, which appeared to fit an Arrhenius plot gave the equation

$$\log \frac{k_A}{k_C^{1/2}} = 4.74 - \frac{7990}{2.303RT}$$

While this hardly qualifies as a determination of the Arrhenius parameters, it nevertheless agrees closely with the earlier value of

$$\log \frac{k_A}{k_C^{1/2}} = 4.6 - \frac{7900}{2.303RT}$$

found by Calvert and Kerr (66), who used a circulating system, and the result has been adopted for further use in this work. An analogous study of the reaction of iso-propyl radicals with azo-iso-propane yielded

$$\log \frac{k_A}{k_C^{1/2}} = 4.01 \pm 0.37 - \frac{7030 \pm 630}{2.303RT}$$

(All error limits quoted in this work are for a 95% confidence level unless otherwise specified.) This result is also in satisfactory agreement with the values of

$$\log \frac{k_A}{k_C} = 3.5 - \frac{6700}{2.303RT} \quad (46)$$

and

$$\log \frac{k_A}{k_C} = 3.4 - \frac{6500}{2.303RT} \quad (65)$$

reported previously. Rate constant data for these reactions are summarized in Tables IX and X and the Arrhenius plots are shown in Figure 9.

2) Photolysis of Azo-n-propane in the Presence of Propane:

When propane was added to the system, 2-methyl pentane appeared among the products at room temperature. With increasing temperature, many products of vapor pressure lower than azo-n-propane began to appear, and the mass balance, as calculated from the hydrocarbon products decreased steadily.

Four of the heavy products were trapped, and their identification was attempted. One of them proved to be the hydrazone isomer of azo-n-propane, propanal propylhydrazone. It was identified by mass spectrometry and NMR. Only mass

Table IX
Reaction of n-Propyl Radicals with Azo-n-propane

Temp (°C)	Time (min)	[Azo] x10 ⁶ mole/cc	Rate x10 ¹² mole/cc s				$\frac{k_A}{k_C^{1/2}}$	
			N ₂	Propane (total)	C ₃ H ₈ R _B	C ₃ H ₈ R _A		C ₆ H ₁₄ R _C
90.0	120.00	0.469	6.83	2.01	0.72	1.29	4.77	1.259 *
119.0	120.00	0.309	6.51	2.19	0.67	1.52	4.45	2.332
149.0	120.00	0.322	6.91	2.81	0.47	2.34	3.15	4.095
61.0	120.00	0.424	6.70	1.42	0.73	0.69	4.88	0.7367*
27.0	120.00	0.460	6.89	1.28	0.85	0.43	5.64	0.3936*
213.0	120.00	0.226	6.38	4.20	0.25	3.95	1.68	13.48
177.0	120.00	0.285	6.67	3.38	0.34	3.04	2.26	7.095
53.0	60.00	0.420	5.79	1.00	0.78	0.22	5.21	0.2295
24.0	30.00	0.500	5.15	0.98	0.64	0.34	4.28	0.3287*
24.0	60.00	0.450	4.59	0.72	0.59	0.13	3.96	0.1452*
71.0	60.00	0.417	5.66	0.97	0.71	0.26	4.70	0.2876*
113.0	61.00	0.372	6.13	1.89	0.62	1.27	4.14	1.678

Cell volume 218 cc. Illuminated volume 192 cc.

* Not used in least squares calculation.

Table X
Reaction of iso-Propyl Radicals with Azo-iso-propane

Temp (°C)	Time (min)	[Azo] $\times 10^6$ mole/cc	Rate $\times 10^{12}$ mole/cc s				$\frac{k_4}{k_C^{1/2}}$	
			N ₂	Propane (total) C ₃ H ₈ R _B	C ₃ H ₈ R _A	C ₆ H ₁₄ R _C		
89.0	32.10	1.125	16.28	6.90	4.92	1.98	8.95	0.5883
121.0	37.00	1.140	19.12	9.90	5.28	4.62	9.60	1.308
149.0	30.00	1.239	20.66	13.20	4.58	8.62	8.33	2.411
132.0	30.00	1.048	16.38	8.31	4.11	4.20	7.47	1.466
105.0	30.00	1.571	19.88	10.30	5.60	4.70	10.19	0.9372
75.0	32.00	1.435	18.45	7.62	5.78	1.84	10.50	0.3957
61.0	30.00	2.058	19.82	8.05	6.03	2.02	10.97	0.2964
44.0	30.00	1.981	18.12	6.66	5.82	0.84	10.59	0.1303

Cell volume 218 cc. Illuminated volume 192 cc.

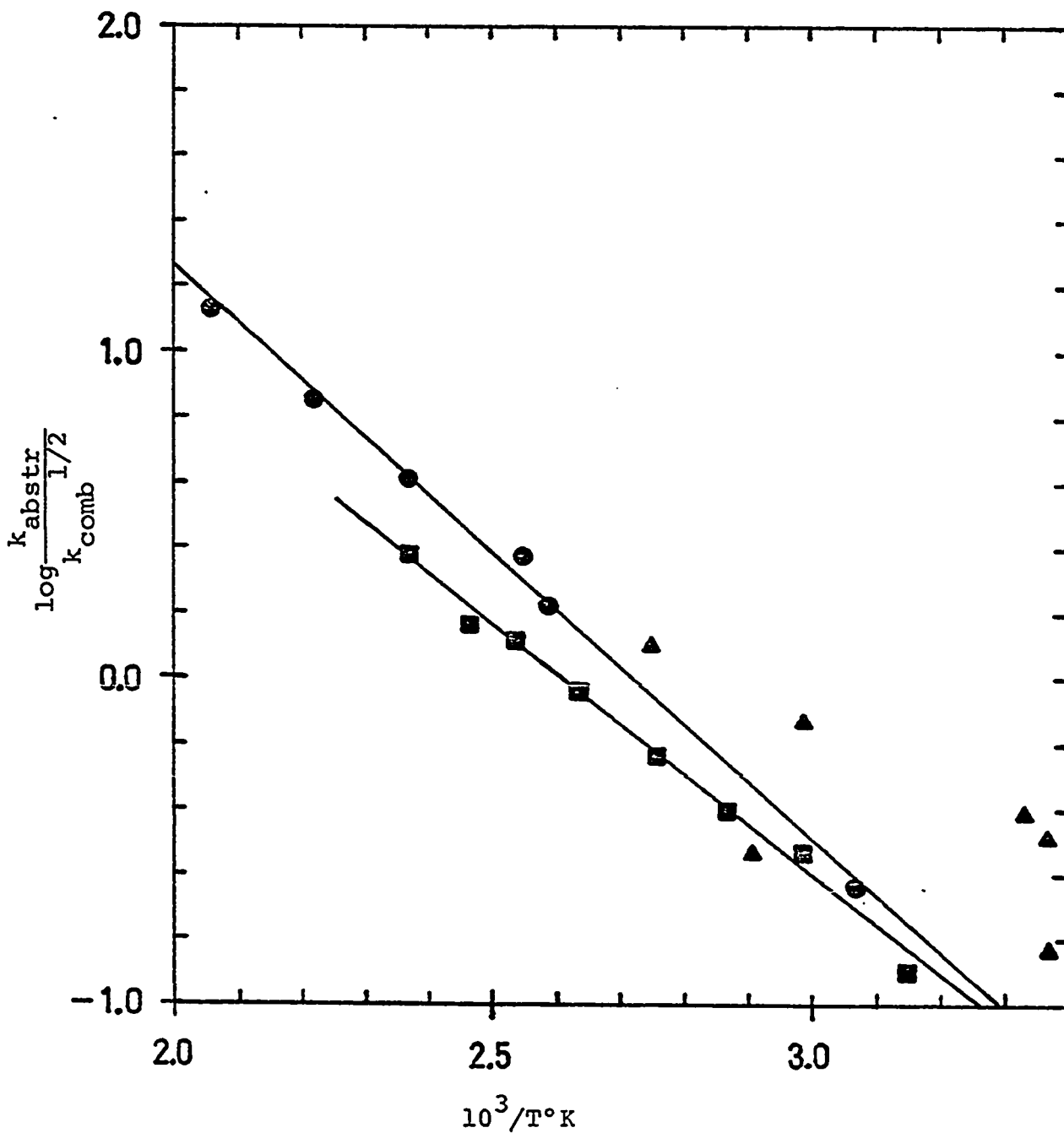


Figure 9. Arrhenius plots for reaction of isopropyl radicals with azo-iso-propane \blacksquare , and n-propyl radicals with azo-n-propane \bullet . Points rejected in least squares calculation for azo-n-propane are marked by \blacktriangle .

spectra were obtained for the other three products, since it was impractical to obtain large enough samples for NMR spectra. An exact mass measurement indicated that the lightest of these products was a hydrocarbon, or mixture of hydrocarbons, C_9H_{20} . The cracking pattern did not match closely the known cracking pattern of any individual isomer. The other two products both had molecular formulae $C_9H_{20}N_2$. The two cracking patterns were virtually identical, except that the product with the shorter retention time had a slightly larger peak at mass 15. The two mass spectra appear closely analogous to that of ethyl 2-butyl diimide, and it seems reasonable to suppose that the one with shorter retention time and larger mass 15 peak is propyl 2-methyl-3-pentyl diimide, and that the other one is propyl-3-hexyl diimide. This tentative identification is supported by the fact that the first product is produced in increasing amounts as temperature and isopropyl concentration increase, while the second product is produced throughout the temperature range of the study. The possibility of these products being cis-trans isomers of propanal dipropylhydrazone can be dismissed, since dialkyl hydrazones are known not to display cis-trans isomerism (128), and the mass spectrum is not analogous to that of ethanal diethylhydrazone. NMR and mass spectral data are summarized in Tables XI and XII, and the NMR spectra of propanal propylhydrazone and n-propane-azo-iso-propane are shown in Figures 10 and 11.

Table XI
 NMR Spectra for Products of Azo-n-propane Decomposition

Compound	Structure	τ	Splitting	J
Azo-n-propane	CH ₃ -	9.04	3	3.5
	-CH ₂ -	8.23	6	3.5
	-CH ₂ -N	6.36	3	3.5
Propanal propylhydrazone	CH ₃ -	9.02	3	3.5
	-CH ₂ -	7.93	Complex	-
	-CH=N (trans)	3.26	3	2.5
	-CH=N (cis)	3.88	3	2.5
	-NH-	~5.5	Broad	-
n-propane-azo-iso-propane	N-CH ₂ -	7.10	3	3.5
	-CH ₂ -	8.52	Complex	-
	-CH ₃	9.12	3	3.5
n-propane-azo-iso-propane	CH ₃ -	8.84	2	3.5
	-CH-N	~6.5	Complex	-

Table XI (continued)

Compound	Structure	τ	Splitting	J
n-propane-azo-iso-propane	N-CH ₂ -	6.41	3	3.5
	-CH ₂ -	8.27	6	3.5
	-CH ₃	9.09	3	3.5

Table XII
Mass Spectral Data for Products of Azo-n-propane Decomposition

Compound	m/e	Intensity
Azo-n-propane		
Parent	114	
1	43	100
2	41	67
3	27	56
4	28	16
5	42	12
6	39	11
7	30	7
8	29	6
9	15	5
10	44	4
Propanal propylhydrazone $C_6H_{14}N_2^*$		
Parent	114	
1	30	100
2	28	66
3	85	55
4	18	48
5	27	33
6	29	32
7	41	24
8	56	20
9	43	19
10	17	11

Table XII (continued)

Compound	m/e	Intensity
Azo-iso-propane		
Parent	114	
1	43	100
2	41	34
3	42	24
4	27	24
5	39	6
6	15	6
7	114	6
8	56	4
9	44	4
10	29	4
n-Propane-azo-iso-propane		
Parent	114	
1	43	100
2	41	39
3	27	27
4	42	21
5	39	7
6	114	7
7	44	5
8	15	5
9	56	4
10	28	4

Table XII (continued)

Compound	m/e	Intensity
Unknown $C_9H_{20}N_2^*$		
Tentatively propyl 2-methyl-3pentyl diimide		
Parent	156	
1	43	100
2	41	16
3	85	14
4	57	10
5	27	9
6	29	6
7	28	4
8	39	3
9	44	3
10	55	2
Unknown $C_9H_{20}N_2^*$		
Tentatively propyl 3-hexyl diimide		
Parent	156	
1	43	100
2	41	15
3	85	10
4	57	10
5	27	9
6	29	8
7	44	4
8	55	3
9	39	3
10	28	3

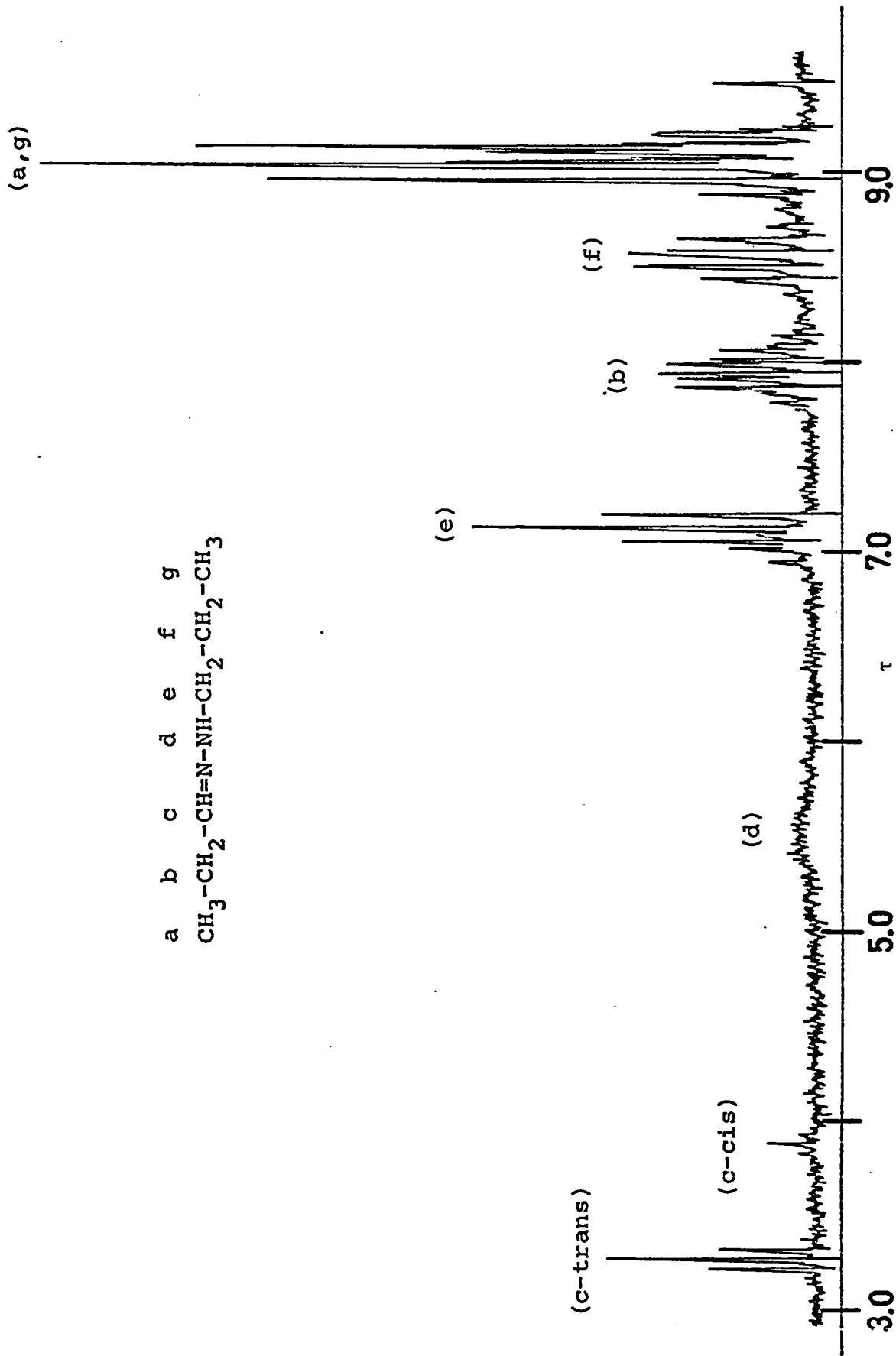


Figure 10. NMR spectrum of propanal propylhydrazone.

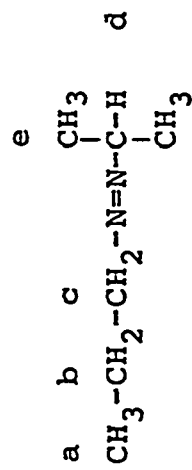
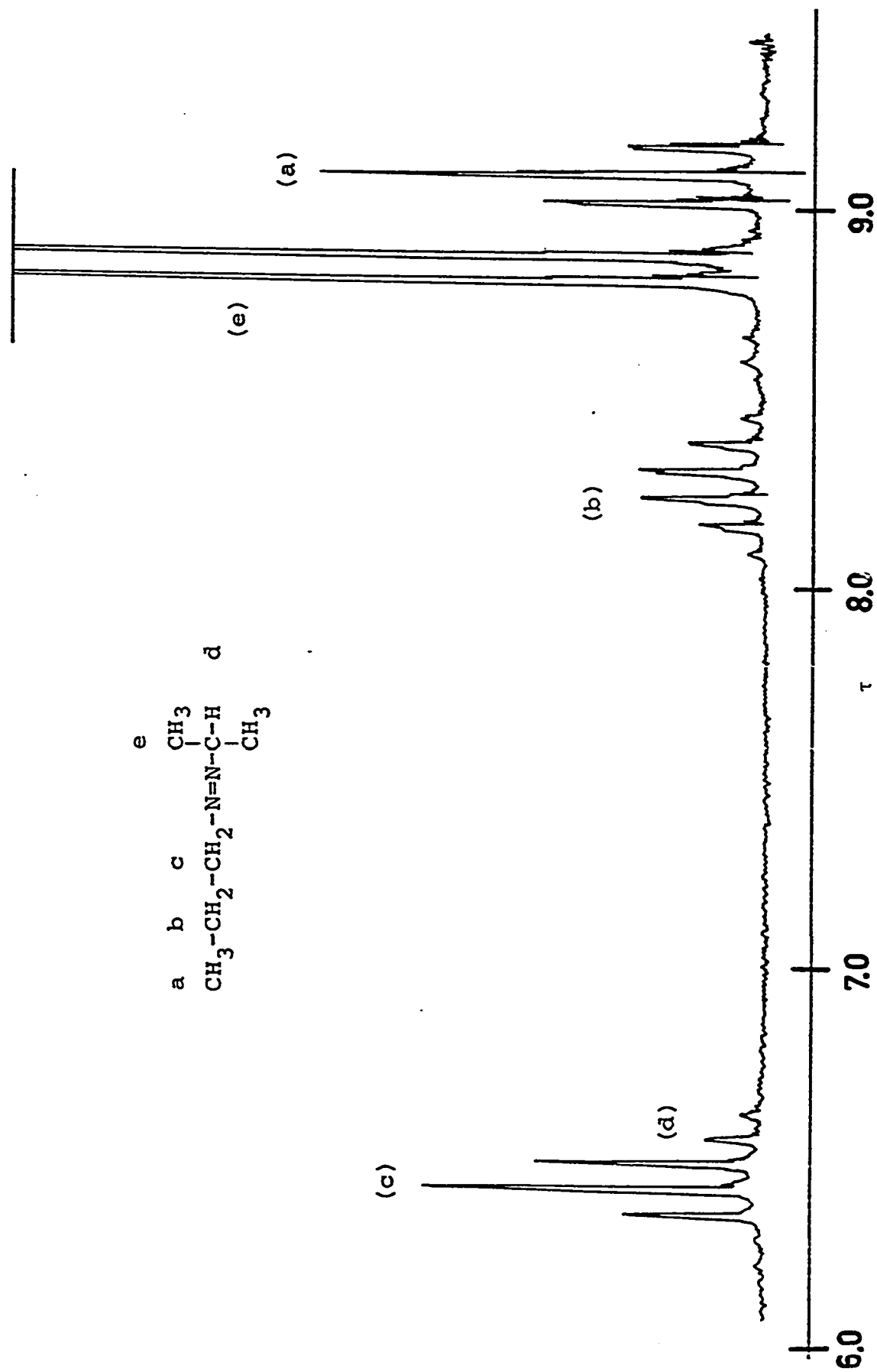
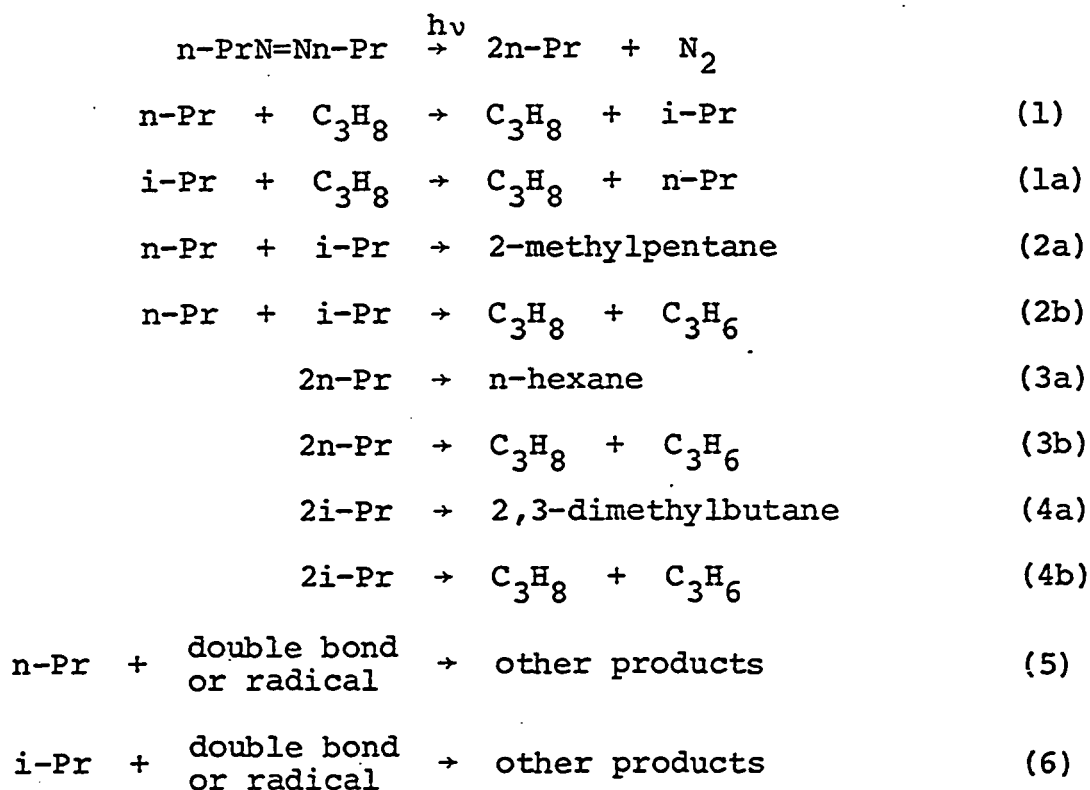


Figure 11. NMR spectrum of n-propane-azo-iso-propane.

The heavy products were eluted from the column as very broad peaks with long retention times when the column was operated under conditions optimal for separation of hydrocarbon products, and it was impractical to attempt quantitative analysis of them. Account of these products was taken in the kinetic treatment in terms of the mass balance defect. The mechanism used for the kinetic treatment is summarized below:



The following assumption is made:

$$k_{2a} + k_{2b} = 2(k_{3a} + k_{3b}) = 2(k_{4a} + k_{4b})$$

Using

$$\frac{k_{2b}}{k_{2a}} = 0.35 \quad \frac{k_{3b}}{k_{3a}} = 0.15 \quad \frac{k_{4b}}{k_{4a}} = 0.55$$

we obtain

$$\frac{R_{2a}}{R_{3a}} = 1.70 \frac{[i-Pr]}{[n-Pr]}$$

and

$$r = \frac{[i-Pr]}{[n-Pr]} = 0.59 \frac{R_{2a}}{R_{3a}}$$

The rates of Reactions 5 and 6 may be expressed in terms of mass balance:

$$R_0 = R_{N_2} - (R_{2a} + R_{2b} + R_{4a} + R_{4b} + R_{3a} + R_{3b})$$

Using the known values of k_b/k_a

$$R_0 = R_{N_2} - 1.35R_{2a} - 1.55R_{4a} - 1.15R_{3a}$$

Since R_0 represents the mass balance defect in terms of radical pairs, while R_5 and R_6 account for the disappearance of single radicals, then

$$R_5 + R_6 = 2R_0$$

Now k_5 and k_6 will not, in general, be equal. They will be related at a given temperature by

$$q = \frac{k_5}{k_6}$$

Thus

$$\frac{R_6}{R_5} = \frac{k_6 [i-Pr] [X]}{q k_6 [n-Pr] [X]} = \frac{1}{q} \frac{[i-Pr]}{[n-Pr]} = \frac{r}{q}$$

where [X] represents the collective concentration of double bonds and radicals other than propyl radicals. The steady state assumption for [i-Pr] gives

$$\frac{d[i-Pr]}{dt} = 0 = R_1 - R_{1a} - R_{2a} - R_{2b} - 2R_{4a} - 2R_{4b} - R_6$$

The rate constants k_1 and k_{1a} are related thermodynamically and from the known entropies and heats of formation of the isopropyl and n-propyl radicals (1)

$$k_{1a} = k_1 \exp(0.91 - 3500/RT)$$

This further leads to the expression (Appendix A):

$$\frac{k_1}{k_{3a}^{1/2}} = \frac{1.35R_{2a} + 3.10R_{4a} + \frac{2rR_0}{r+q}}{R_{3a}^{1/2} [C_3H_8] [1-r \exp(0.91 - 3600/RT)]}$$

3) Determination of the Radical Disappearance Ratio:

All the unknown quantities needed for determination of $k_1/k_{3a}^{1/2}$ can be evaluated from the results of photolysis of azo-n-propane in the presence of propane with the exception of q . At higher temperatures, reactions of radicals with the azo compound and perhaps with propylene formed in the system are evidently of substantial importance, and, in order to evaluate $k_1/k_{3a}^{1/2}$, the value of q must be known. This value was determined from the photolysis of n-propane-azo-iso-propane in the presence of C_3F_8 , added as a pressure stabilizer, at several different temperatures. The

ratio of n-propyl/iso-propyl radicals consumed in reactions other than combination and disproportionation with each other can be obtained from the mass balance ratio

$$\frac{R_5}{R_6} = \frac{R_{N_2} - (1.35R_{2a} + 2.30R_{3a})}{R_{N_2} - (1.35R_{2a} + 3.10R_{4a})} = M$$

Since $q = rR_5/R_6$, one obtains

$$q = 0.59 \frac{R_{2a}}{R_{3a}} M$$

Least squares treatment of the data gives a straight line relation corresponding to the equation

$$\log q = 0.157 - 15/T$$

The data are summarized in Table XIII and Figure 12.

4) Arrhenius Parameters:

Rate constants for the reaction of n-propyl radicals with propane are summarized in Table XIV and Figure 13. Least squares treatment of the data gives the Arrhenius equation

$$\log \frac{k_1}{k_{3a}^{1/2}} = 2.54 \pm 0.25 - \frac{7800 \pm 410}{2.303RT}$$

The interference of reactions accounted for collectively under Reactions 5 and 6 is most important under the same conditions which favor high rates of abstraction

Table XIII
Photolysis of n-Propane-azo-iso-propane with Added C₃F₈

T°C	Azo (torr)	C ₃ F ₈ (torr)	SN ₂ * (μmole)	S _{2a} * (μmole)	S _{3a} * (μmole)	S _{4a} * (μmole)	Mass** Balance	q
28	2.8	0	5.11	1.86	1.09	0.78	1.02	-
62	1.2	0	3.20	1.19	0.70	0.52	1.05	-
90	2.6	0	5.94	2.22	1.33	0.94	1.05	-
126	1.7	0	4.36	1.56	0.89	0.67	1.00	-
123.0	6.4	48.2	9.13	2.15	1.03	1.01	0.619	1.535
120.0	5.4	102.4	11.02	2.33	1.06	1.18	0.562	1.672
119.0	4.5	206.2	3.59	0.74	0.37	0.37	0.557	1.422
90.0	6.5	50.4	7.78	2.19	1.15	0.99	0.747	1.395
91.0	6.3	203.4	12.82	3.05	1.33	1.54	0.627	1.944
60.0	8.7	101.5	7.70	2.18	1.07	0.99	0.741	1.635
60.0	8.8	201.5	8.04	1.96	0.98	0.94	0.650	1.494

*S_i is the quantity of product formed in reaction i.

**Mass balance is given by (1.35 S_{2a} + 1.15 S_{3a} + 1.55 S_{4a})/SN₂.

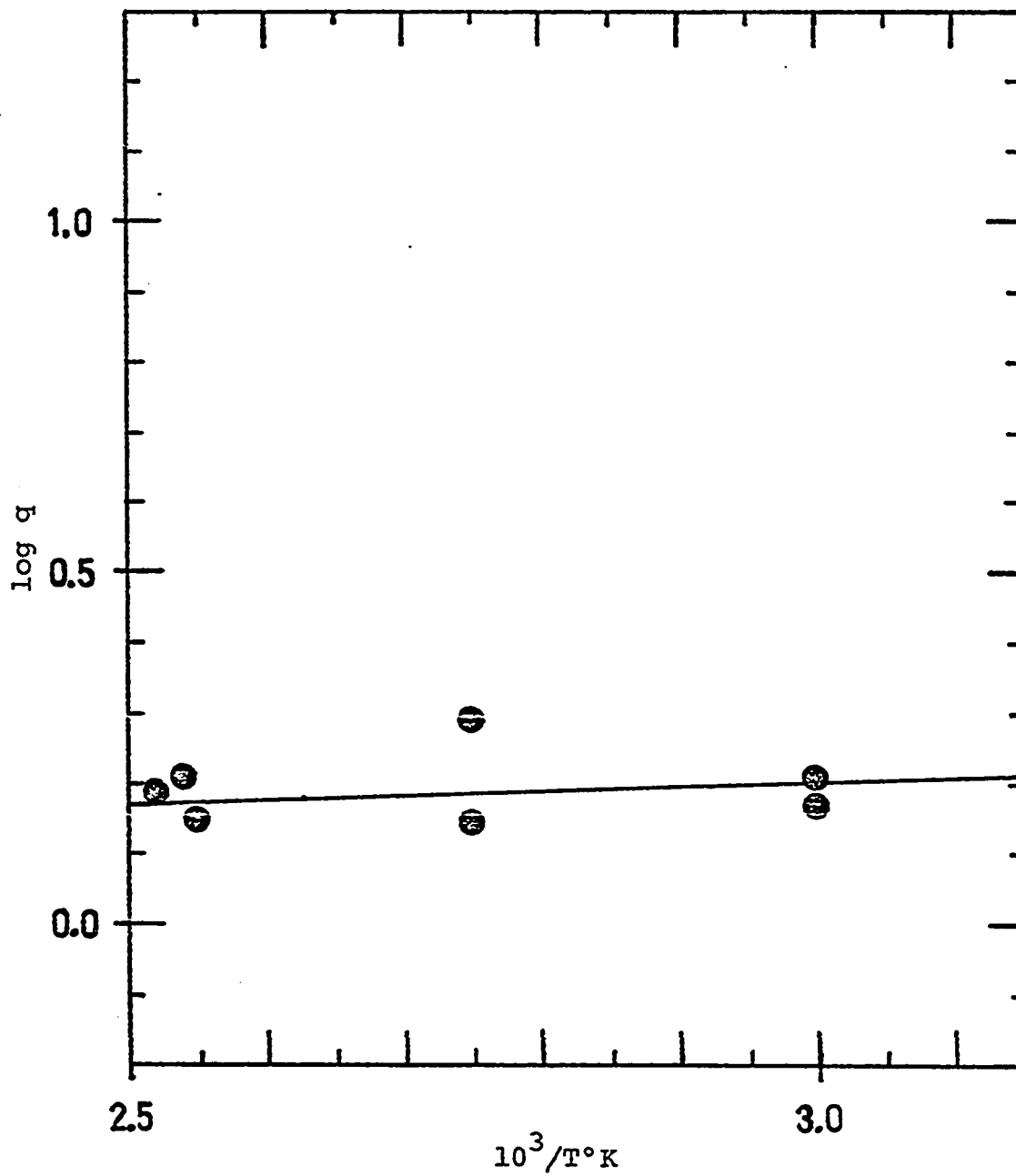


Figure 12. Determination of n-propyl/iso-propyl radical disappearance ratio q .

Table XIV
Temperature study of the Reaction of n-Propyl Radicals with Propane

$\frac{10^3}{T^\circ K}$	Time (hours)	N_2	Rate $\times 10^{14}$ mole/cc s	R_{2a}	R_{3a}	R_{4a}	R_0	$[C_3H_8] \times 10^5$	r	q	$\frac{k_1}{k_{3a}} \times 10^4$
3.30 ^a	36	24.4	1.13	16.5	---	---	3.90	4.93	0.040	1.61	8.575
3.30 ^a	36	18.8	0.96	14.5	---	---	0.83	4.38	0.039	1.61	8.008
2.75 ^a	36	22.3	3.86	6.63	0.52	0.52	8.66	4.93	0.343	1.58	78.65
2.79 ^a	36	25.5	3.54	7.68	0.40	0.40	11.27	4.93	0.272	1.58	68.60
2.75 ^a	36	26.7	3.94	7.60	0.48	0.48	11.90	4.93	0.306	1.58	78.96
2.75 ^a	36	24.9	3.94	7.64	0.48	0.48	10.05	4.93	0.304	1.58	74.23
2.75 ^a	36	24.2	3.78	7.84	0.44	0.44	9.40	4.38	0.284	1.58	76.55
2.75 ^a	36	22.1	3.22	5.95	0.44	0.44	10.23	4.38	0.319	1.58	86.21
2.75 ^a	36	16.8	3.01	5.39	0.40	0.40	5.92	4.38	0.329	1.58	72.71
2.56 ^a	36	23.1	3.30	3.22	0.84	0.84	13.64	4.93	0.605	1.57	168.4
2.53 ^a	36	20.5	3.01	2.73	0.84	0.84	11.99	4.38	0.651	1.57	193.0
2.38 ^a	36	21.0	2.57	1.57	1.04	1.04	14.11	4.38	0.966	1.56	330.8
2.36 ^a	36	27.2	3.58	2.29	1.45	1.45	17.49	4.93	0.922	1.56	310.5

Table XIV (continued)

$\frac{10^3}{T^\circ K}$	Time (hours)	N_2	Rate $\times 10^{14}$ mole/cc s	R_{2a}	R_{3a}	R_{4a}	R_0	$[C_3H_8] \times 10^5$ mole/cc	x	q	$\frac{k_1}{k_{3a}} \times 10^4$
2.22 ^a	36	33.0	5.63	2.97	2.61	17.94	4.93	1.118	1.55	382.9	
2.21 ^a	36	37.5	7.23	3.82	3.46	17.98	4.38	1.117	1.55	440.1	
3.00 ^a	36	27.2	2.57	12.9	0.08	8.77	4.93	0.118	1.59	27.85	
3.06 ^a	36	24.6	1.77	15.8	0.04	3.98	4.38	0.066	1.60	16.27	
3.34 ^b	24	33.3	0.42	17.1	--	13.07	3.04	0.014	1.61	6.364	
3.08 ^b	24	16.7	0.45	5.26	--	10.04	3.04	0.050	1.60	17.55	
2.89 ^b	24	23.0	0.57	4.22	0.03	17.33	3.04	0.080	1.59	40.41	
2.59 ^b	20	18.1	0.68	1.66	0.10	15.12	3.04	0.242	1.57	135.2	
1.98 ^b	12	189.0	17.8	10.2	11.1	136.04	3.04	1.030	1.54	1871.	
3.33 ^c	36	0.5	nil	nil	nil	--	0.00	--	--	--	
2.18 ^c	36	0.5	0.28	0.03	nil	--	4.93	--	--	--	

^a Cell 238 cm³; illuminated volume 192 cm³; 1 lamp.

^b Cell 418 cm³; illuminated volume 409 cm³; 2 lamps.

^c Blank runs.

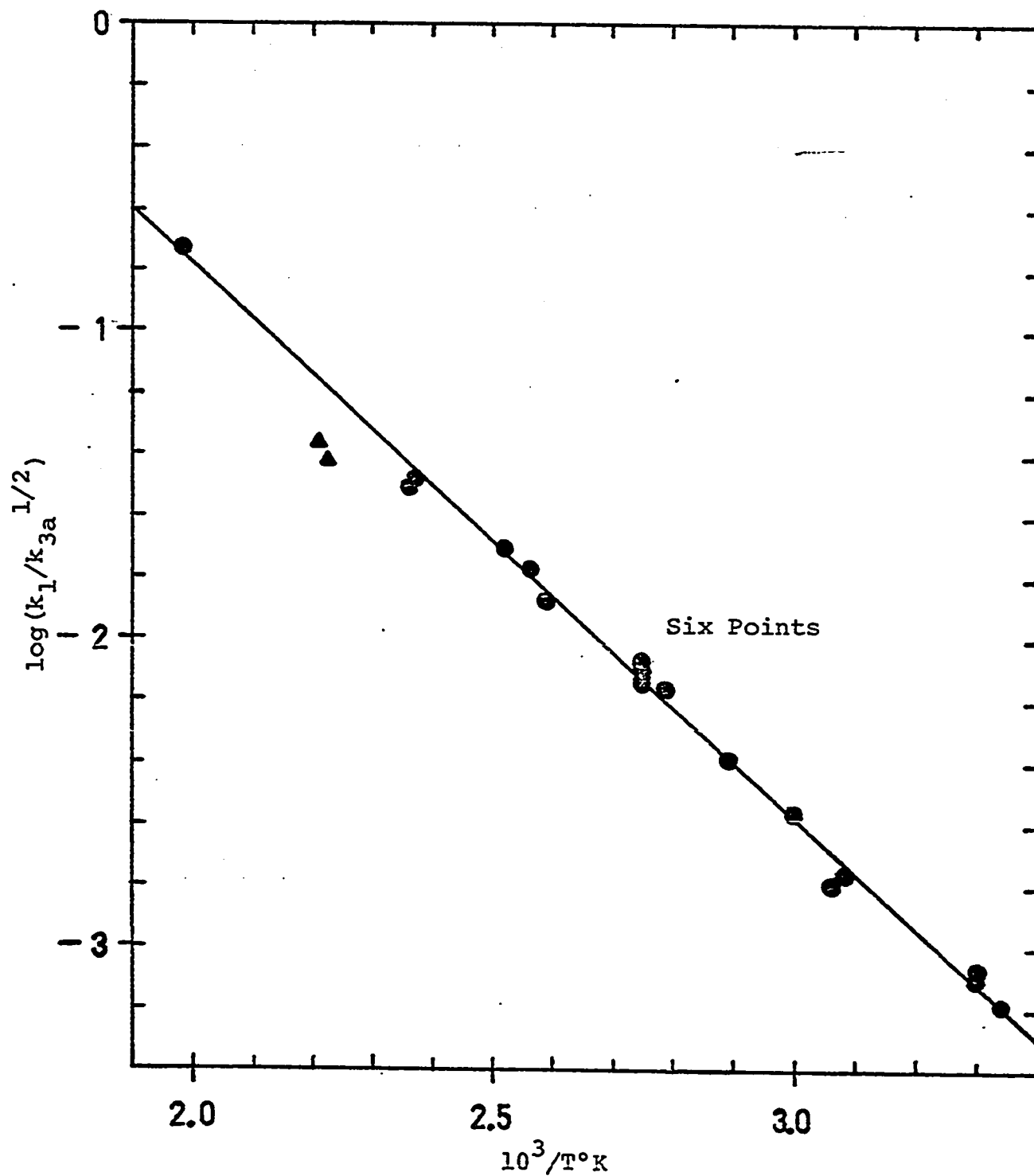


Figure 13. Arrhenius plot for reaction of n-propyl radicals with propane.

● r less than 1.1

▲ r greater than 1.1, not used in least squares calculation.

compared to combination. Hence these reactions will be most important in runs with a high value of r , the steady state concentration ratio of isopropyl to n -propyl radicals. The Arrhenius parameters have been recalculated eliminating the two runs with the highest values of r . Thus, for r less than 1.1,

$$\log \frac{k_1}{k_{3a}^{1/2}} = 2.78 \pm 0.17 - \frac{8170 \pm 280}{2.303RT}$$

In order to determine the value for k_1 it is necessary to know the value of k_{3a} . The measured value reported in the literature (23,138)

$$k_{3a} = 10^{15.8} \text{ cc mole}^{-1} \text{ sec}^{-1}$$

appears to be too high and cannot be considered reliable. It is probably best to assume that n -propyl radicals recombine with the same rate as ethyl radicals and accept the value for the latter reported by Shepp and Kutschke (16)

$$\log k_{3a} = 14.2 - (2000 \pm 1000)/2.3RT$$

This would lead to

$$\log k_1 = 9.9 - \frac{9200}{2.3RT}$$

Combining these Arrhenius parameters with the equation for k_{1a} , the Arrhenius parameters of the reverse reaction are given by

$$\log k_{1a} = 10.3 - \frac{12700}{2.3RT}$$

Both the activation energy and the A factor determined here for n-propyl radicals are lower than those found in the case of methyl radicals reacting with propane (71,76).

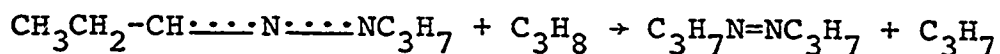
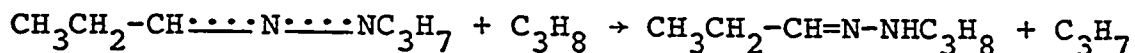
$$\log k_A = 11.87 - \frac{10200}{2.3RT}$$

DISCUSSION

1) Possible Consequences of the Mass Balance Defect:

The most obvious sources of uncertainty in the determination of k_1 are the processes treated collectively under Reactions 5 and 6 which are not directly monitored. These processes include addition and abstraction reactions with propylene and azo-n-propane and combination with the resulting radicals. The concentration of propylene should always be very small in the system, and, although small quantities of C_9H_{20} were detected among the products, it is doubtful if radical reactions with propylene are of great significance. On the other hand, alkyl radicals are known to react very readily with azo-alkanes under the conditions used in this study, and this is undoubtedly the dominant cause of their "disappearance" from the system. There are two plausible reactions involving the resonance stabilized azo-alkyl radical formed in the abstraction reaction which are not included in the kinetic treatment; the thermal

decomposition, and the abstractive attack on propane:



Studies of the formation of heavy products in the azoethane system led to the conclusion that neither decomposition nor abstraction could be very important under ordinary conditions. Although significant quantities of propanal propylhydrazone were formed in the azo-n-propane system, it must be remembered that the equilibrium constant for isomerization of azo-n-propane is larger than for isomerization of azoethane, and it is possible that much of the hydrazone arose from wall catalyzed reaction during the 36 hour runs. If a significant proportion of the propanal propylhydrazone was formed from hydrogen atom abstraction by the azo-alkyl radical, this could significantly influence the mechanism, since it would form predominantly iso-propyl radicals. On the other hand, if it resulted from disproportionation with propyl radicals, it would probably remove more iso-propyl than n-propyl radicals from the system. Of these possibilities, the one which could have the most serious effect on the results of this study is the abstraction of hydrogen from propane by the azo-alkyl radical. The effect of such a reaction would not be accounted for through the radical "disappearance ratio" q , because, in the system where q was determined, there was no large concentration of substrate present from which hydrogen atoms could be

abstracted. In a study of the pyrolysis of azo-n-propane, Geiseler and Hoffman (139) have concluded that although formation of azo-alkyl radicals is important, they do not act as chain carriers at temperatures less than 400°C, and it is reasonable to suppose that the activation energy for abstraction of hydrogen from propane by the azoalkyl radical must be higher than for its abstraction of hydrogen from azo-n-propane.

2) Conclusion:

Either the result reported here is correct, and the activation energy for abstraction by n-propyl radicals is actually lower than for abstraction by methyl radicals, or else the system is being influenced by some process which has not been accounted for in the kinetic treatment. If there were an activation energy for n-propyl radical combination larger than the 2 kcal/mole found for ethyl radicals by Shepp and Kutschke (16), then this might be sufficient to account for the result. The studies of isopropyl and t-butyl radical combination rate constants reported by Metcalfe and Trotman-Dickenson (14,15) indicate no activation energy at all. However, measurements of radical combination rates by intermittent illumination techniques are tedious to perform, and temperature studies typically take the form of a few (usually 3) careful determinations at different temperatures. The possibility of an activation energy for radical combination cannot be

ruled out by such results, but it is clear that any activation energy must be no larger than a few kcal/mole. It would be of great benefit if more precise information were available on the rates of higher alkyl radical combination reactions. Information on the kinetic parameters for the reactions of azo-alkyl radicals would also be very useful in assessing the potential effect of their reactions on the system.

Campbell and co-workers (140) have conducted a temperature study of the mercury photosensitized decomposition of propane, and they have found that the Arrhenius parameters determined for Reaction 1 in this study appear to predict reasonable values for the rate constants in their system. However, this is not a rigorous test of the validity of the results reported here.

CHAPTER V

THE REACTIONS OF HIGHER ALKYL RADICALS WITH SILANE AND DISILANE

RESULTS

- 1) Reaction of Methyl Radicals with Monosilane.
- 2) Reaction of Ethyl Radicals with Silane, Silane-d₄, Disilane, and Disilane-d₆.
- 3) Reaction of n-Propyl and iso-Propyl Radicals with Silane.
- 4) Determination of Relative Rates of Abstraction from Silane, Silane-d₄, Disilane, and Disilane-d₆ by n-Propyl and iso-Propyl Radicals.
- 5) Calculations.

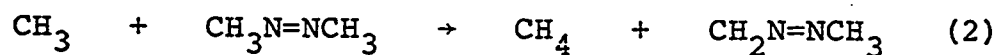
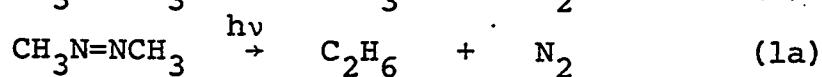
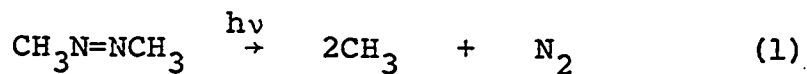
DISCUSSION

- 1) Comparison of Arrhenius Parameters for Alkyl Radicals Reacting with Silanes and with Hydrocarbons.
- 2) Possible Reasons for the Lack of a Definite Trend in Activation Energies for a Series of Alkyl Radicals Reacting with Silane.
- 3) Kinetic Isotope Effect.
- 4) BEBO Calculations.

RESULTS

1) Reaction of Methyl Radicals with Monosilane:

The photolysis of azomethane proceeds via the following sequence:



The quantum yield of nitrogen in Reaction 1 is unity, and that of ethane in Reaction 1a (54-57) is 0.007. Allowance has been made for this in determining the ethane produced in Reaction 3. A temperature study of Reaction 2 has been carried out using the relation

$$\frac{k_2}{k_3^{1/2}} = \frac{R_{\text{CH}_4}}{[\text{Azo}]R_3^{1/2}}$$

The Arrhenius equation was found to be

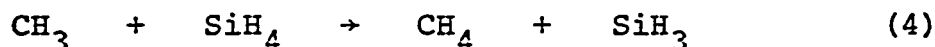
$$\log \frac{k_2}{k_3^{1/2}} = 4.49 \pm 0.25 - \frac{8050 \pm 440}{2.303RT}$$

The Arrhenius parameters are in reasonable agreement with the values

$$\log \frac{k_2}{k_3^{1/2}} = 4.2 - \frac{7800}{2.303RT}$$

found by Kerr and co-workers (60). They also agree satisfactorily with a number of previous determinations (61-63), and they have been adopted here for use in further work with methyl radicals. The data for this determination are summarized in Table XV and the Arrhenius plot is given in Figure 14.

When methyl radicals are produced in the presence of monosilane, they react by abstraction of a hydrogen atom.



A temperature study of Reaction 4 was performed, and rate constants were determined from the expression

$$\frac{k_4}{k_3^{1/2}} = \frac{R_{\text{CH}_4} - R_2}{[\text{SiH}_4]R_3^{1/2}}$$

where R_2 was calculated using the equation

$$R_2 = \frac{k_2}{k_3^{1/2}} R_3^{1/2} [\text{Azo}]$$

Least squares treatment of the data gave the Arrhenius equation

$$\log \frac{k_4}{k_3^{1/2}} = 4.49 \pm 0.17 - \frac{7470 \pm 290}{2.303RT}$$

Table XV
 Reaction of Methyl Radicals with Azomethane

Temp (°C)	Time (min)	[Azo] $\times 10^6$ mole/cc	Rate $\times 10^{12}$ mole/cc s			$\frac{k_2}{k_3^{1/2}}$	
			N ₂	CH ₄ R ₂	C ₂ H ₆ (total)		
25.0	7.00	6.970	156.11	3.62	138.18	137.13	0.04435
61.0	7.30	4.312	108.09	6.07	81.50	80.78	0.1566
89.0	7.10	3.735	99.84	10.85	56.90	56.16	0.3876
124.0	7.10	3.485	101.18	21.54	31.50	30.75	1.115
151.0	7.00	3.517	102.62	29.38	16.73	15.97	2.090
178.0	7.00	1.862	62.84	19.44	7.23	6.78	4.010
218.0	7.00	1.568	57.71	25.62	3.77	3.32	8.967

Cell volume 186.5 cc. Illuminated volume 158 cc.

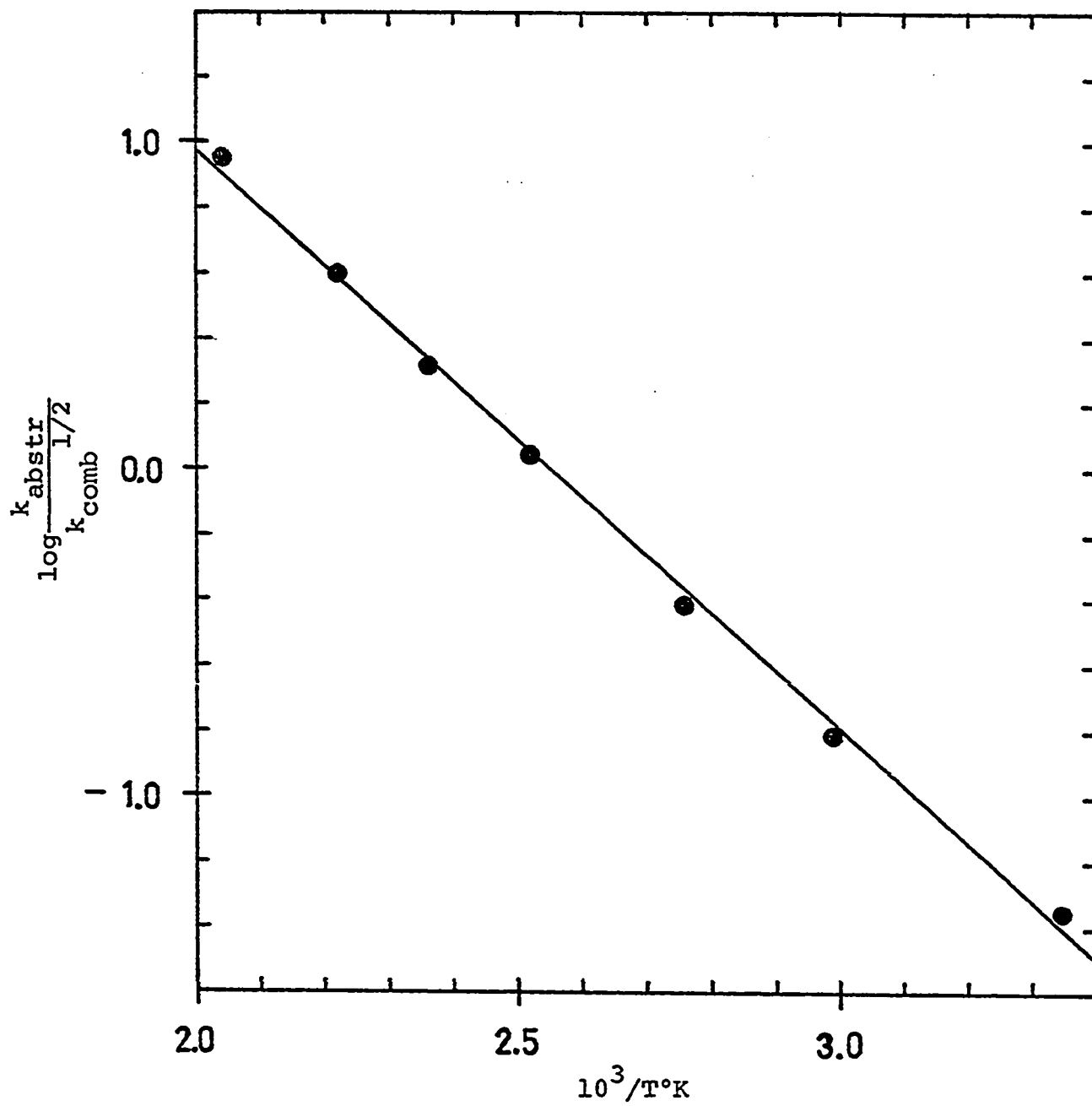


Figure 14. Arrhenius plot for reaction of methyl radicals with azomethane.

This is in reasonable agreement with the equations

$$\log \frac{k_4}{k_3^{1/2}} = 5.13 - \frac{6990}{2.303RT} \quad (115)$$

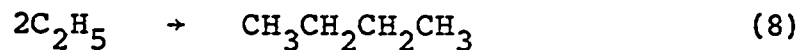
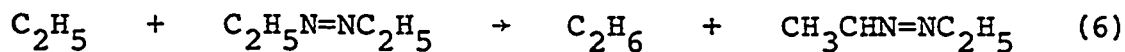
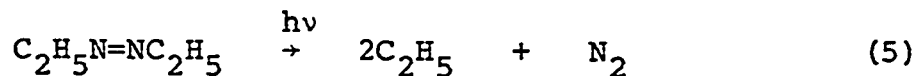
and

$$\log \frac{k_4}{k_3^{1/2}} = 5.15 - \frac{6890}{2.303RT} \quad (118)$$

reported previously. The rate constant data for Reaction 4 are given in Table XVI, and the Arrhenius plot is shown in Figure 15.

2) Reaction of Ethyl Radicals with Silane, Silane-d₄,
Disilane, and Disilane-d₆:

The photolysis of azoethane proceeds via the sequence (45,64):



A temperature study of Reaction 6 was carried out. The ratio of disproportionation to combination of ethyl radicals (23) was taken to be 0.14, and rate constants were determined using the relationship

$$\frac{k_6}{k_8^{1/2}} = \frac{R_{\text{C}_2\text{H}_6} - 0.14R_8}{[\text{Azo}]R_8^{1/2}}$$

Table XVI
Reaction of Methyl Radicals with Silane

Temp (°C)	Time (min)	[Azo] $\times 10^6$ mole/cc	[SiH ₄]	Rate $\times 10^{12}$ mole/cc s						$\frac{k_4}{k_3^{1/2}}$
				N ₂	CH ₄ (total)	CH ₄ R ₂	CH ₄ R ₄	C ₂ H ₆ (total)	C ₂ H ₆ R ₃	
113.0	5.10	2.016	0.307	40.17	24.34	1.90	22.44	8.85	8.51	25.06
148.0	5.00	1.849	0.269	39.58	27.60	2.68	24.92	3.82	3.47	49.73
137.0	5.00	1.895	0.320	40.62	28.47	2.20	26.27	4.17	3.82	42.00
127.0	6.00	1.858	0.375	38.05	27.34	1.81	25.53	4.63	4.34	32.68
101.0	6.00	1.867	0.536	36.31	24.45	1.34	23.11	7.96	7.67	15.57
91.0	6.00	1.895	0.412	38.77	18.81	1.18	17.63	13.02	12.73	11.99
74.0	7.00	1.756	0.428	35.22	14.14	0.73	13.41	16.00	15.75	7.895
28.0	10.00	1.375	0.670	22.66	3.99	0.11	3.88	17.01	16.84	1.411
45.0	10.00	1.459	0.501	28.04	6.86	0.24	6.62	18.49	18.32	3.087
62.0	10.00	1.607	0.481	27.78	10.16	0.44	9.72	15.10	14.93	5.230

Cell volume 218 cc. Illuminated volume 192 cc.

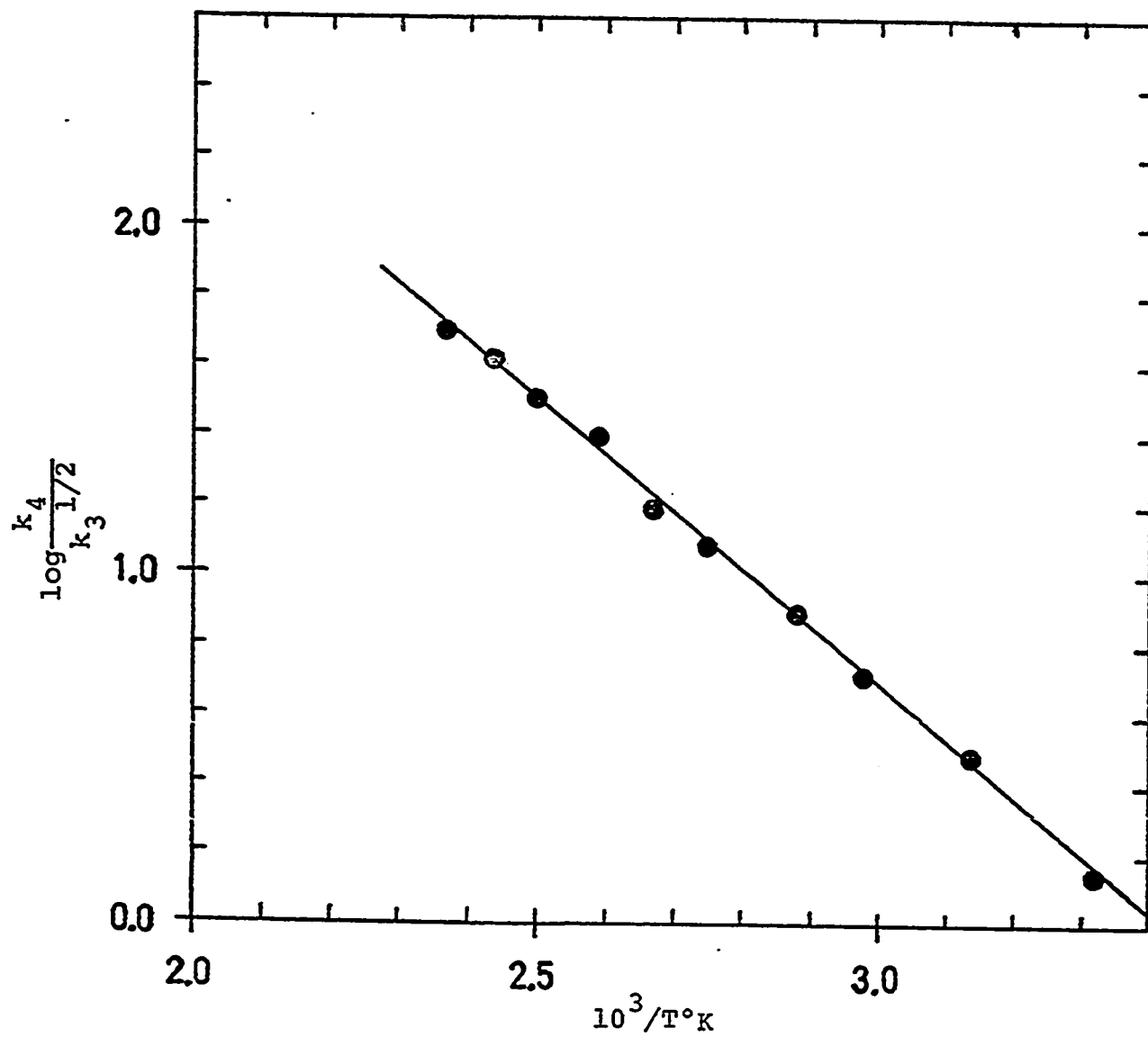


Figure 15. Arrhenius plot for reaction of methyl radicals with silane.

The Arrhenius equation

$$\log \frac{k_6}{k_8^{1/2}} = 4.87 \pm 0.35 - \frac{8570 \pm 590}{2.303RT}$$

was found. This is in fair agreement with the equations

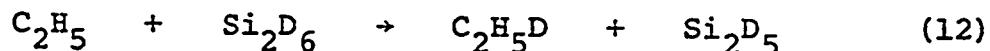
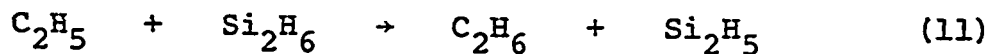
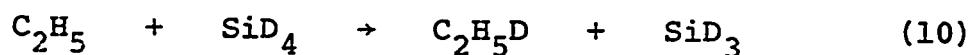
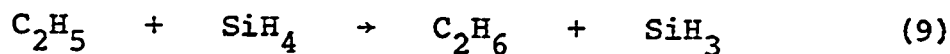
$$\log \frac{k_6}{k_8^{1/2}} = 4.6 - \frac{8000}{2.303RT} \quad (45)$$

and

$$\log \frac{k_6}{k_8^{1/2}} = 4.2 - \frac{7500}{2.303RT} \quad (64)$$

which have been reported previously. The data are given in Table XVII, and the Arrhenius plot is shown in Figure 16.

When a silane compound is present, the ethyl radicals react by abstracting a hydrogen atom.



Rate constants for these reactions were determined using the expression

$$\frac{k_x}{k_8^{1/2}} = \frac{R_{\text{C}_2\text{H}_6} - 0.14R_8 - R_6}{[\text{silane}]R_8^{1/2}}$$

Temperature studies of the reaction of ethyl radicals with

Table XVII
Reaction of Ethyl Radicals with Azoethane

Temp (°C)	Time (min)	[Azo] $\times 10^6$ mole/cc	Rate $\times 10^{12}$ mole/cc s					$\frac{k_6}{k_8^{1/2}}$
			N ₂	Ethane (total)	C ₂ H ₆ R ₇	C ₂ H ₆ R ₆	C ₄ H ₁₀ R ₈	
92.0	15.00	3.630	47.74	14.12	3.76	10.36	26.85	0.5508
120.0	15.00	2.190	38.31	12.79	2.03	10.76	14.53	1.289
149.0	15.00	1.900	34.66	17.25	1.44	15.81	10.30	2.593
135.0	15.00	1.940	37.27	16.55	2.23	14.32	15.91	1.851
104.0	15.00	2.760	41.15	13.43	3.15	10.28	22.51	0.7851
78.0	15.00	3.260	42.71	10.07	4.17	5.90	29.80	0.3315
60.0	15.00	3.410	42.19	8.22	4.17	4.05	29.80	0.2176
26.0	15.00	3.830	42.59	5.79	4.97	0.82	35.53	0.03592

Cell volume 218 cc. Illuminated volume 192 cc.

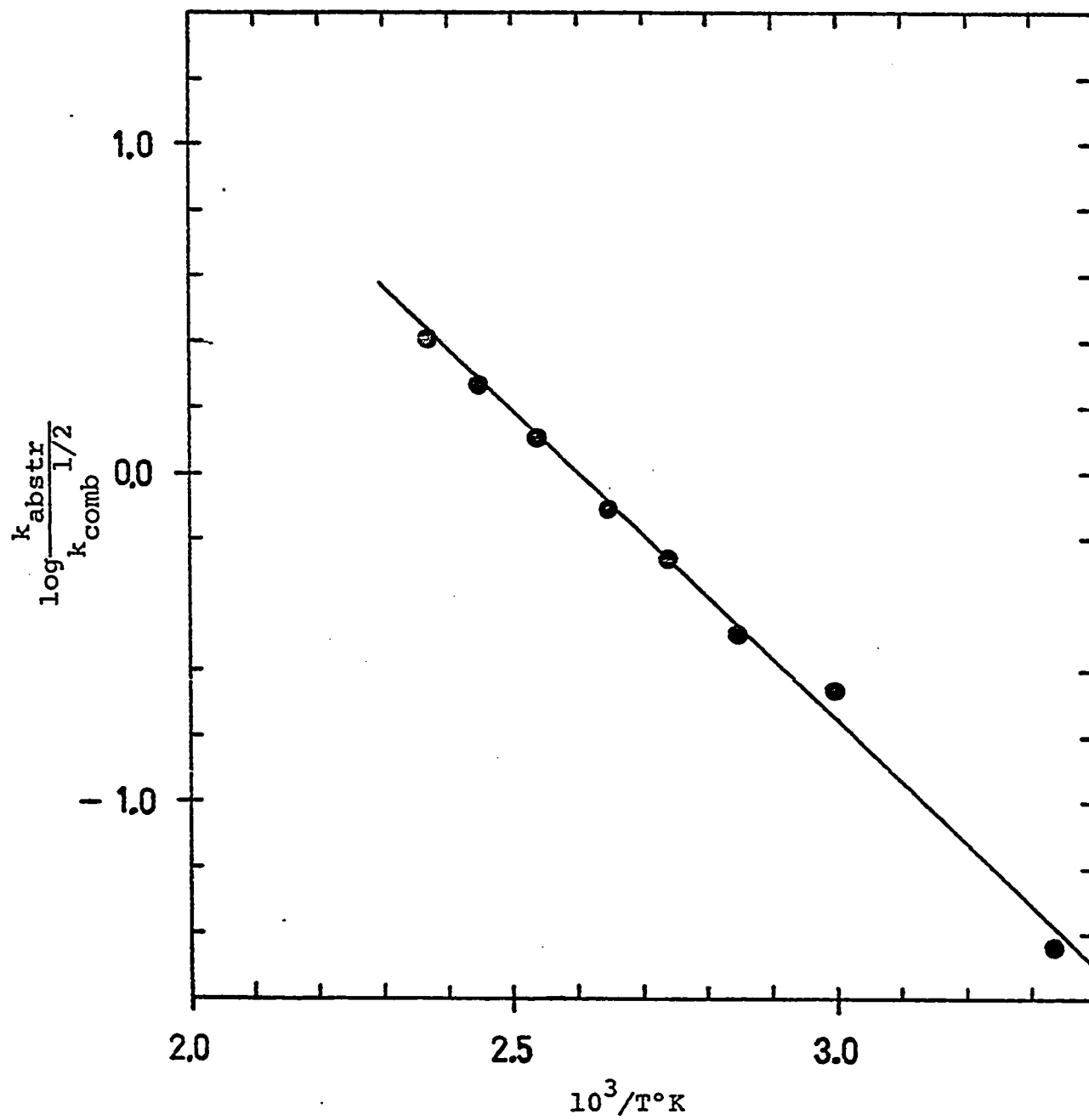


Figure 16. Arrhenius plot for reaction of ethyl radicals with azoethane.

each of the silane compounds gave the following Arrhenius equations:

$$\log \frac{k_9}{k_8^{1/2}} = 5.06 \pm 0.23 - \frac{7250 \pm 380}{2.303RT}$$

$$\log \frac{k_{10}}{k_8^{1/2}} = 5.20 \pm 0.35 - \frac{8350 \pm 670}{2.303RT}$$

$$\log \frac{k_{11}}{k_8^{1/2}} = 5.08 \pm 0.28 - \frac{5650 \pm 450}{2.303RT}$$

$$\log \frac{k_{12}}{k_8^{1/2}} = 5.36 \pm 0.16 - \frac{6840 \pm 270}{2.303RT}$$

The data for ethyl radical reactions with silane and silane-d₄ are given in Table XVIII, and the data for the reactions with disilane and disilane-d₆ are given in Table XIX. The Arrhenius plots are shown in Figure 17.

3) Reaction of n-Propyl and iso-Propyl Radicals with Silane:

Rate constants as a function of temperature for reaction of n-propyl and iso-propyl radicals with silane were determined relative to the recombination of these radicals:

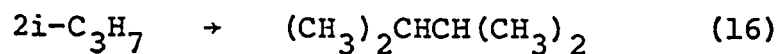
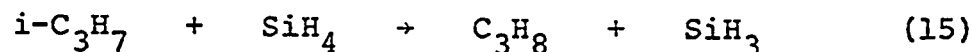
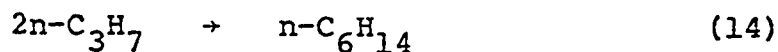
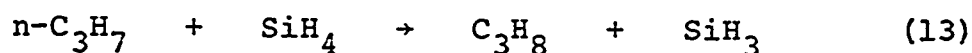


Table XVIII
Reaction of Ethyl Radicals with Silane

Temp (°C)	Time (min)	[Azo] $\times 10^6$ mole/cc	[SiH ₄]	N ₂	Ethane (total)	C ₂ H ₆ R ₆	C ₂ H ₆ R ₇	C ₂ H ₆ R ₉	C ₄ H ₁₀ R ₈	$\frac{k_9}{k_8^{1/2}}$
45.0	10.00	1.997	0.578	55.21	11.72	1.27	6.06	4.39	43.32	1.154
63.0	10.00	1.812	0.496	15.10	5.38	0.96	1.07	3.35	7.64	2.444
76.0	10.00	1.784	0.472	56.86	17.97	3.40	4.86	9.71	34.72	3.491
89.0	10.00	1.942	0.706	58.86	25.87	5.17	3.99	16.71	28.47	4.436
120.0	10.00	1.468	0.506	57.03	35.85	8.53	2.84	24.48	20.31	10.74
149.0	10.00	1.793	0.554	68.32	57.82	16.82	1.70	39.30	12.15	20.35
180.0	10.50	1.997	0.692	90.36	91.10	26.60	0.87	63.63	6.20	36.93
103.0	10.00	1.774	0.589	63.72	35.51	7.33	4.07	24.11	29.08	7.591
92.0	10.00	2.025	1.031	61.37	19.27	6.27	4.55	8.45	32.47	1.438

[SiD₄]
C₂H₅D
R₁₀
 $\frac{k_{10}}{k_8^{1/2}}$

Table XVIII (continued)

Temp (°C)	Time (min)	[Azo] x10 ⁶ mole/cc	[SiD ₄]	Rate x10 ¹² mole/cc s					$\frac{k_{10}}{k_8^{1/2}}$	
				N ₂	Ethane (total) C ₂ H ₆ R ₆	C ₂ H ₆ R ₇	C ₂ H ₅ D R ₁₀	C ₄ H ₁₀ R ₈		
123.0	10.00	1.375	1.096	52.87	31.51	8.56	2.75	20.20	19.62	4.161
148.0	10.00	1.022	1.189	48.70	37.07	8.86	1.46	26.75	10.42	6.970
179.0	10.00	1.031	1.189	54.60	54.60	12.13	0.68	41.79	4.86	15.94
212.0	10.00	0.640	1.022	40.28	47.70	8.64	0.24	38.82	1.74	28.80
105.0	15.00	0.546	1.096	25.69	12.27	1.50	1.51	9.26	10.82	2.569
232.0	10.00	0.598	0.807	44.10	49.05	11.39	0.24	37.42	1.74	35.15

Cell volume 218 cc. Illuminated volume 192 cc.

Table XIX

Reaction of Ethyl Radicals with Disilane

Temp (°C)	Time (min)	[Azo] x10 ⁶ mole/cc	[Si ₂ H ₆]	Rate x10 ¹² mole/cc s						$\frac{k_{11}}{k_8^{1/2}}$
				N ₂	Ethane (total)	C ₂ H ₆ R ₆	C ₂ H ₆ R ₇	C ₂ H ₆ R ₁₁	C ₄ H ₁₀ R ₈	
24.0	10.00	1.096	0.855	40.02	27.26	0.14	1.82	25.30	13.02	8.201
46.0	10.00	1.031	0.746	33.86	31.25	0.27	0.94	30.04	6.68	15.58
60.0	10.00	1.013	0.406	34.55	31.25	0.54	1.26	29.45	9.03	24.14
75.0	10.00	1.161	0.676	41.50	52.43	0.69	0.51	51.23	3.65	39.67
90.0	10.00	1.115	0.546	41.58	51.48	1.07	0.47	49.94	3.39	49.68
106.0	10.00	0.743	0.647	31.69	43.23	0.71	0.18	42.34	1.30	57.40
122.0	10.00	1.050	0.780	45.14	68.06	1.44	0.15	66.47	1.04	83.56
137.0	10.00	1.096	0.657	59.20	89.15	2.30	0.16	86.69	1.13	124.1
152.0	10.00	1.078	0.655	48.35	85.77	2.62	0.10	83.05	0.69	152.6
24.0	10.00	1.210	0.945	36.55	13.80	0.21	3.18	10.41	22.74	2.310

 $\frac{k_{12}}{k_8^{1/2}}$
 $\frac{C_2H_5D}{R_{12}}$

Table XIX (continued)

Temp (°C)	Time (min)	[Azo] x10 ⁶ mole/cc	[Si ₂ D ₆]	Rate x10 ¹² mole/cc s							$\frac{k_{12}}{k_8^{1/2}}$
				N ₂	Ethane (total)	C ₂ H ₆ R ₆	C ₂ H ₆ R ₇	C ₂ H ₅ D R ₁₂	C ₄ H ₁₀ R ₈		
48.0	10.00	1.031	1.059	34.98	22.05	0.45	2.20	19.40	15.71	4.622	
64.0	10.00	1.152	1.013	42.02	34.90	0.86	1.94	32.10	13.89	8.502	
84.0	10.00	1.087	1.003	39.50	42.28	1.24	0.98	40.06	7.03	15.06	
105.0	10.50	1.078	0.929	39.60	52.50	1.78	0.54	50.18	3.89	27.39	
130.0	10.00	1.106	1.068	44.97	63.46	2.31	0.22	60.93	1.56	45.68	
154.0	10.00	1.115	0.676	43.41	60.68	4.02	0.19	56.47	1.39	70.85	
180.0	10.00	1.078	0.535	45.84	83.68	7.04	0.21	76.43	1.48	117.4	

Cell volume 218 cc. Illuminated volume 192 cc.

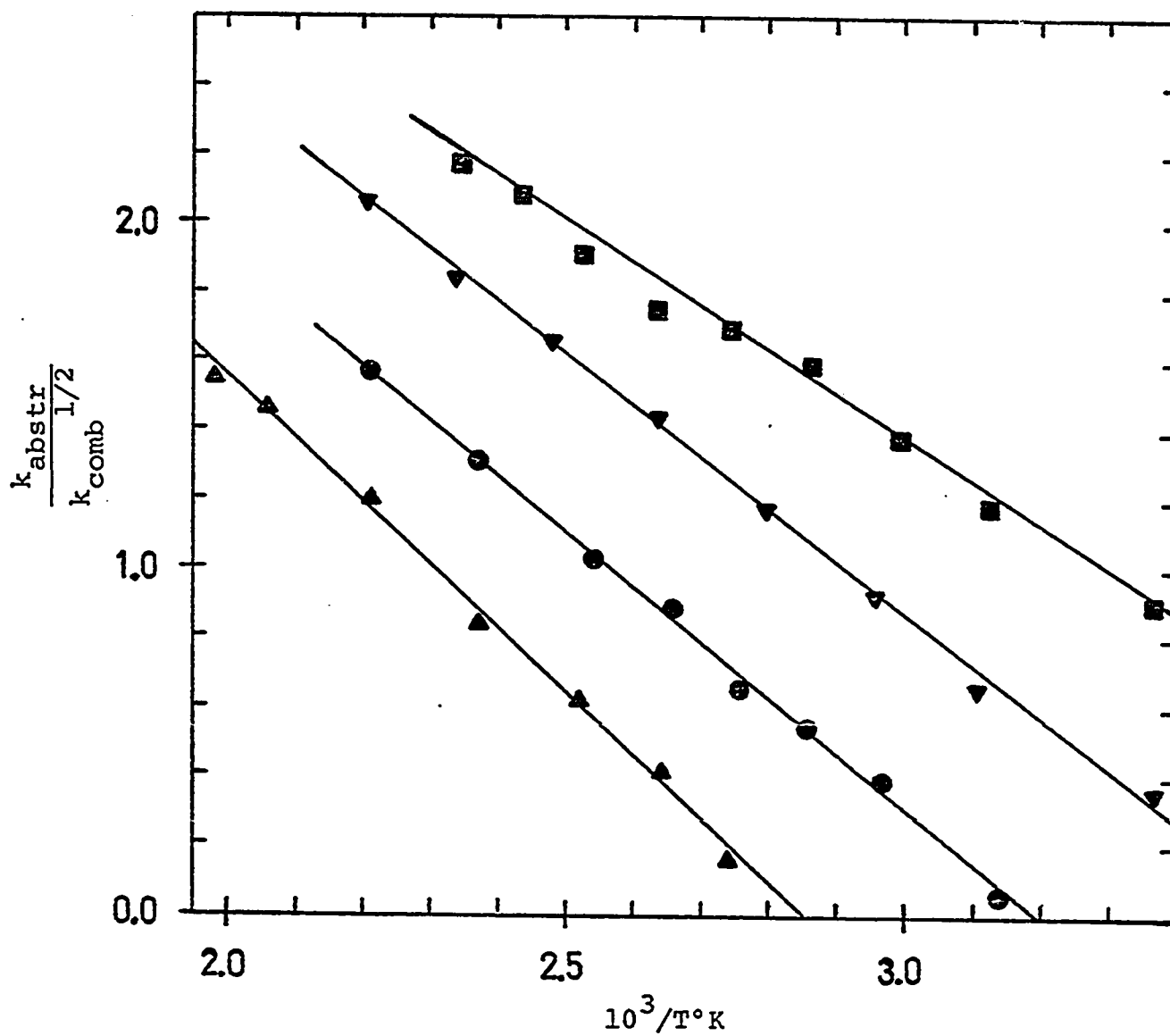


Figure 17. Arrhenius plots for reaction of ethyl radicals with silane ●, silane-d₄ ▲, disilane ■, and disilane-d₆ ▼.

The following Arrhenius equations were derived:

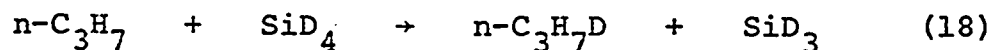
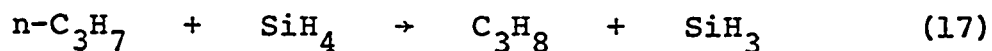
$$\log \frac{k_{13}}{k_{14}^{1/2}} = 4.85 \pm 0.21 - \frac{6910 \pm 340}{2.303RT}$$

$$\log \frac{k_{15}}{k_{16}^{1/2}} = 5.17 \pm 0.21 - \frac{7640 \pm 330}{2.303RT}$$

The data for reactions of propyl radicals with silane are given in Table XX and the Arrhenius plots are shown in Figure 18.

4) Determination of Relative Rates of Abstraction from Silane, Silane-d₄, Disilane, and Disilane-d₆ by n-Propyl and iso-Propyl Radicals:

When n-propyl radicals are produced in the presence of a mixture of large quantities of silane and silane-d₄ at elevated temperatures, so that they react exclusively by abstraction from silane compounds, the relative rates of reaction with deuterated and light silane may be determined by measuring the relative amounts of deuterated and light propane which are produced.



The rate constant ratio is given by the equation

$$\frac{k_D}{k_H} = \frac{R_D[H]}{R_H[D]}$$

Table XX

Reaction of Propyl Radicals with Silane

Temp (°C)	Time (min)	[Azo] x10 ⁶ mole/cc	[SiH ₄]	Rate x10 ¹² mole/cc s						$\frac{k_{13}}{k_{14}^{1/2}}$
				N ₂	Propane (total)	C ₃ H ₈ (Abstr. from azo)	C ₃ H ₈ (Disp.)	C ₃ H ₈	C ₆ H ₁₄ R ₁₃ R ₁₄	
90.0	165.00	0.466	2.930	5.11	6.05	0.18	0.03	5.84	0.20	4.457
119.0	160.00	0.284	1.280	4.81	5.97	0.25	0.03	5.69	0.19	10.20
149.0	160.00	0.285	0.514	5.47	6.08	0.63	0.04	5.41	0.29	19.54
63.0	160.00	0.392	3.560	4.05	4.76	0.09	0.04	4.63	0.26	2.551
76.0	160.00	0.420	2.290	4.53	4.98	0.15	0.06	4.77	0.41	3.253
42.0	80.00	0.519	2.330	4.24	3.23	0.09	0.16	2.98	1.18	1.177
107.0	60.00	0.403	0.853	5.99	6.08	0.49	0.11	5.48	0.72	7.571
128.0	94.00	0.363	1.340	4.85	6.65	0.37	0.03	6.25	0.17	11.31
25.0	67.00	0.509	4.160	2.90	2.22	0.04	0.12	2.06	0.78	0.5607
52.0	62.00	0.434	4.350	3.40	3.89	0.05	0.04	3.80	0.27	1.681

(1) n-propyl Radicals

Table XX (continued)

Temp (°C)	Time (min)	[Azo] x10 ⁶ mole/cc	[SiH ₄]	Rate x10 ¹² mole/cc s						$\frac{k_{16}}{k_{15}}$
				N ₂	Propane (total)	C ₃ H ₈ (Abstr. from azo)	C ₃ H ₈ (Disp.)	C ₃ H ₈ R ₁₅	C ₆ H ₁₄ R ₁₆	
25.0	30.00	1.014	6.762	8.97	4.95	0.11	1.19	3.65	2.17	0.3664
90.0	51.20	1.072	3.454	15.31	13.14	0.61	0.48	12.05	0.88	3.719
118.0	40.00	0.595	1.537	10.20	9.29	0.53	0.30	8.46	0.54	7.490
149.0	42.05	0.559	0.961	10.79	11.50	0.78	0.19	10.53	0.35	18.52
132.0	40.00	0.540	1.041	9.70	9.09	0.67	0.31	8.11	0.56	10.41
105.0	40.00	0.724	1.820	11.00	10.16	0.58	0.44	9.14	0.80	5.615
78.0	40.00	0.739	3.707	10.29	8.90	0.28	0.43	8.19	0.78	2.502
61.0	40.00	0.656	3.279	8.48	6.42	0.19	0.72	5.51	1.30	1.474
43.0	40.00	0.630	3.454	7.27	4.73	0.11	0.92	3.70	1.67	0.8289

(2) Iso-propyl Radicals

Cell volume 218 cc. Illuminated volume 192 cc.

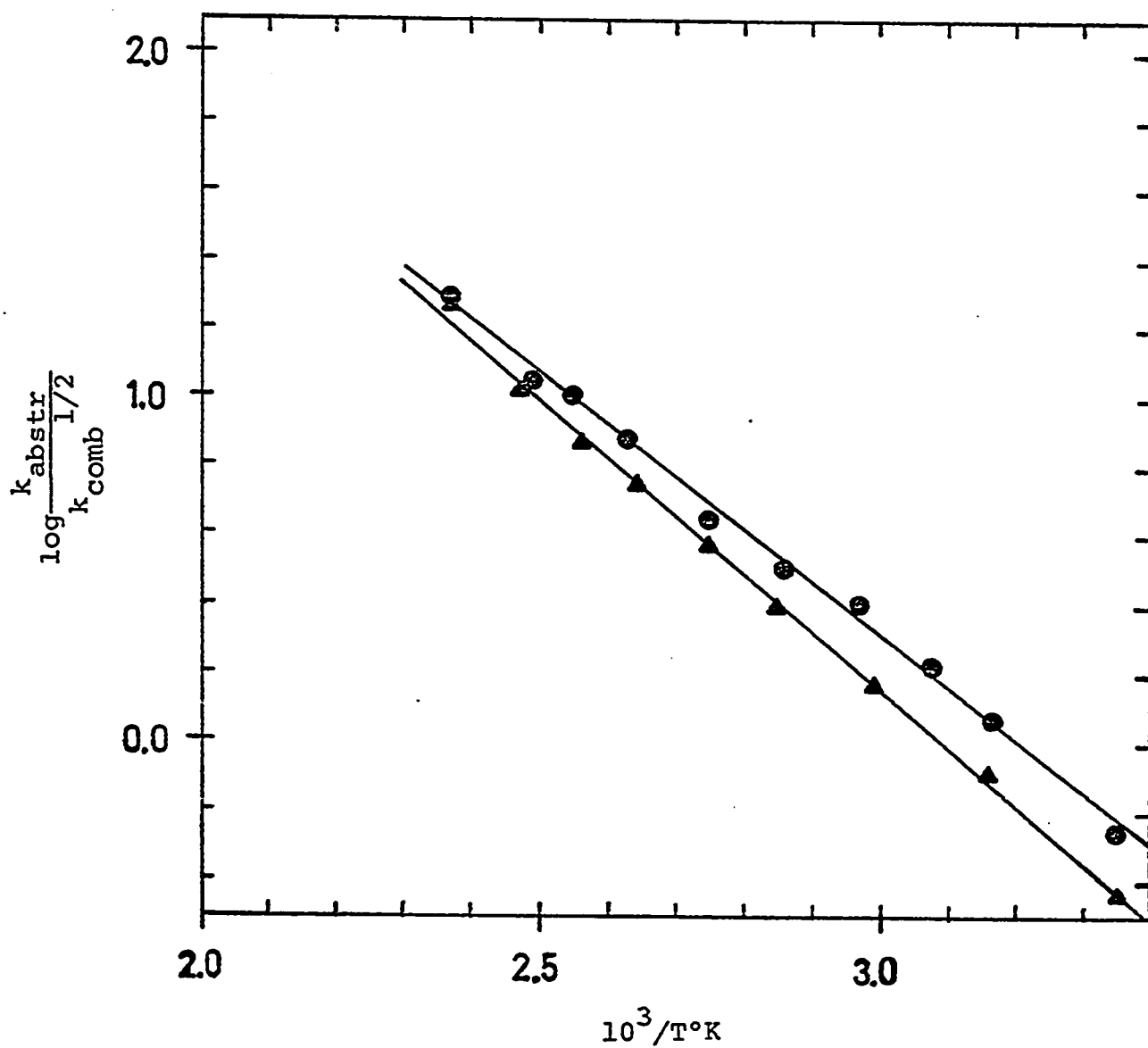
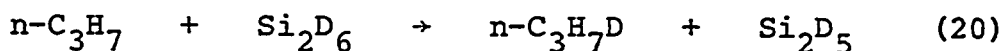
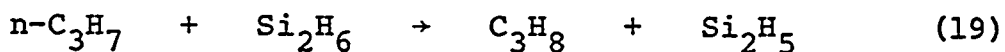
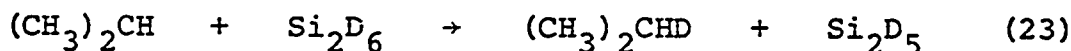
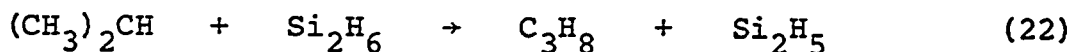
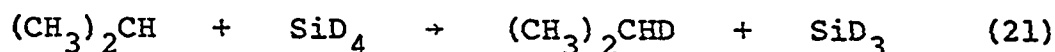
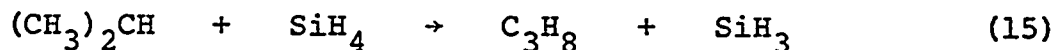


Figure 18. Arrhenius plots for reaction of n-propyl radicals ●, and iso-propyl radicals ▲, with silane.

In addition to the ratio of isotopic propanes produced, it is only necessary to know the pressures of deuterated and nondeuterated silane in the cell in order to evaluate the ratio k_D/k_H . Azo-bis-(n-propane-2,2-d₂) was used as the radical source, since propane which is deuterated on the second carbon atom has a very small n-1 peak in its mass spectrum, and determination of isotopic ratios is simplified. The ratios were also determined as a function of temperature for mixtures of silane with disilane-d₆ and disilane with disilane-d₆.



Relative rate constants for these reactions are listed in Table XXI. Similar determinations of relative rate constants were made for iso-propyl radicals, and the rate constants



are given in Table XXII. Arrhenius plots are shown in Figures 19 and 20. The Arrhenius parameters for n- and iso-propyl radicals are identical within experimental error, as shown in Table XXIII. The results of these determinations have been used to calculate Arrhenius parameters for reaction with the individual silanes, and these parameters

Table XXI
Relative Rates of Reaction of n-Propyl Radicals
with Deuterated and Nondeuterated Silanes

Temp (°C)	Time (min)	Azo	Pressure (torr)		Ratio D/H	$\frac{k_D}{k_H}$
			SiH ₄	SiD ₄		
			(1) Silane and Silane-d ₄			
120.0	250.00	7.6	51.9	150.9	0.7760	0.2669
135.0	181.00	7.6	54.6	162.3	0.8210	0.2762
170.0	210.00	6.2	49.8	152.8	1.0080	0.3285
152.0	142.00	7.0	41.4	160.6	1.2170	0.3137
191.0	150.00	7.9	58.7	165.4	0.9490	0.3368
213.0	131.00	6.5	61.3	150.2	0.8900	0.3632
107.0	200.00	7.0	32.2	175.5	1.3700	0.2514
89.0	173.00	7.7	44.1	159.4	0.8380	0.2318
			(2) Silane and Disilane-d ₆			
			SiH ₄	Si ₂ D ₆		
93.0	241.00	3.7	91.6	47.2	1.8410	3.5728

Table XXI (continued)

Temp (°C)	Time (min)	Azo	Pressure (torr) SiH ₄	Si ₂ D ₆	Ratio D/H	$\frac{k_D}{k_H}$
164.0	185.00	4.3	72.5	39.1	1.9670	3.6472
212.0	209.00	3.5	77.8	41.3	1.9240	3.6244
194.0	194.00	3.3	63.2	40.6	2.3900	3.7204
179.0	225.00	2.7	74.2	39.6	1.9590	3.6706
143.0	306.00	2.5	63.1	42.0	2.4840	3.7319
128.0	241.00	3.8	80.3	47.0	2.1550	3.6818
104.0	253.00	3.9	73.9	36.3	1.7620	3.5871
(3) Disilane and Disilane-d ₆						
			Si ₂ H ₆	Si ₂ D ₆		
130.0	250.00	9.5	49.7	147.4	1.1320	0.3817
149.0	153.00	8.2	57.7	149.9	1.0240	0.3942
168.0	226.00	7.7	50.8	150.0	1.2270	0.4155
189.0	202.00	8.1	52.6	149.9	1.3360	0.4688

Table XXI (continued)

Temp (°C)	Time (min)	Azo	Pressure (torr) Si ₂ H ₆	Si ₂ D ₆	Ratio D/H	$\frac{k_D}{k_H}$
208.0	325.00	8.0	48.3	145.9	1.4570	0.4823
89.0	300.00	6.8	52.8	152.4	0.9840	0.3409

Table XXII
 Relative Rates of Reaction of iso-Propyl Radicals
 with Deuterated and Nondeuterated Silanes

Temp (°C)	Time (min)	Azo	Pressure (torr)		SilD ₄	D/H	$\frac{k_D}{k_H}$
(1) Silane and Silane-d ₄							
209.0	170.00	7.4	106.3		302.6	1.0460	0.3674
191.0	236.00	7.6	106.4		300.2	0.9910	0.3512
150.0	120.00	8.1	106.2		304.0	0.9250	0.3231
131.0	277.00	4.8	102.3		303.1	0.8500	0.2869
112.0	244.00	5.8	102.5		306.6	0.7560	0.2527
90.0	336.00	4.3	102.5		299.6	0.7070	0.2419
172.0	452.00	6.7	105.8		301.8	0.8760	0.3071
(2) Silane and Disilane-d ₆							
			SiH ₄		Si ₂ D ₆		
90.0	132.00	5.2	137.8		68.2	1.7440	3.5238
111.0	334.00	6.9	153.2		59.4	1.4610	3.7681

Table XXII (continued)

Temp (°C)	Time (min)	Azo	Pressure (torr) SiH ₄	Si ₂ D ₆	D/H	$\frac{k_D}{k_H}$
131.0	188.00	7.1	152.4	59.2	1.5110	3.8898
151.0	189.00	8.1	199.9	51.9	0.9173	3.5331
211.0	300.00	7.8	202.6	48.6	0.8336	3.4750
191.0	140.00	11.1	198.7	50.5	0.9009	3.5447
231.0	136.00	7.5	202.1	49.4	0.8720	3.5674
171.0	181.00	7.6	200.8	52.2	0.9353	3.5979
(3) Disilane and Disilane-d ₆						
			Si ₂ H ₆	Si ₂ D ₆		
90.0	174.00	5.9	36.8	122.4	1.1400	0.3427
193.0	150.00	5.1	43.5	101.9	1.0380	0.4431
174.0	150.00	4.8	40.2	109.8	1.1580	0.4240
151.0	187.00	6.0	40.4	107.1	1.0590	0.3995
132.0	140.00	3.6	38.5	90.1	0.8832	0.3774

Table XXII (continued)

Temp (°C)	Time (min)	Azo	Pressure (torr) Si ₂ H ₆	Si ₂ D ₆	D/H	$\frac{k_D}{k_H}$
110.0	234.00	4.3	42.1	111.3	0.9553	0.3613
220.0	201.00	5.8	47.5	104.3	1.0520	0.4791

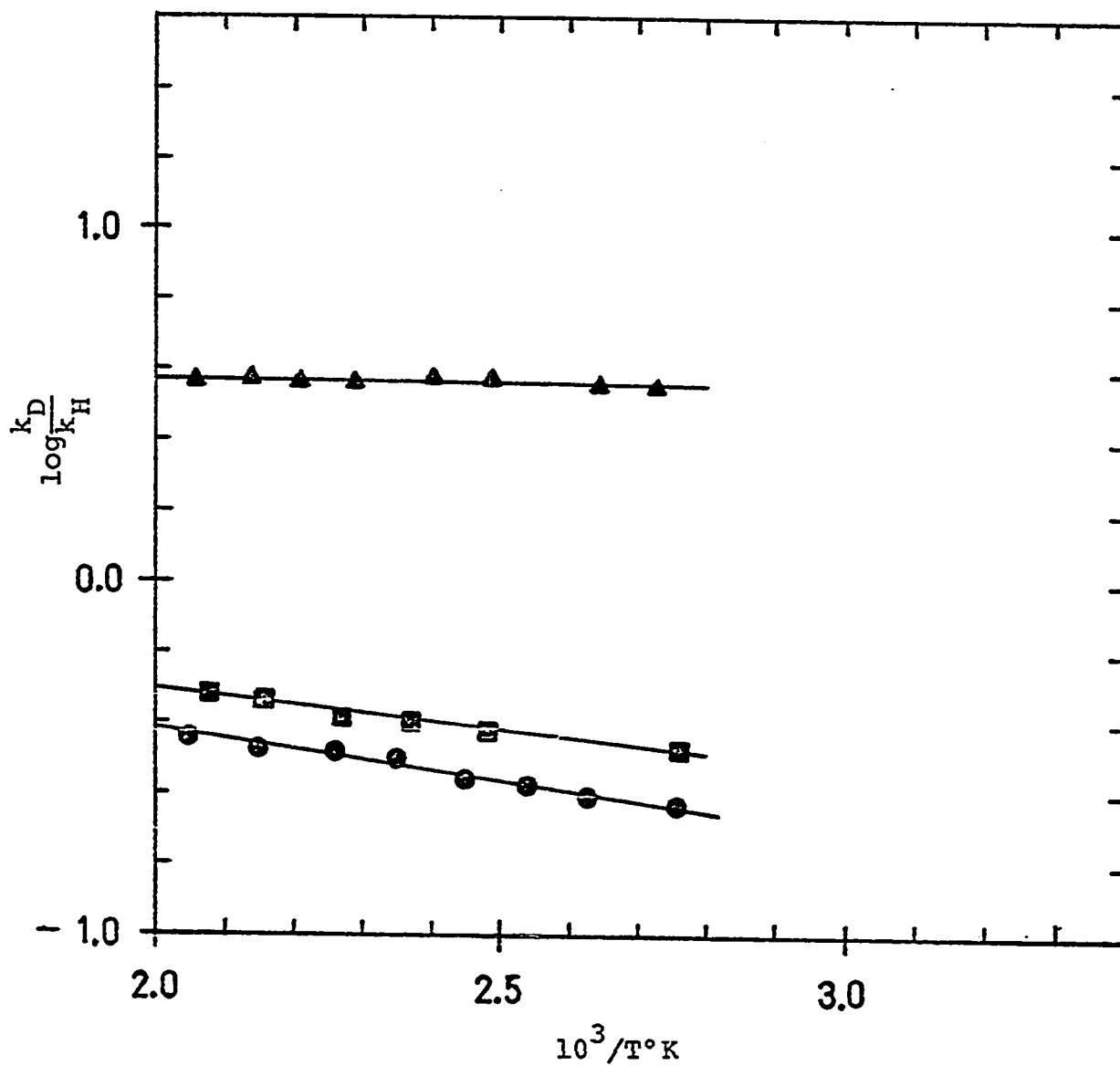


Figure 19. Arrhenius plots for relative rates of reaction of n-propyl-2,2-d₂ radicals with silane and silane-d₄ ●, silane and disilane-d₆ ▲, and disilane and disilane-d₆ ■.

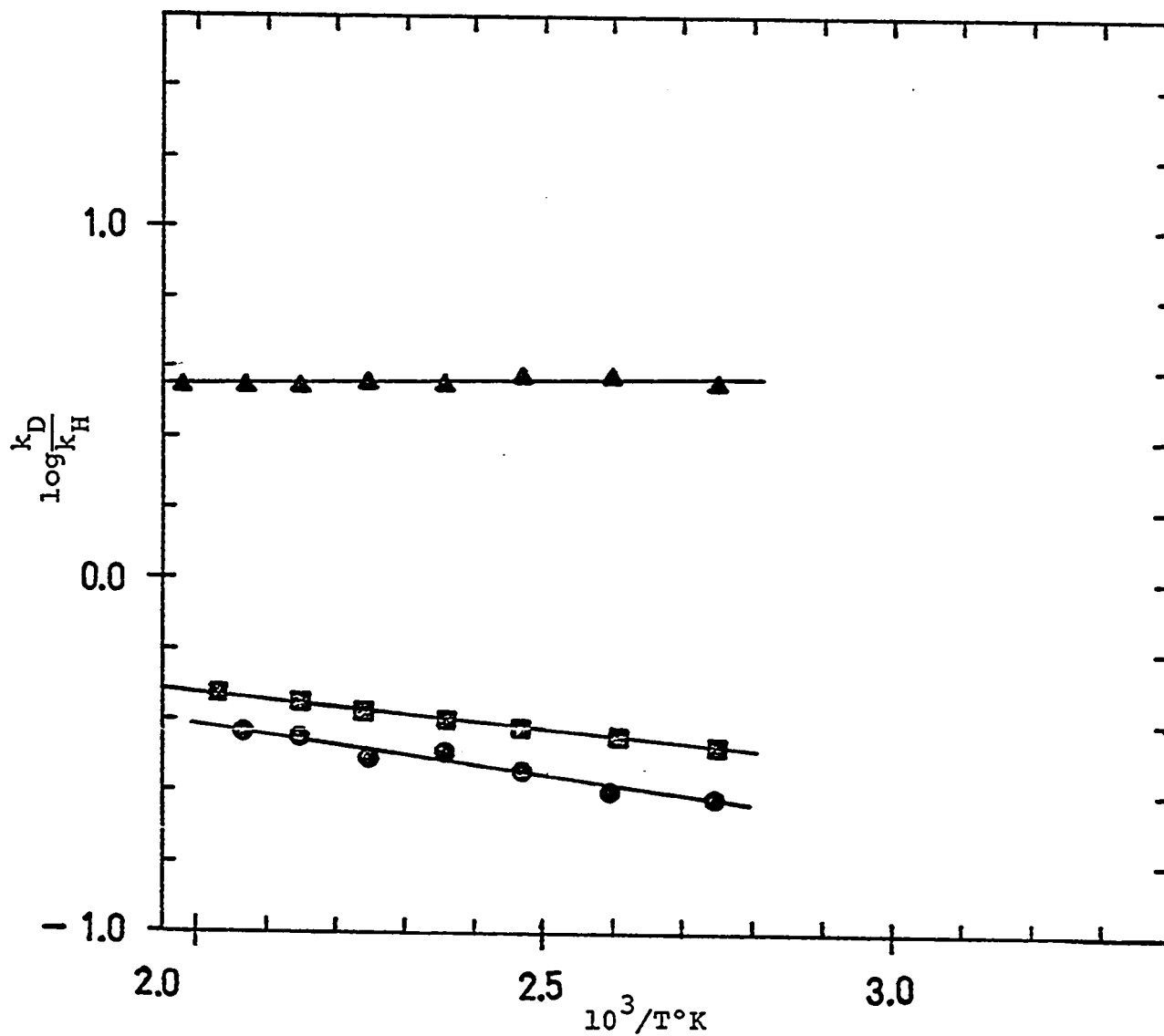


Figure 20. Arrhenius plots for relative rates of reaction of isopropyl radicals with silane and silane- d_4 ●, silane and disilane- d_6 ▲, and disilane and disilane- d_6 ■.

Table XXIII
 Arrhenius Parameters for Relative Rates of Reaction
 of Propyl Radicals with Silanes

Reaction	$\log \frac{A_D}{A_H}$	$E_D - E_H$ kcal/mole
$n\text{-C}_3\text{H}_7 + \text{SiH}_4 + \text{SiD}_4$	0.14 ± 0.09	1.29 ± 0.17
$n\text{-C}_3\text{H}_7 + \text{SiH}_4 + \text{Si}_2\text{D}_6$	0.60 ± 0.06	0.08 ± 0.11
$n\text{-C}_3\text{H}_7 + \text{Si}_2\text{H}_6 + \text{Si}_2\text{D}_6$	0.14 ± 0.17	1.03 ± 0.33
$\text{iso-C}_3\text{H}_7 + \text{SiH}_4 + \text{SiD}_4$	0.12 ± 0.20	1.24 ± 0.38
$\text{iso-C}_3\text{H}_7 + \text{SiH}_4 + \text{Si}_2\text{D}_6$	0.50 ± 0.13	-0.12 ± 0.26
$\text{iso-C}_3\text{H}_7 + \text{Si}_2\text{H}_6 + \text{Si}_2\text{D}_6$	0.07 ± 0.06	0.90 ± 0.12

Error limits are for 95% confidence level.

are listed in Table XXIV.

5) Calculations:

Experimental kinetic isotope effects over a temperature range from 300 to 500°K were calculated from the Arrhenius parameters obtained in this work. They are contrasted with the isotope effects obtained for methyl radicals reacting with silanes and with hydrocarbons in Figure 21 to 24. In addition, the kinetic isotope effects at room temperature are listed in Table XXV.

Potential energies of activation for the abstraction of hydrogen from monosilane by methyl, ethyl, n-propyl, and iso-propyl radicals have been calculated (Appendix B) by the Bond Energy Bond Order method of Johnston (121), using a three mass point model. Similar calculations were also performed for the reaction of methyl and ethyl radicals with methane. The parameters used in these calculations are given in Table XXVI, and the calculated potential energies of activation are listed in Table XXVII.

DISCUSSION

1) Comparison of Arrhenius Parameters for Alkyl Radicals
Reacting with Silanes and with Hydrocarbons:

The A factors for alkyl radical abstraction from the silanes all have similar values, and they are all about equal

Table XXIV
Arrhenius Parameters for Hydrogen
Abstraction Reactions of Alkyl Radicals

Reaction	$\log A^C$ $\frac{\text{cm}^3}{\text{mole sec}}$	E kcal/mole	Refer- ence
$\text{CH}_3 + \text{SiH}_4$	12.26 ± 0.17	7.47 ± 0.29	a
$\text{C}_2\text{H}_5 + \text{SiH}_4$	11.73 ± 0.23	7.25 ± 0.38	a
$\text{C}_2\text{H}_5 + \text{SiD}_4$	11.87 ± 0.35	8.35 ± 0.67	a
$\text{C}_2\text{H}_5 + \text{Si}_2\text{H}_6$	11.75 ± 0.28	5.65 ± 0.45	a
$\text{C}_2\text{H}_5 + \text{Si}_2\text{D}_6$	12.03 ± 0.16	6.84 ± 0.27	a
$n\text{-C}_3\text{H}_7 + \text{SiH}_4$	11.52 ± 0.21	6.91 ± 0.34	a
$n\text{-C}_3\text{H}_7 + \text{SiD}_4$	11.66 ± 0.30	8.20 ± 0.51	a, b
$n\text{-C}_3\text{H}_7 + \text{Si}_2\text{H}_6$	11.98 ± 0.44	5.96 ± 0.78	a, b
$n\text{-C}_3\text{H}_7 + \text{Si}_2\text{D}_6$	12.12 ± 0.27	6.98 ± 0.45	a, b
$\text{iso-C}_3\text{H}_7 + \text{SiH}_4$	11.84 ± 0.21	7.64 ± 0.33	a
$\text{iso-C}_3\text{H}_7 + \text{SiD}_4$	11.96 ± 0.41	8.88 ± 0.72	a, b
$\text{iso-C}_3\text{H}_7 + \text{Si}_2\text{H}_6$	12.27 ± 0.40	6.62 ± 0.71	a, b
$\text{iso-C}_3\text{H}_7 + \text{Si}_2\text{D}_6$	12.34 ± 0.34	7.52 ± 0.59	a, b
$\text{CH}_3 + \text{SiH}_4$	11.80	6.99	115
$\text{CH}_3 + \text{SiD}_4$	11.98	8.19	115
$\text{CH}_3 + \text{Si}_2\text{H}_6$	11.96	5.63	115
$\text{CH}_3 + \text{Si}_2\text{D}_6$	12.19	6.96	115
$\text{CH}_3 + \text{SiH}_4$	11.82	6.89	118
$\text{CH}_3 + \text{C}^{14}\text{H}_4$	11.83	14.65	141
$\text{CD}_3 + \text{C}^{14}\text{D}_4$	12.60	17.80	142

Table XXIV (continued)

Reaction	$\log A^c$ $\frac{\text{cm}^3}{\text{mole sec}}$	E kcal/mole	Refer- ence
$\text{CD}_3 + \text{C}_2\text{H}_6$	12.21	11.8	143
$\text{CD}_3 + \text{C}_2\text{D}_6$	12.21	13.3	143

Error limits are for 95% confidence level.

^a This work

^b Calculated from relative rate Arrhenius parameters.

^c Assuming (11) $\log(k_{\text{comb}}) = 13.34$ in all cases.

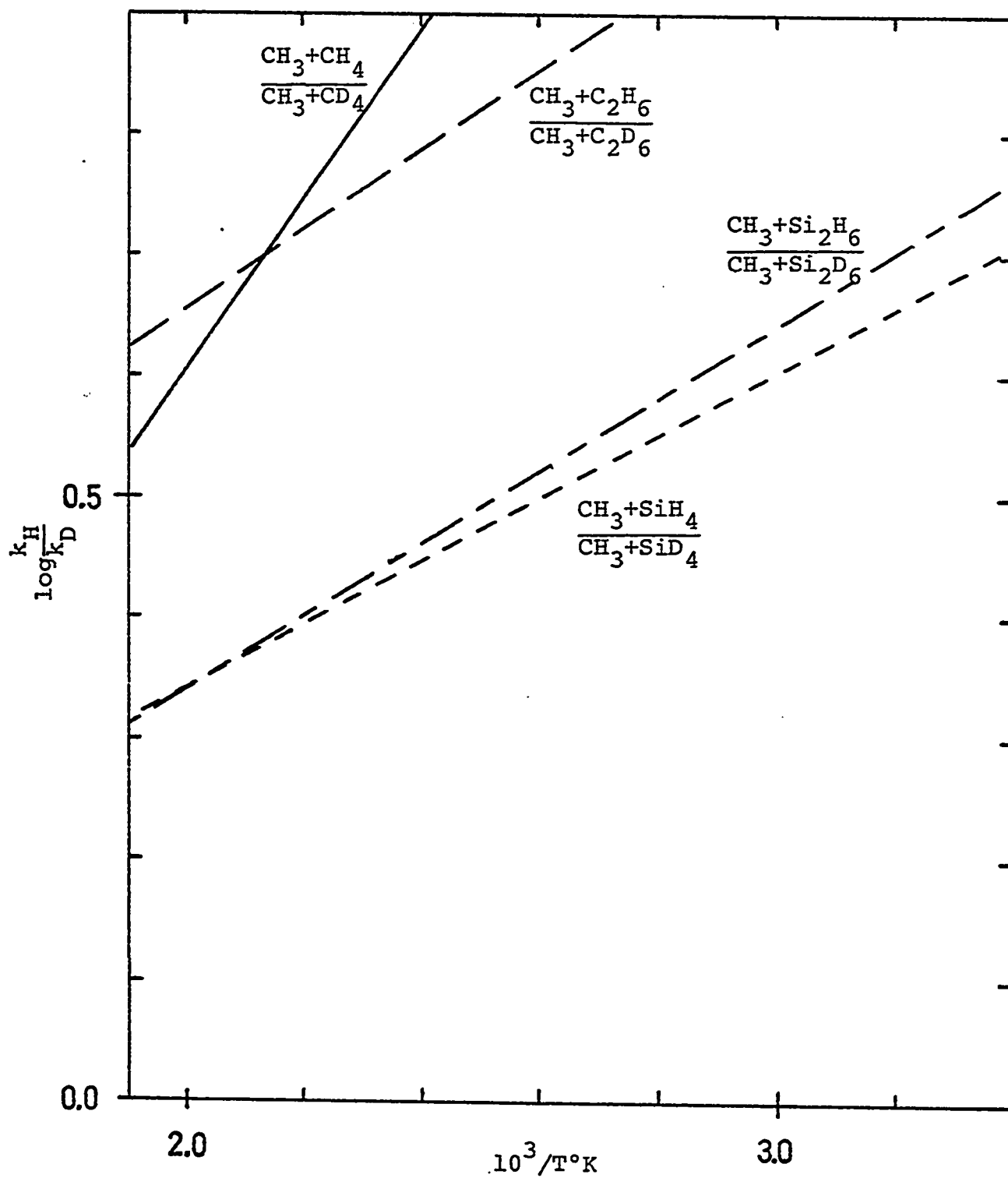


Figure 21. Kinetic isotope effect for methyl radicals reacting
 with: methane ——— (141,142) silane - - - (115)
 ethane — — — (143) disilane — - (115)

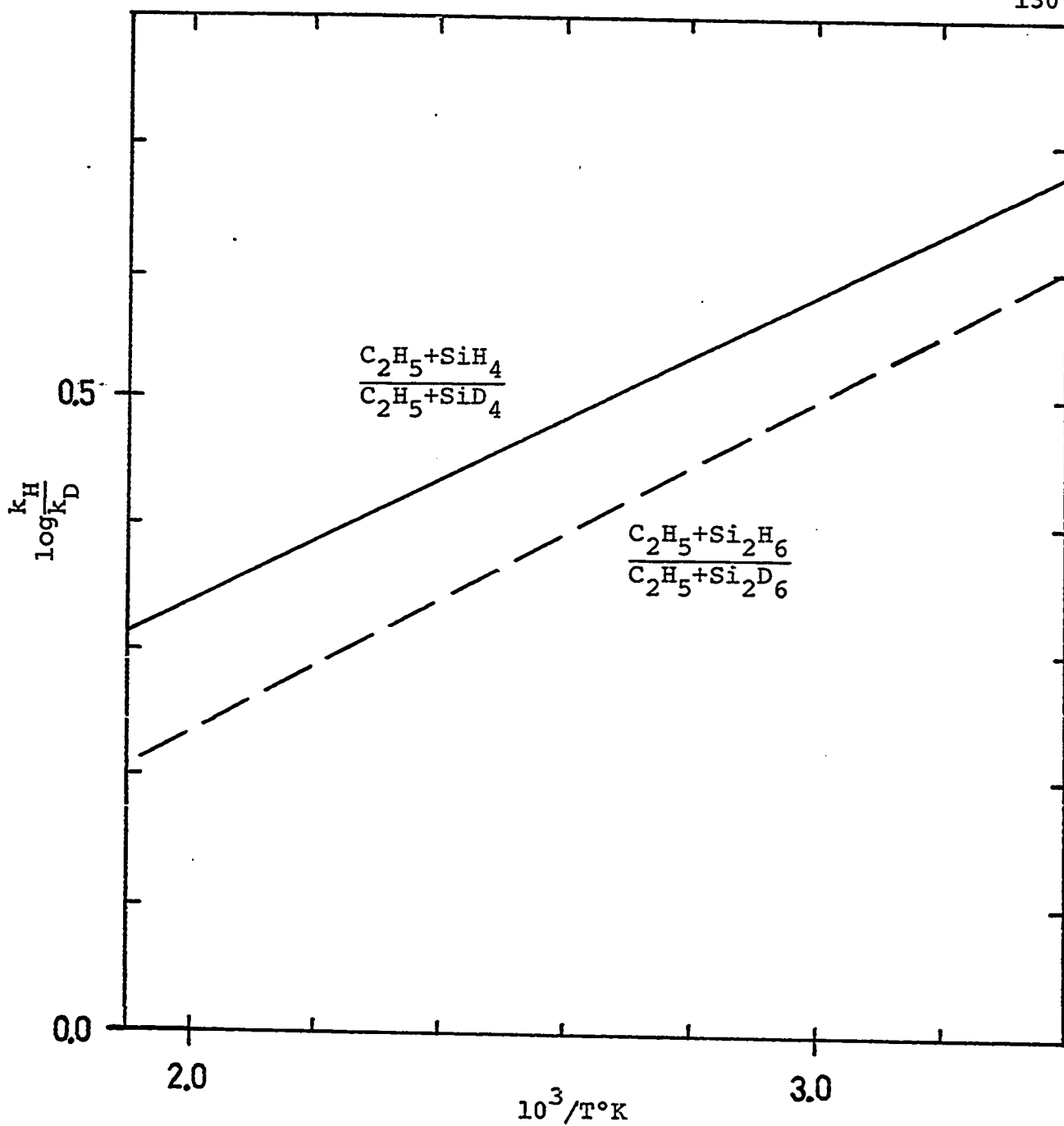


Figure 22. Kinetic isotope effect calculated from experimental data for ethyl radicals reacting with:
silane ———
disilane - - -

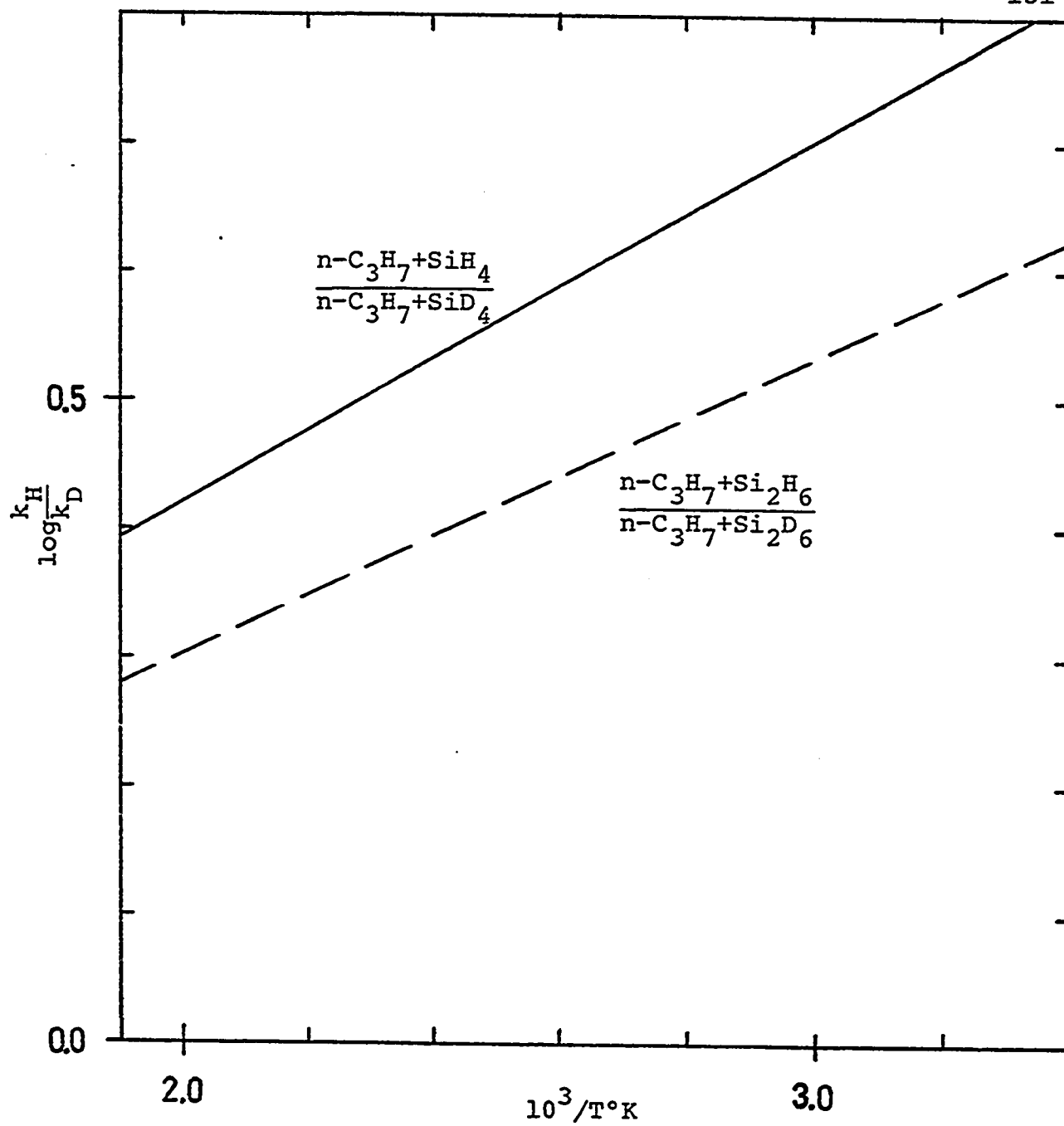


Figure 23. Kinetic isotope effect calculated from experimental data for n-propyl radicals reacting with:

silane —————

disilane - - - - -

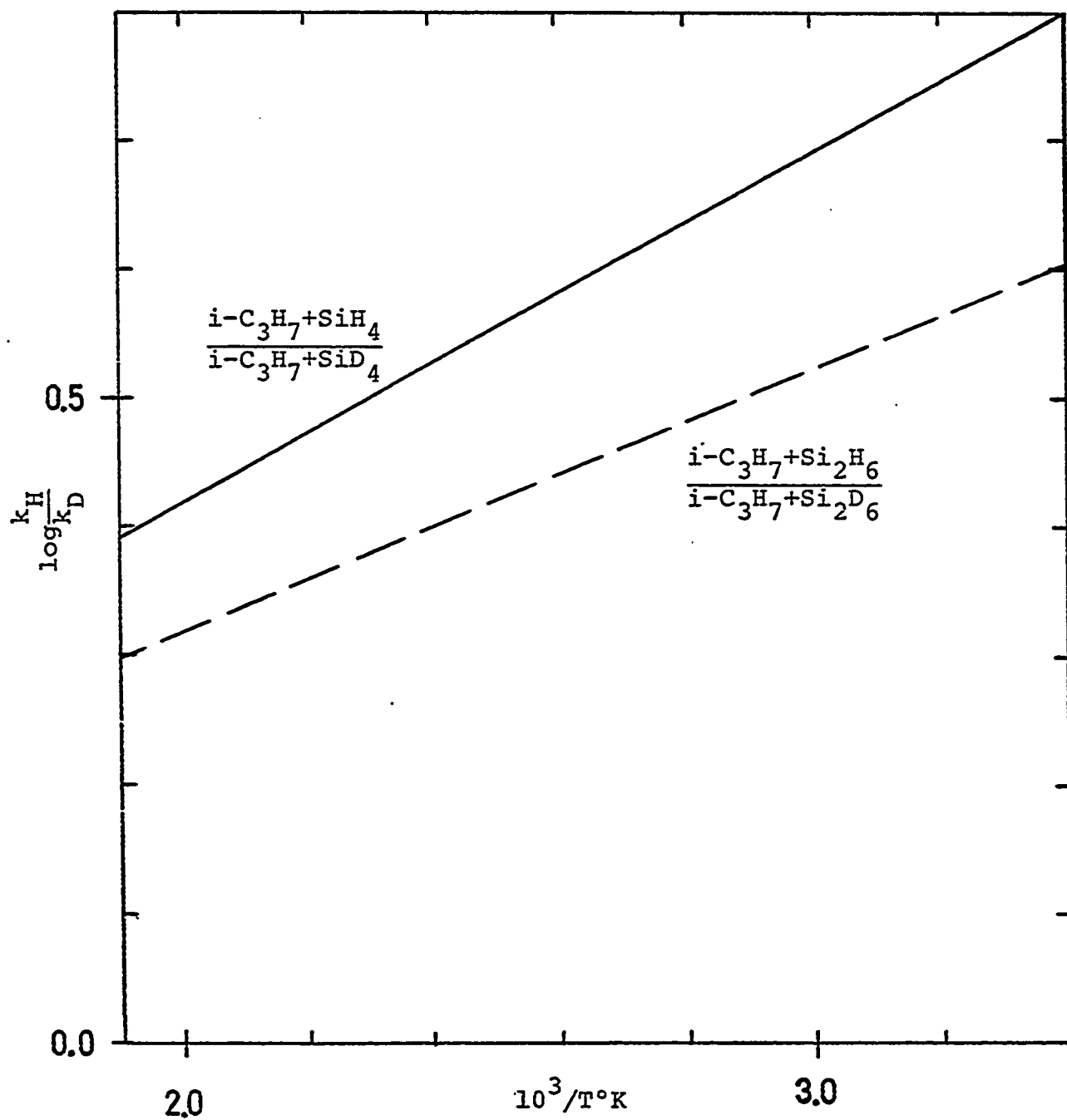


Figure 24. Kinetic isotope effect calculated from experimental data for iso-propyl radicals reacting with:

silane —————

disilane — — — —

Table XXV
 Experimentally Determined Kinetic
 Isotope Effects at 300°K

Reaction	$\frac{k_H}{k_D}$
$\text{CH}_3 + \text{Silane}^a$	4.9
$\text{CH}_3 + \text{Disilane}^a$	5.5
$\text{C}_2\text{H}_5 + \text{Silane}^b$	4.6
$\text{C}_2\text{H}_5 + \text{Disilane}^b$	3.9
$n\text{-C}_3\text{H}_7 + \text{Silane}^b$	6.2
$n\text{-C}_3\text{H}_7 + \text{Disilane}^b$	4.0
$\text{iso-C}_3\text{H}_7 + \text{Silane}^b$	6.0
$\text{iso-C}_3\text{H}_7 + \text{Disilane}^b$	3.9
$\text{CH}_3 + \text{Methane}^c$	33.5
$\text{CH}_3 + \text{Ethane}^d$	12.4

^a Reference 115

^b This work

^c References 141 and 142

^d Reference 143

Table XXVI

Input Parameters for BEBO Calculations

Bond Dissociation Energies ^a (kcal mole ⁻¹)		Refer- ence
D(CH ₃ -H)	108.3	2
D(CH ₃ CH ₂ -H)	102.1	2
D(C ₂ H ₅ CH ₂ -H)	102.1	2
D[(CH ₃) ₂ CH-H]	98.6	2
D(SiH ₃ -H)	98.3	100
D(CH ₃ -SiH ₃)	85.1	102
D(C ₂ H ₅ -SiH ₃)	82.1	102
D(CH ₃ CH ₂ CH ₂ -SiH ₃)	79.4	102
D[(CH ₃) ₂ CH-SiH ₃]	81.2	102
Bond Distances Å		
Si-H	1.48	144
C-H	1.09	144
C-Si	1.87	144
C-C	1.54	1
Stretching Frequency, cm ⁻¹		
C-Si	701	144
C-C	1000	1
Morse Parameter β, cm ⁻¹		
CH ₃ + SiH ₄	1.435	b
C ₂ H ₅	1.461	b
n-C ₃ H ₇	1.485	b
iso-C ₃ H ₇	1.469	b

Table XXVI (continued)

Bond Energy Indexes		Refer- ence
Si-H	1.003	c
CH ₃ -H	1.089	c
C ₂ H ₅ -H	1.081	c
C ₂ H ₅ CH ₂ -H	1.081	c
(CH ₃) ₂ CH-H	1.076	c

^a Includes zero point energy.

^b Calculated (121) from $\beta = 1.2177 \times 10^7 W_e \sqrt{\frac{\mu}{E_{SS}}}$.

^c Calculated (121) from $p = \frac{0.26 [\ln(E_{1S}/E_x)]}{R_x - R_{1S}}$.

Table XXVII
 Potential Energies of Activation Calculated
 by the BEBO Method

Reaction	Bond Order (Bond breaking)	Energy (kcal /mole)	Bond Lengths (Å)	
			Bond Breaking	Bond Forming
$\text{CH}_3 + \text{SiH}_4$	0.70	10.0	1.57	1.40
$\text{C}_2\text{H}_5 + \text{SiH}_4$	0.61	11.0	1.61	1.33
$n\text{-C}_3\text{H}_7 + \text{SiH}_4$	0.62	10.4	1.60	1.34
$\text{iso-C}_3\text{H}_7 + \text{SiH}_4$	0.55	12.0	1.64	1.30
$\text{CH}_3 + \text{CH}_4$	0.50	15.8	1.27	1.27
$\text{C}_2\text{H}_5 + \text{CH}_4$	0.41	18.1	1.32	1.23

to those reported for abstraction from hydrocarbons. The activation energies for abstraction from silanes are generally lower than for abstraction from hydrocarbons, and this is clearly the reason that silanes react faster. The activation energies for different radicals attacking the same silane compound are all about the same. It is remarkable that they should differ by so little, in view of the differences in energy of the bond being formed.

2) Possible Reasons for the Lack of a Definite Trend in Activation Energies for a Series of Alkyl Radicals Reacting with Silane:

Abstraction from silanes is more exothermic than abstraction from hydrocarbons. More energy is supplied from bond formation than is required for bond breaking, and the transition state is reached at a point less than halfway along the reaction coordinate. Because of this, it will resemble reactants more than products. As a consequence, variations in the energy contributed by carbon-hydrogen bond formation would have a relatively smaller effect on the magnitude of the activation energy than if the reaction were thermoneutral. For a series of different radicals reacting with the same substrate, this should result in a smaller increase in activation energy for a given decrease in energy of the bond being formed. It seems unlikely, however, that the observed results could be explained solely on the basis of the exothermicity of the reaction.

It has been reported that there is an activation energy of 2 kcal/mole for combination of ethyl radicals (16). An activation energy of this magnitude could have an effect of one kcal/mole on the measured activation energy of hydrogen atom abstraction, since the rate of this abstraction is determined relative to the rate of radical combination. It would seem plausible that the higher alkyl radicals might have an activation energy of combination about equal in magnitude to the barriers to rotation around the bond which is formed in the resulting hydrocarbon. Such barriers may be expected to have a magnitude in the range of 2-6 kcal/mole (1), and the existence of activation energies for radical combination in this range could easily account for the results found in this work. The temperature studies of higher alkyl radical combination rates which have been carried out do not unanimously indicate activation energies, however, and unfortunately, they cannot be considered sufficiently reliable to answer definitely whether or not there is an activation energy for radical combination (14-16).

3) Kinetic Isotope Effect:

The variation of experimental kinetic isotope effect with temperature observed in this work may be seen, by reference to Figures 21 to 24, to be quite similar to that found previously for methyl radicals reacting with silanes (115). The isotope effects are generally consistent with

the other features of the data. They are lower than the corresponding isotope effects found for hydrocarbons, which is in keeping with the greater exothermicities and smaller activation energies of the silane reactions. They show a slight trend toward increasing isotope effect with decreasing exothermicity along the series methyl, ethyl, n-propyl, and iso-propyl, and there is a significant decrease in isotope effect in going from monosilane to disilane which must be due to the smaller zero point energy of the latter compound. One must be cautious not to read too much into minor variations in the isotope effects. For n- and iso-propyl radicals the isotope effects were determined directly by competitive reaction, and, at 300°K, the isotope effects for n-propyl appear to be higher than for iso-propyl. However, they were calculated from the Arrhenius parameters for the relative rates of reaction, and these did not differ outside statistical error. Consequently, the difference between the experimental isotope effects for these two radicals must be more apparent than real. Greater caution must be used in assessing the significance of variations in the isotope effects for the other radicals, since they were not determined from relative rates of reaction and are therefore probably less accurate.

4) BEBO Calculations:

Examining the results of BEBO calculations may provide some insight into the peculiar features of alkyl

radical reactivity with silanes. The calculated potential energies of activation are smaller and closer together for silanes than they are for hydrocarbons. While the BEBO calculations do suggest less difference between activation energies for a series of alkyl radicals reacting with silane, they do not necessarily suggest that there should be no difference at all.

The predicted potential energies of activation are 3 to 5 kcal/mole higher than the experimental activation energies. Inspection of Figures 25-27 shows that the triplet repulsion energy, which predominates only slightly in the case of alkyl radicals reacting with hydrocarbons, is the dominant source of the predicted energy barrier to reaction of alkyl radical with silanes. This is primarily true because the energy barrier associated with bond breaking and formation is very small for alkyl radicals reacting with silanes. It is also noteworthy that the differences in the maxima of the "bonding" energies predicted for different radicals are quite small.

The small magnitude of the energy of the bonding term is partly due to the fact that the reactions are all exothermic. Of greater importance in the calculations is the fact that the bond energy index for the Si-H bond is very near unity, while that for C-H bonds is somewhat higher. A bond having an energy index near unity will show a lower energy requirement for effecting a given decrease in its

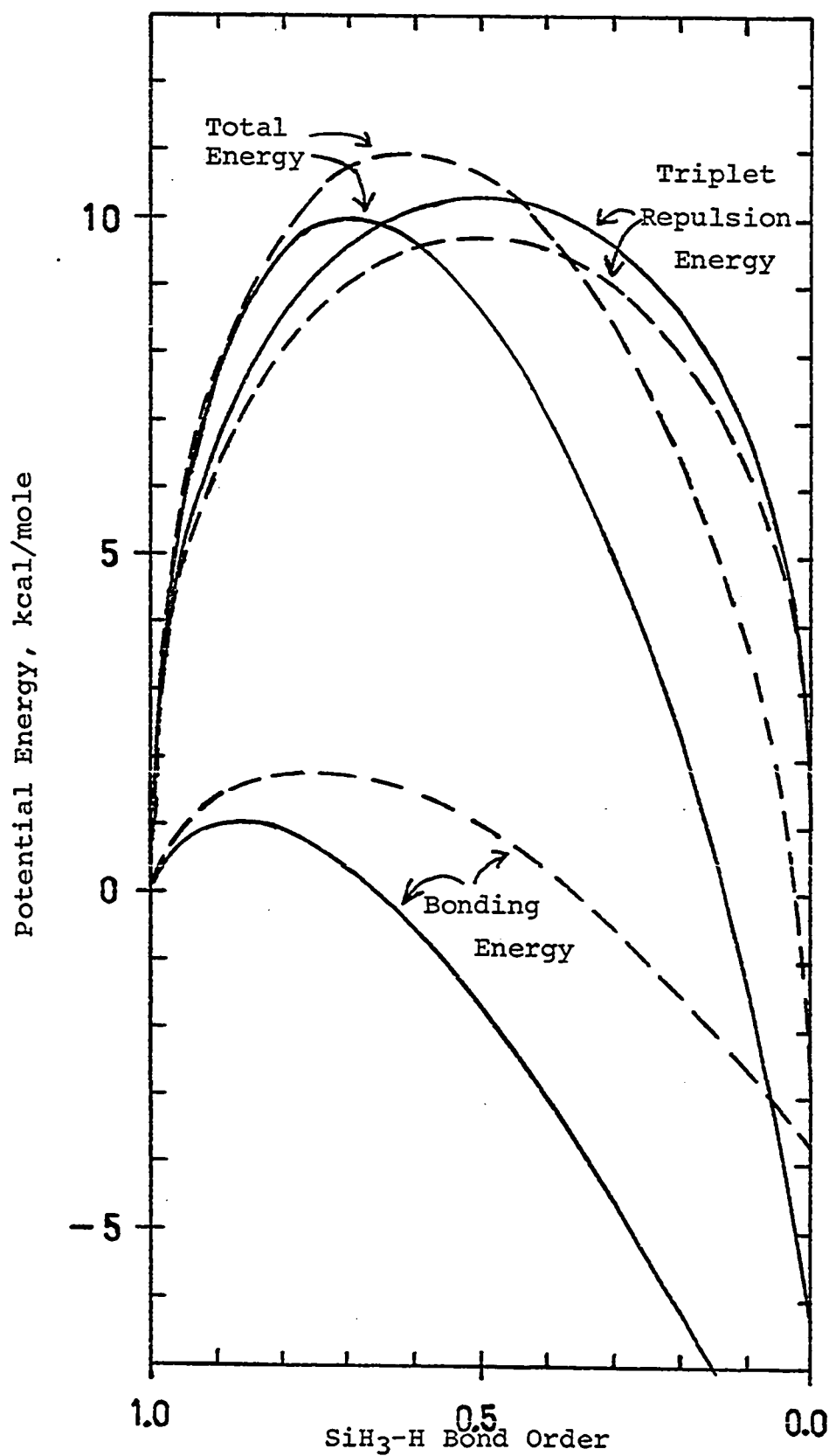


Figure 25. Potential energy vs. SiH₃-H bond order for methyl radicals — and ethyl radicals - - reacting with silane.

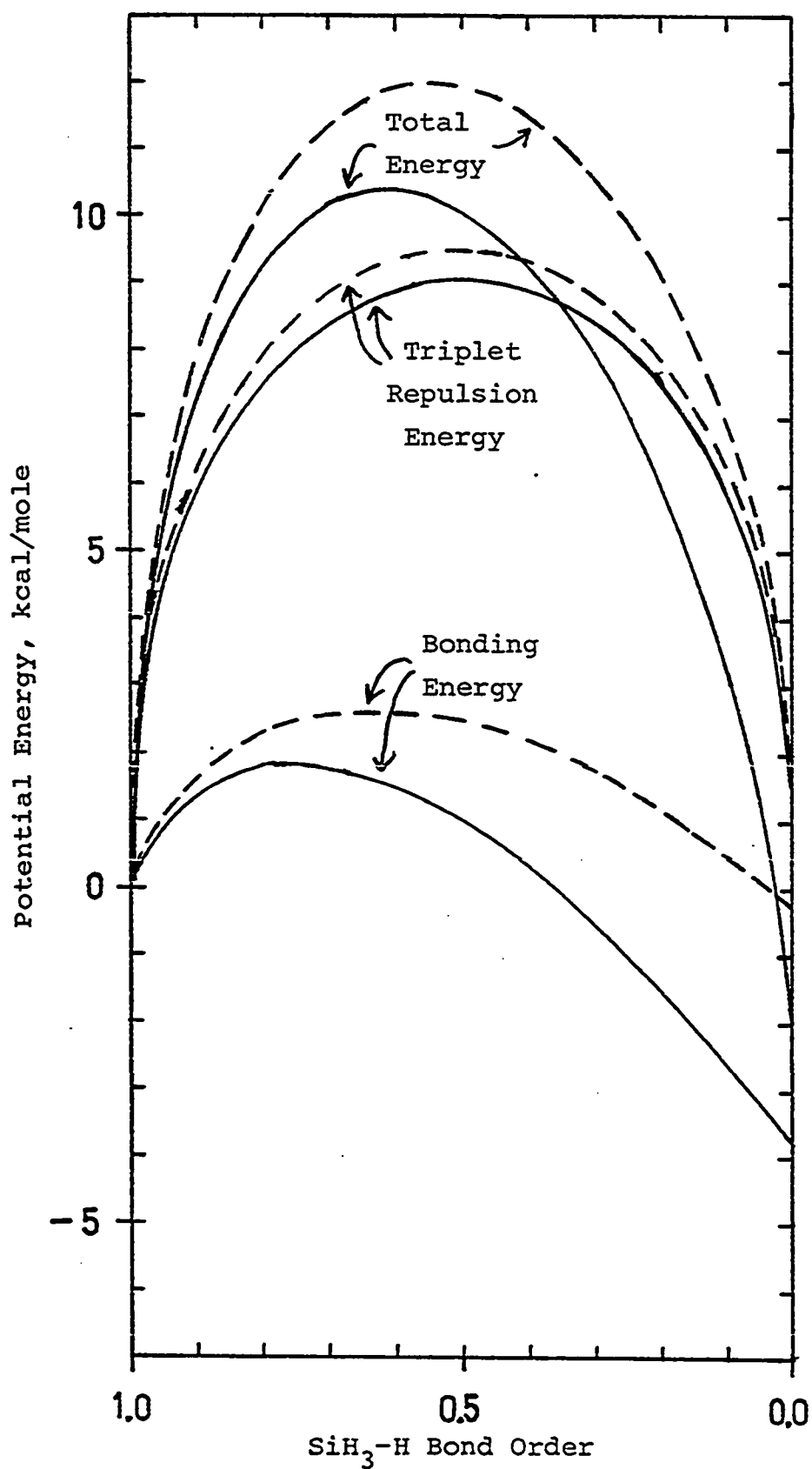


Figure 26. Potential energy vs. SiH₃-H bond order for n-propyl radicals — and iso-propyl radicals — — reacting with silane.

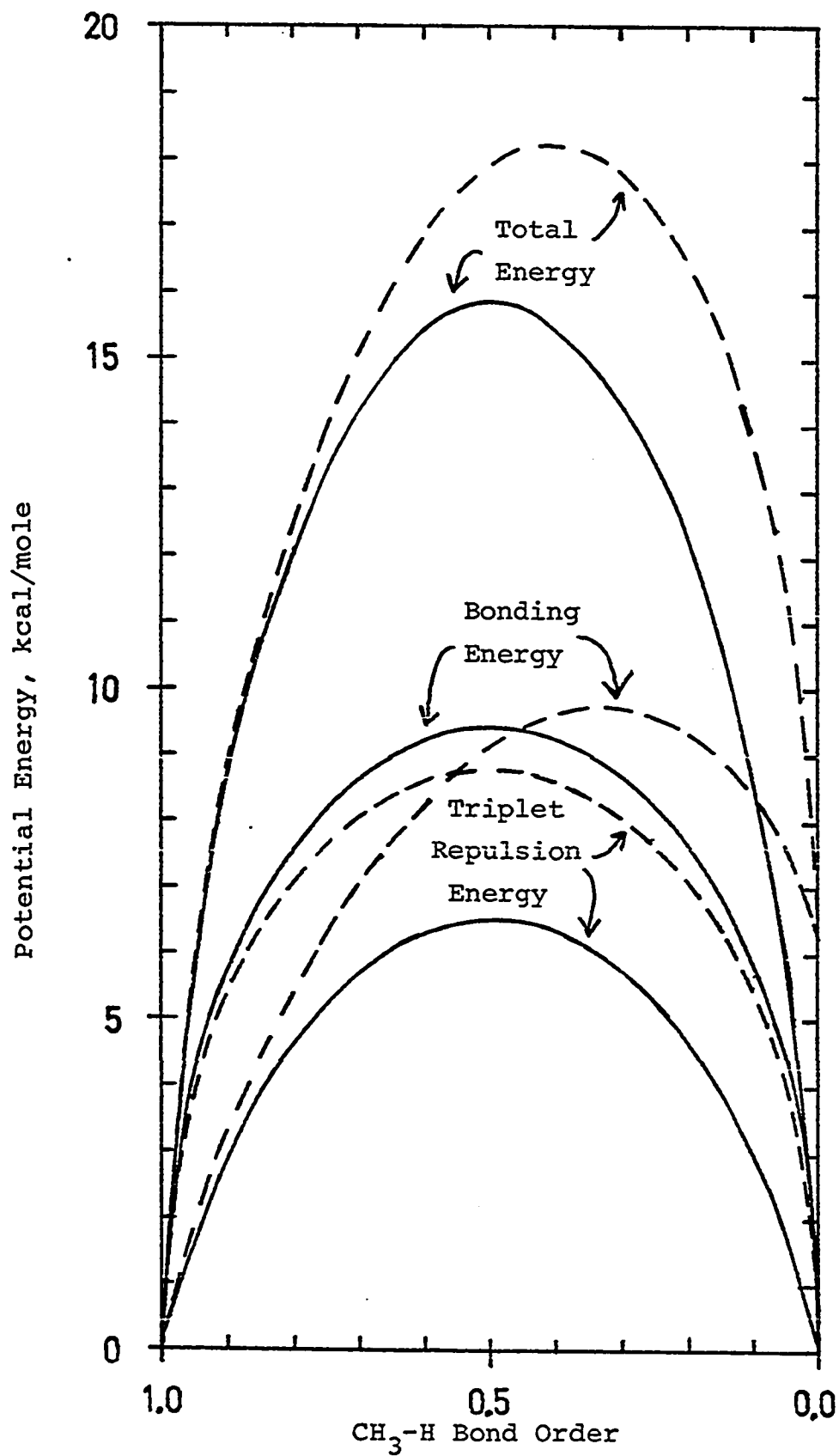


Figure 27. Potential energy vs. CH₃-H bond order for methyl radicals——and ethyl radicals——reacting with methane.

order than a bond with a higher index. Thus Si-H bonds are predicted to be more easily broken than C-H bonds when attacked by alkyl radicals.

Examination of the potential energy curves for the silanes reveals that the differences in the predicted potential energies of activation do not arise directly from differences in the maxima of the bonding energy terms. The bonding terms are much smaller than the triplet repulsion energy terms, and, since the reactions are exothermic, the maxima of the bonding terms are displaced toward higher order of the bond being broken. Since the triplet terms are symmetrical, they tend to displace the point of maximum total energy toward their own maxima at bond order 0.5, thus obscuring to some extent the differences in the maxima of the bonding terms. For methyl and ethyl radicals reacting with methane, the bonding terms are much larger. The bonding term for methyl is symmetrical, while that for ethyl is nearly so, and the maximum values of the bonding terms add directly to the maximum values of the triplet terms.

It is necessary to remember that the BEBO method is empirical, and that its principal justification lies in the fact that it often predicts reasonable potential energies of activation. Obviously there can be no guarantee that the behavior of the calculated "bonding" and "triplet" terms corresponds closely to reality, but it is interesting to

observe that in this case they seem to offer some insight into observed behavior.

It would be prudent to consider some of the more hazardous features of the calculations presented here. Except for methylsilane, the C-Si stretching frequencies needed for calculation of the triplet repulsion energy are not known, and it has been assumed that they are all the same as for methylsilane. The bond dissociation energies for the alkyl silanes used were calculated from electron impact data and appear to be reasonably reliable. It is clear, however, that variations in C-Si stretching frequencies and bond energies can have a substantial effect on the magnitude of the triplet repulsion energy. Since the bonding energy terms are small, any significant variation in triplet repulsion energy between two different radicals attacking silane would have a substantial effect on the relative magnitude of their calculated potential energies of activation.

For the interaction of hydrogen atoms, the triplet energy falls off more rapidly with increasing distance than the Morse function predicts, and this is particularly true for distances in excess of two Angstroms (121). In the case of the alkyl radical-silane system, the closest approach of carbon to silicon predicted by the calculations is just under three Angstroms. The triplet repulsion considered here is not that between hydrogen atoms, however, but

between alkyl and silyl groups. The electrons involved in triplet repulsion are not highly localized in the $1s$ orbitals of hydrogen atoms, but are spread out in the larger orbitals of the alkyl and silyl groups. Because of this they may interact meaningfully at greater internuclear distances. The combined effect of the longer internuclear distances and the larger orbitals is impossible to assess quantitatively. James and Stuart (145) have reported Arrhenius parameters and calculated potential energies of activation for hydrogen abstraction from cyclohexadiene by methyl, ethyl, iso-propyl, and tert-butyl radicals. They found that the measured activation energies were all approximately equal for the different radicals, while BEBO calculations predicted increasing potential energy of activation with decreasing energy of the bond being formed, and they also have suggested that the triplet repulsion energy may not be given accurately by the Morse function for systems where there is considerable delocalization of electrons.

CHAPTER VI

THE REACTIONS OF METHYL RADICALS WITH METHYL SUBSTITUTED SILANE

RESULTS

- 1) Reaction of Methyl Radicals with Tetramethylsilane and neo-Pentane.
- 2) Reaction of Methyl Radicals with Methylsilane-d₃.
- 3) Reaction of Methyl-d₃ Radicals with Deuterated Methylsilanes.
- 4) Reaction of Methyl Radicals with Methylsilanes.

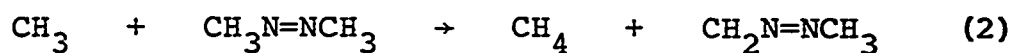
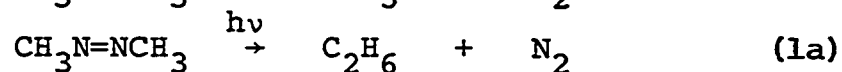
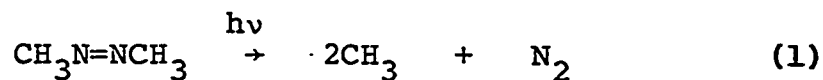
DISCUSSION

- 1) Comparison of Arrhenius Parameters with Previous Values for Silanes and for Hydrocarbons.
- 2) Kinetic Isotope Effect.
- 3) Correlation of Kinetic Data and Magnetic Shielding.

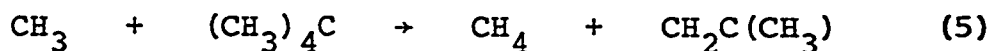
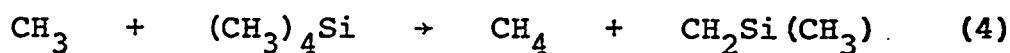
RESULTS

1) Reaction of Methyl Radicals with Tetramethylsilane and neo-Pentane:

The photolysis of azomethane was used as the source of methyl radicals. Photolytic decomposition of azomethane proceeds by the following sequence:



Temperature studies of the reaction of methyl radicals with tetramethylsilane and with neo-pentane were carried out.



The rate constant data for these reactions are summarized in Table XXVIII. Least squares treatment of the data yielded the Arrhenius equations

$$\log \frac{k_4}{k_3^{1/2}} = 4.67 \pm 0.23 - \frac{9660 \pm 410}{2.303RT}$$

and

Table XXVIII

Reaction of Methyl Radicals with Tetramethyl-silane and neo-Pentane

Temp (°C)	Time (min)	[Azo] [(CH ₃) ₄ Si] x10 ⁶ mole/cc	Rate x10 ¹² mole/cc s						$\frac{k_4}{k_3} \frac{1}{2}$	
			N ₂	Methane (total)	CH ₄ R ₂	CH ₄ R ₄	C ₂ H ₆ (total)	C ₂ H ₆ R ₃		
58.0	10.00	1.361	6.033	40.82	1.79	1.10	0.69	29.12	28.80	0.02131
91.0	10.00	1.634	5.739	49.58	5.91	3.90	2.01	28.38	28.06	0.06612
119.0	10.00	1.274	16.814	42.93	17.09	4.98	12.11	14.87	14.56	0.1868
178.0	10.00	1.220	12.110	41.67	32.17	9.16	23.01	4.11	3.80	0.9747
214.0	10.00	1.416	13.711	54.43	53.91	14.10	39.81	2.11	1.69	2.233
61.0	10.00	1.209	13.057	36.71	2.64	1.07	1.57	26.90	26.69	0.02327
150.0	10.00	1.416	14.952	47.05	29.01	8.34	20.67	7.60	7.28	0.5124
			[(CH ₃) ₄ C]				CH ₄ R ₅			$\frac{k_5}{k_3} \frac{1}{2}$
151.0	10.00	1.220	16.215	43.78	16.25	7.83	8.42	8.97	8.65	0.1766
92.0	11.00	1.383	33.617	44.40	6.43	3.33	3.10	26.76	26.47	0.01792

Table XXVIII (continued)

Temp (°C)	Time (min)	[Azo] [(CH ₃) ₄ C] x10 ⁶ mole/cc	Rate x10 ¹² mole/cc s						$\frac{k_5}{k_3^{1/2}}$	
			N ₂	Methane (total)	CH ₄ R ₂	CH ₄ R ₅	C ₂ H ₆ (total)	C ₂ H ₆ R ₃		
120.0	11.00	1.372	33.367	45.26	13.04	5.97	7.07	17.36	17.07	0.05128
183.0	10.00	1.220	31.777	45.04	32.49	9.60	22.89	3.59	3.27	0.3983
222.0	10.00	1.252	16.705	48.42	41.35	14.09	27.26	2.00	1.69	1.255

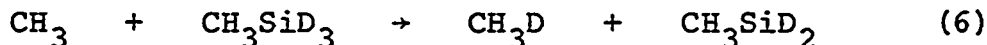
Cell volume 186.5 cc. Illuminated volume 158 cc.

$$\log \frac{k_5}{k_3^{1/2}} = 5.25 \pm 0.48 - \frac{11720 \pm 920}{2.303RT}$$

The Arrhenius plots are shown in Figure 28.

2) Reaction of Methyl Radicals with Methylsilane-d₃:

When methyl radicals are produced in the presence of methylsilane, they may react either with the silyl group or with the methyl group. In an attempt to assess the relative importance of the two reactions, methyl radicals were reacted with methylsilane-d₃.



Methane was produced by Reaction 2, and methane-d was produced by Reaction 6. The rate constants for Reaction 6 were determined by means of the expression

$$\frac{k_6}{k_3^{1/2}} = \frac{R_{\text{CH}_3\text{D}}}{R_3^{1/2} [\text{CH}_3\text{SiD}_3]}$$

The Arrhenius equation

$$\log \frac{k_6}{k_3^{1/2}} = 5.58 \pm 0.09 - \frac{9220 \pm 150}{2.303RT}$$

was found. Data for the reaction of methyl radicals with methylsilane-d₃ are given in Table XXIX and the Arrhenius plot is shown in Figure 29.

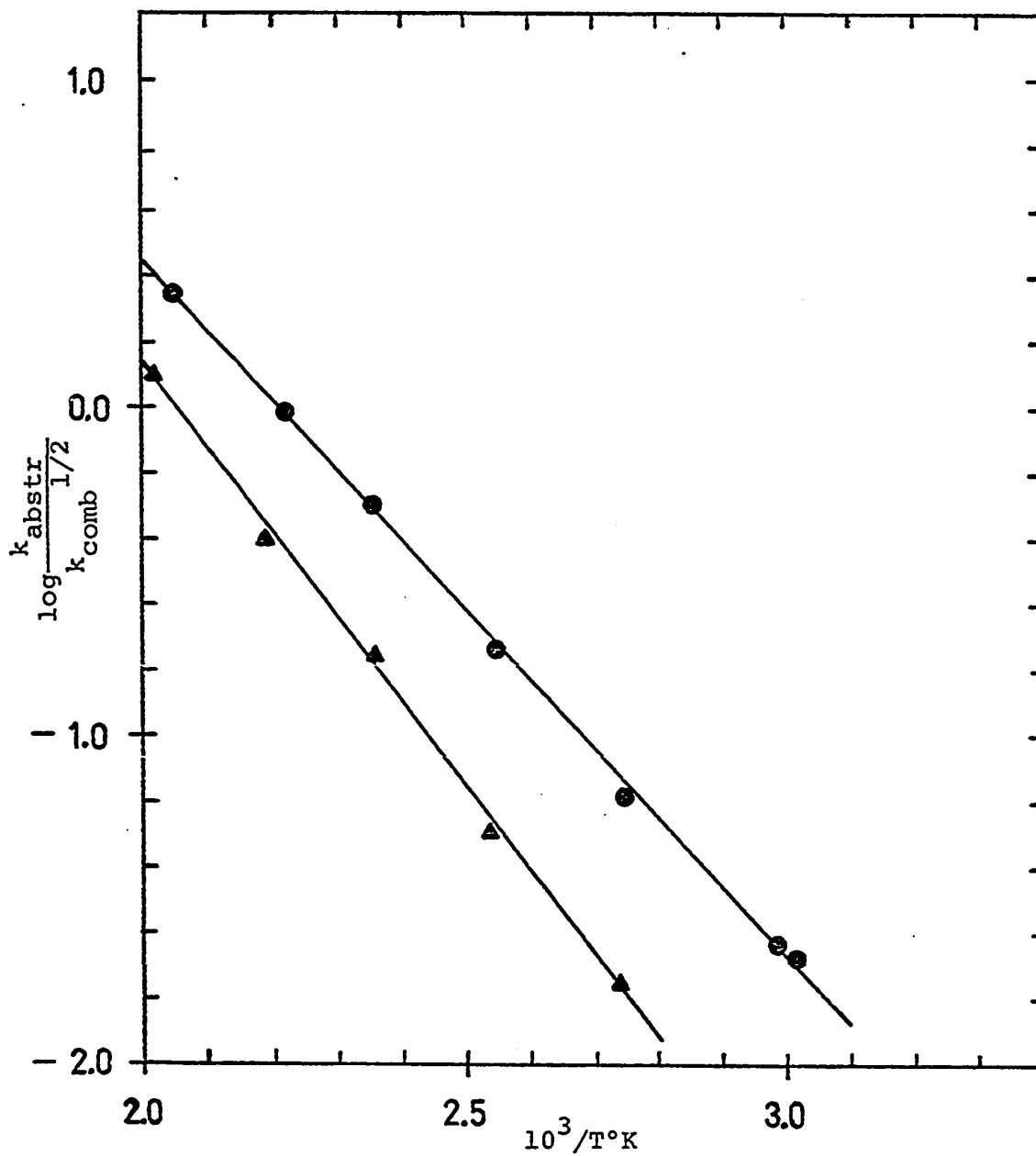


Figure 28. Arrhenius plots for reaction of methyl radicals with tetramethylsilane ●, and neo-pentane ▲.

Table XXIX

Reaction of Methyl Radicals with Methylsilane-d₃

Temp (°C)	Time (min)	[Azo] x10 ⁶ mole/cc	[CH ₃ SiD ₃] N ₂	Rate x10 ¹² mole/cc s						$\frac{k_6}{k_3^{1/2}}$	
				CH ₄ (total) R ₂	CH ₄ R ₂	CH ₄ (Excess) R ₂	CH ₃ D R ₆	C ₂ H ₆ (total) R ₃	C ₂ H ₆ R ₃		
24.0	40.00	1.158	2.834	11.52	0.46	0.14	0.320	0.59	10.31	10.22	0.06512
48.0	40.00	1.197	2.608	12.61	1.15	0.38	0.770	1.76	9.46	9.37	0.2205
61.0	40.00	1.070	2.637	11.00	1.58	0.48	1.100	2.52	7.10	7.01	0.3609
75.0	40.00	1.041	2.462	11.33	1.54	0.67	0.870	3.30	5.51	5.43	0.5752
92.0	45.00	1.041	1.829	10.51	1.99	0.92	1.070	4.05	3.65	3.57	1.172
103.0	40.10	1.158	1.965	11.00	2.36	1.21	1.150	5.17	2.66	2.58	1.638
117.0	40.00	1.080	1.508	10.76	2.37	1.36	1.010	5.36	1.76	1.69	2.734
135.0	43.00	1.119	1.343	13.02	3.29	1.86	1.430	6.40	1.25	1.15	4.444
150.0	42.00	1.070	1.187	13.10	3.76	2.08	1.680	6.97	0.87	0.79	6.606
167.0	40.00	1.070	1.323	13.26	3.84	2.15	1.690	8.94	0.50	0.41	10.55
184.0	40.00	1.051	0.983	13.28	4.54	2.60	1.940	8.22	0.41	0.33	14.56
201.0	40.00	1.099	1.041	13.41	4.84	2.98	1.860	10.61	0.28	0.20	22.79

Cell volume 218 cc. Illuminated volume 192 cc.

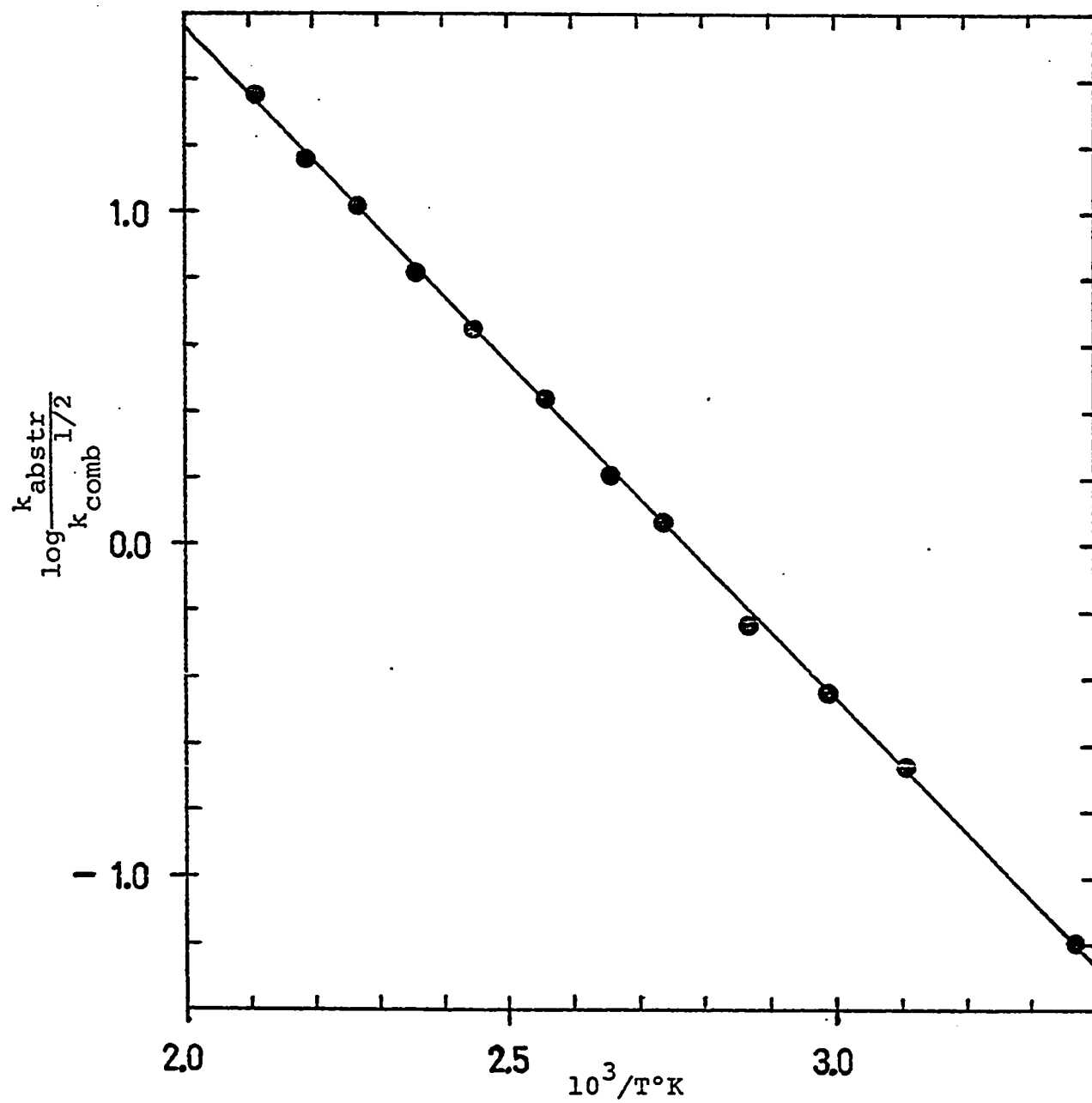
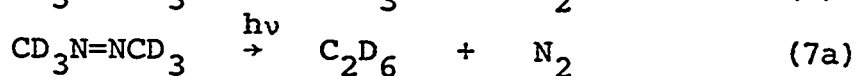
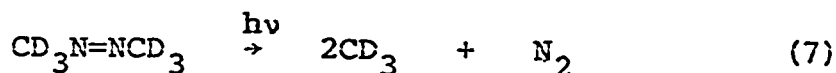


Figure 29. Arrhenius plot for reaction of methyl radicals with methylsilane- d_3 .

A small amount of methane was produced in addition to that which could be accounted for by Reaction 2. In order to establish whether this was produced by abstraction from the methyl group, it was decided to repeat the study using trideuteromethyl radicals produced in the photolysis of azomethane-d₆.

3) Reaction of Methyl-d₃ Radicals with Deuterated Methyl-silanes:

It is reasonable to assume that the mechanism of azomethane-d₆ photolysis is perfectly analogous to that of azomethane photolysis.



except that, of course, the rate constant for Reaction 8 should be smaller than that of Reaction 2. The rate of Reaction 9 would be expected to be indistinguishable from that of Reaction 3 (121).

A temperature study of the photolysis of azomethane-d₆ was carried out, and the Arrhenius equation

$$\log \frac{k_8}{k_9^{1/2}} = 4.15 \pm 0.15 - \frac{8210 \pm 250}{2.303RT}$$

was found. Data for Reaction 8 are listed in Table XXX and plotted in Figure 30.

The Arrhenius equation for Reaction 2

$$\log \frac{k_8}{k_3^{1/2}} = 4.49 \pm 0.25 - \frac{8050 \pm 440}{2.303RT}$$

is surprisingly similar to that for Reaction 8. Such a small difference in activation energies was not expected, and it would seem probable that one of the determinations must be in error. The rate of Reaction 8 was so small over most of the temperature range of the study that it was difficult to measure accurately, and this may well be the source of the discrepancy. The result obtained was nevertheless used in determination of rate constants for trideuteromethyl radical abstraction reactions, since the rate constants involved are so small that they are unlikely to introduce much error in the results.

Reaction of trideuteromethyl radicals with Si-deuterated methylsilanes is a very effective method of determining the relative importance of abstraction from the methyl group, since any hydrogen abstraction results in the appearance of methane-d₃, the mass spectrum of which has its parent (and principal) peak at mass 19. The mass 19 peak in the mass spectrum of methane-d₄, however, is extremely small, and is, of course, due mainly to isotopic impurity. The

Table XXX
 Reaction of Trideuteromethyl Radicals with Azomethane-d₆

Temp (°C)	Time (min)	[Azo] x10 ⁶ mole/cc	Rate x10 ¹² mole/cc s				$\frac{k_8}{k_9^{1/2}}$
			N ₂	CD ₄ R ₈	C ₂ D ₆ (total)	C ₂ D ₆ R ₉	
27.0	10.00	6.088	145.77	1.05	131.96	130.90	0.01507
94.0	7.00	5.652	152.80	8.44	73.69	72.63	0.1752
184.0	7.00	3.653	113.02	14.92	7.08	6.33	1.623
151.0	7.20	3.642	110.90	12.01	14.65	13.92	0.8839
123.0	7.20	4.229	122.62	9.96	33.26	32.38	0.4139
60.0	7.00	5.641	144.36	3.32	106.24	105.18	0.05739

Cell volume 186.5 cc. Illuminated volume 158 cc.

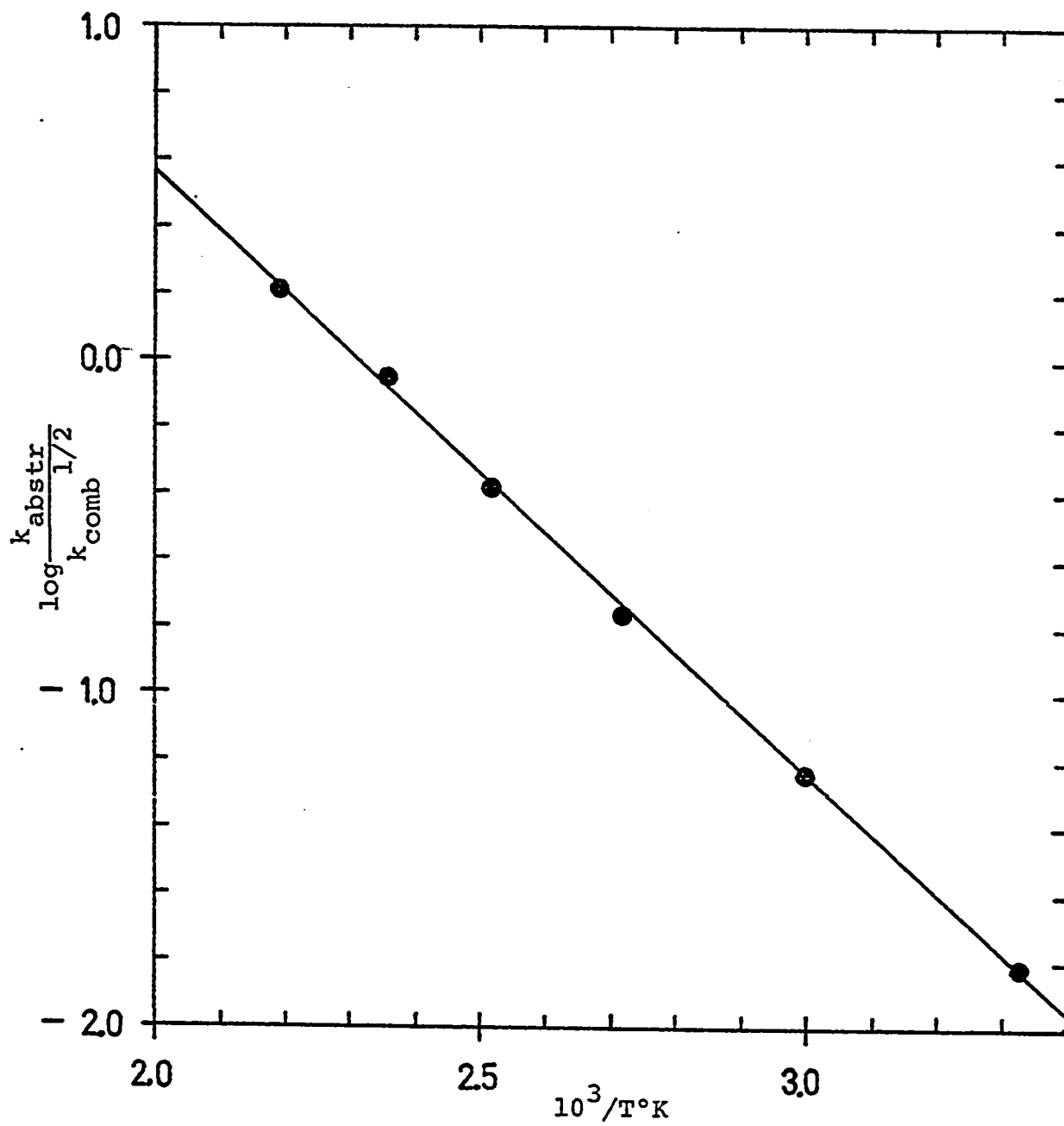
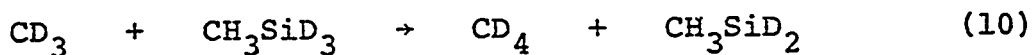


Figure 30. Arrhenius plot for reaction of trideuteromethyl radicals with azomethane- d_6 .

relative abundance of mass 19 in the mass spectrum of methane-d₄ produced in photolysis of azomethane-d₆ alone was noted, and a comparison was made with the abundance of mass 19 in the spectrum of methane produced by reaction of trideuteromethyl radicals with methylsilane-d₃. It was evident that formation of methane-d₃ in the reaction of trideuteromethyl radicals with methylsilane-d₃ was too slight to measure. A trace of methane-d₃ was obtained at room temperature, and this was probably due to isotopic impurity of the methylsilane-d₃.

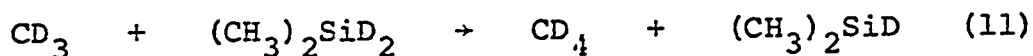
A temperature study of the reaction of trideuteromethyl radicals with methylsilane-d₃ was carried out.



The Arrhenius equation for Reaction 10 was found to be

$$\log \frac{k_{10}}{k_9^{1/2}} = 5.82 \pm 0.34 - \frac{9200 \pm 550}{2.303RT}$$

Rate constants for trideuteromethyl radical abstraction from dimethylsilane-d₂



were similarly determined, and again, no significant abstraction from the methyl groups could be detected. The Arrhenius equation

$$\log \frac{k_{11}}{k_9^{1/2}} = 5.25 \pm 0.24 - \frac{8820 \pm 390}{2.303RT}$$

was found for Reaction 11.

In the reaction of trideuteromethyl radicals with trimethylsilane-d, a measurable amount of abstraction from the methyl group occurred.



From the methane-d₄ produced, the Arrhenius equation for reaction with the silyl group

$$\log \frac{k_{12}}{k_9^{1/2}} = 5.11 \pm 0.19 - \frac{9210 \pm 330}{2.303RT}$$

was found. The methane-d₃ was also measured, and the Arrhenius equation

$$\log \frac{k_{13}}{k_9^{1/2}} = 4.31 \pm 0.53 - \frac{9070 \pm 920}{2.303RT}$$

for reaction with the methyl groups was determined. Rate constants for reactions of trideuteromethyl radicals with the series of deuterated, methyl substituted silanes are listed in Table XXXI, and the Arrhenius plots are shown in Figure 31. The result obtained for Reaction 13 does not differ greatly from that obtained for tetramethylsilane. It

Table XXXI

Reactions of Trideutromethyl Radicals with Deuterated Methyl Silanes

Temp (°C)	Time (min)	[AzO] x10 ⁶ mole/cc	[CH ₃ ⁻ SiD ₃] mole/cc	N ₂	Rate x10 ¹² mole/cc s			$\frac{k_{11}}{k_9^{1/2}}$			
					CD ₄ total R ₈	CD ₄ C ₂ H ₆ R ₁₀ total	C ₂ H ₆ C ₂ H ₆ R ₉				
69.0	40.00	1.068	3.121	8.14	4.60	0.13	4.47	2.47	2.41	0.9226	a
102.0	42.40	1.106	3.261	8.35	7.10	0.20	6.90	0.68	0.61	2.709	a
131.0	40.00	0.994	1.709	8.61	7.60	0.29	7.31	0.39	0.33	7.446	a
85.0	40.00	1.124	3.177	8.90	6.84	0.20	6.64	1.65	1.58	1.663	a
115.0	40.00	1.096	2.397	10.35	9.72	0.28	9.44	0.67	0.61	5.042	a
152.0	20.00	1.579	1.124	18.62	11.80	1.15	10.65	0.87	0.74	11.01	a
22.0	40.10	1.339	6.100	37.94	3.76	0.09	3.67	31.91	31.65	0.1069	b
49.0	21.50	1.406	3.797	41.36	7.06	0.29	6.77	28.45	28.16	0.3343	b
			[(CH ₃) ₂ ⁻ SiD ₂]				CD ₄ R ₁₁			$\frac{k_{11}}{k_9^{1/2}}$	
	22.0	10.00	1.339	4.904	38.61	1.69	1.60	34.39	34.07	0.05590 ^b	
	49.0	10.00	1.209	5.020	35.65	5.17	4.94	25.95	25.74	0.1940	b

Table XXXI (continued)

Temp (°C)	Time (min)	[Azo] x10 ⁶	[(CH ₃) ₂ SiD ₂] mole/cc	N ₂	Rate x10 ^{1.2} mole/cc s				$\frac{k_{11}}{k_9}$			
					CD ₄ total	CD ₄ R ₈	CD ₄ total	C ₂ H ₆ R ₉				
69.0	10.50	1.209	4.759	38.17	9.44	0.49	8.95	25.12	24.81	0.3776	b	
89.0	10.00	1.317	4.871	42.61	17.30	0.84	16.46	16.77	16.45	0.8332	b	
111.0	10.00	1.198	4.748	40.72	24.47	1.08	23.39	8.44	8.12	1.729	b	
132.0	10.00	1.198	3.931	41.66	28.37	1.46	26.91	5.38	5.06	3.043	b	
152.0	10.00	1.296	2.396	44.41	27.32	2.03	25.29	3.69	3.38	5.741	b	
26.0	10.00	1.263	9.670	37.02	1.48	0.10	0.32	1.38	31.22	31.01	0.02563	0.00594 ^b
61.0	11.40	1.361	9.725	40.71	6.29	0.42	1.20	5.87	25.63	25.35	0.1199	0.02451 ^b
93.0	10.00	1.492	9.659	48.10	16.67	1.11	2.53	15.56	18.04	17.72	0.3827	0.06222 ^b
124.0	10.00	1.350	5.271	46.83	19.41	1.81	3.06	17.60	10.13	9.81	1.049	0.1824 ^b
157.0	10.00	1.361	3.561	48.31	22.36	2.70	3.59	19.66	4.96	4.64	2.563	0.4680 ^b
184.0	10.00	1.361	2.352	50.42	22.47	3.66	3.59	18.81	2.95	2.64	4.922	0.9394 ^b

Table XXXI (continued)

Temp (°C)	Time (min)	[Azo] x10 ⁶ mole/cc	[SiD] x10 ⁶ mole/cc	[CH ₃] ₃ N ₂	Rate x10 ¹² mole/cc s	CD ₄	CD ₃ H	CD ₄	C ₂ H ₆	C ₂ H ₆	total R ₈	R ₁₃	R ₁₂	total R ₉	$\frac{k_{12}}{k_9^{1/2}}$	$\frac{k_{13}}{k_9^{1/2}}$
216.0	10.00	1.307	1.503	48.31	25.10	4.88	4.43	20.22	1.79	1.48	11.06	2.423				

a Cell volume 218 cc. Illuminated volume 192 cc.

b Cell volume 186.5 cc. Illuminated volume 158 cc.

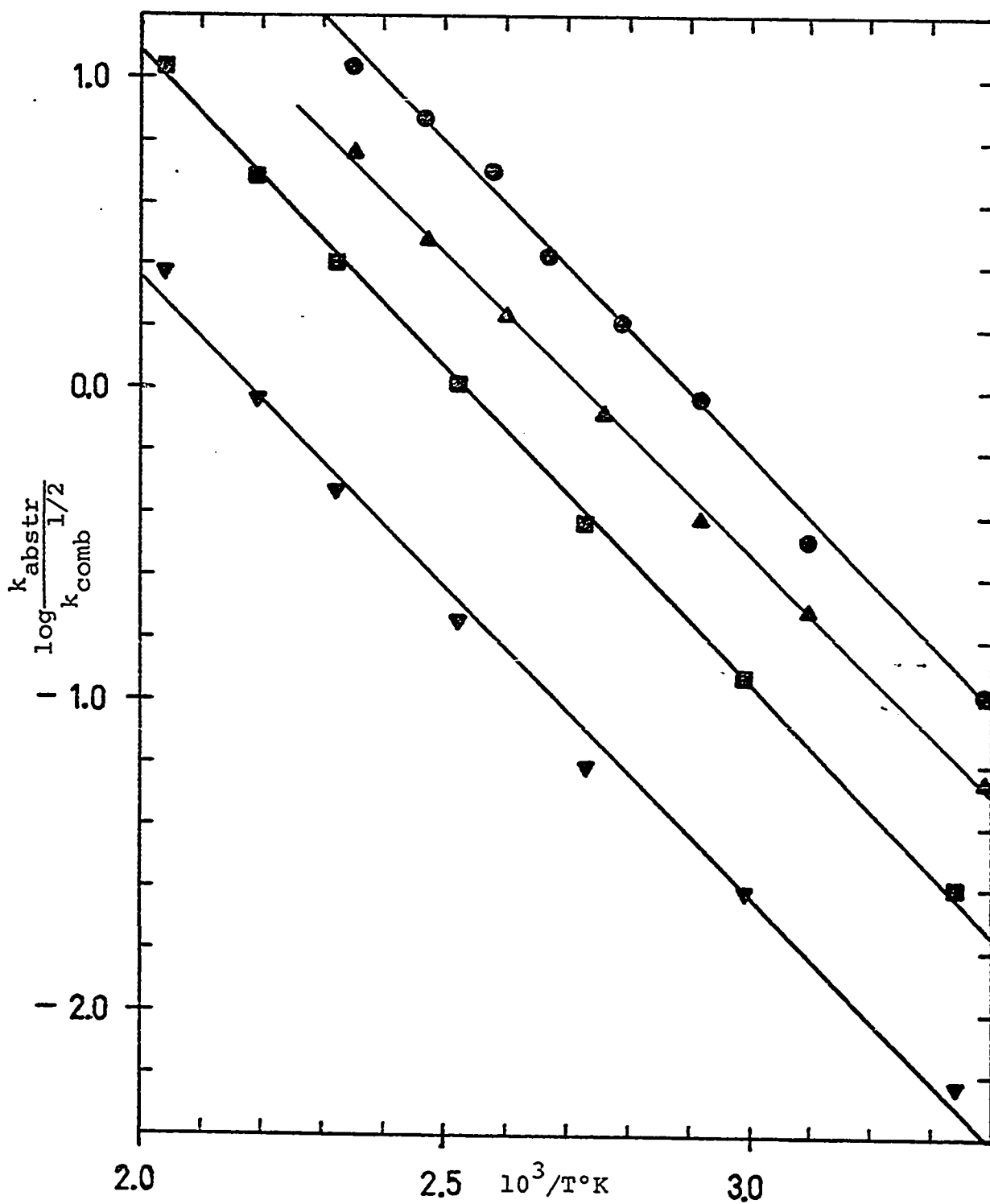
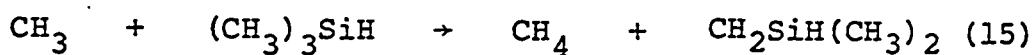
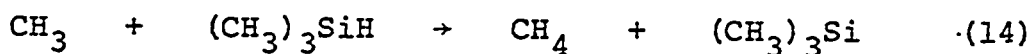


Figure 31. Arrhenius plots for reaction of trideuteromethyl radicals with methylsilane- d_3 \ominus , dimethylsilane- d_2 \blacktriangle , the silyl group of trimethylsilane- d \boxtimes , and the methyl groups of trimethylsilane- d \blacktriangledown .

must be considered that Reaction 13 is small compared to Reaction 12, and at lower temperatures the small quantity of undeuterated trimethylsilane present would make a significant contribution to the methane-d₃ produced. Inspection of the Arrhenius plot for Reaction 13 reveals the curvature that would be expected from this. Also, because of this curvature, the statistical error limits for this set of rate constants are larger than for most of the other reactions in this study. In view of the uncertainty inherent in the treatment of these results, it was decided to use the Arrhenius equation determined for tetramethylsilane in calculating the rate of abstraction from the methyl groups of undeuterated trimethylsilane.

4) Reaction of Methyl Radicals with Methylsilanes:

A temperature study of the reaction of methyl radicals with trimethylsilane was conducted.



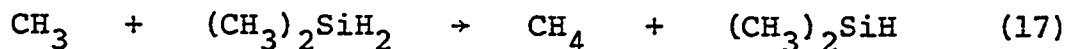
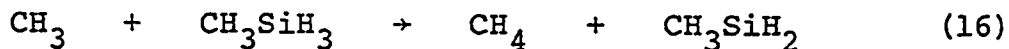
Rate constants for Reaction 14 were calculated from the relation

$$\frac{k_{14}}{k_3^{1/2}} = \frac{R_{\text{CH}_4} - R_2 - R_{15}}{R_3^{1/2} [(\text{CH}_3)_3\text{SiH}]}$$

Least squares treatment of the data resulted in the Arrhenius equation

$$\log \frac{k_{14}}{k_3^{1/2}} = 5.02 \pm 0.27 - \frac{8310 \pm 470}{2.303RT}$$

The reactions of methyl radicals with methylsilane and with dimethylsilane were also studied.



On the basis of the results obtained from the studies of trideuteromethyl radical radical reactions with methylsilane- d_3 and dimethylsilane- d_2 it was assumed that no significant reaction of methyl radicals with the methyl groups of methylsilane and dimethylsilane took place. Temperature studies yielded the following Arrhenius equations:

$$\log \frac{k_{16}}{k_3^{1/2}} = 5.61 \pm 0.24 - \frac{8130 \pm 390}{2.303RT}$$

$$\log \frac{k_{17}}{k_3^{1/2}} = 5.40 \pm 0.18 - \frac{8300 \pm 310}{2.303RT}$$

The rate constant data for methyl radical reactions with methyl substituted silanes are given in Table XXXII, and the Arrhenius plots are shown in Figure 32.

Table XXXII
Reaction of Methyl Radicals with Methyl Silanes

Temp (°C)	Time (min)	[Azo] [CH ₃ SiH ₃] x10 ⁶ mole/cc	N ₂	Rate x10 ¹² mole/cc s				$\frac{k_{16}}{k_3^{1/2}}$		
				Methane (total) R ₂	CH ₄ R ₂	CH ₄ R ₁₆ (total)	C ₂ H ₆ R ₃			
25.0	30.00	0.983	2.549	11.20	3.68	0.11	3.57	8.51	8.42	0.4827 ^a
47.0	30.00	1.090	2.578	13.63	8.45	0.29	8.16	7.06	6.97	1.199 ^a
62.0	30.00	1.099	2.491	13.31	10.59	0.42	10.17	4.72	4.63	1.897 ^a
76.0	30.00	1.012	1.732	12.39	10.62	0.51	10.11	3.15	3.07	3.331 ^a
93.0	31.00	1.022	1.693	13.13	12.29	0.66	11.63	1.85	1.76	5.178 ^a
105.0	31.20	1.177	1.469	14.66	14.63	0.97	13.66	1.50	1.39	7.887 ^a
121.0	25.00	0.834	1.148	10.24	12.57	0.69	11.88	0.69	0.62	13.14 ^a
151.0	25.00	1.051	1.051	13.30	16.53	1.12	15.41	0.35	0.24	29.93 ^a
137.0	20.00	1.090	1.158	13.50	16.01	1.19	14.82	0.56	0.48	18.47 ^a
27.0	10.00	1.535	5.380	41.35	7.81	0.37	CH ₄ R ₁₇ 7.44	31.86	31.54	0.2462 ^b

Table XXXII (continued)

Temp (°C)	Time (min)	[Azo] x10 ⁶	[(CH ₃) ₂ SiH ₂] mole/cc	Rate x10 ¹² mole/cc s						$\frac{k_{17}}{k_3^{1/2}}$
				N ₂	Methane (total)	CH ₄ R ₂	CH ₄ R ₁₇	C ₂ H ₆ (total)	C ₂ H ₆ R ₃	
60.0	12.00	1.394	4.737	40.35	19.87	1.05	18.82	21.27	21.01	0.8668 ^b
91.0	10.00	1.372	3.855	41.14	31.54	1.84	29.70	9.18	8.86	2.588 ^b
119.0	10.00	1.492	3.136	45.99	45.15	3.54	41.61	5.80	5.49	5.663 ^b
151.0	10.00	1.198	2.581	38.08	45.47	2.95	42.52	1.58	1.27	14.62 ^b
183.0	10.00	1.361	1.459	43.15	48.34	6.10	42.24	1.37	1.05	28.25 ^b
212.0	5.00	2.548	1.285	79.32	86.08	21.19	64.89	1.90	1.27	44.81 ^b
29.0	10.00	1.274	6.970	43.78	4.64	0.30	CH ₄ R ₁₅ 0.18	CH ₄ R ₁₄ 4.16	26.90	26.58 ^b
150.0	10.00	1.350	3.757	46.94	41.99	5.07	3.17	33.75	3.27	2.95 ^b
120.0	10.00	1.307	3.670	44.41	30.70	4.05	2.21	24.44	8.97	8.65 ^b
91.0	11.40	1.361	3.855	44.14	19.62	2.58	1.20	15.84	18.04	17.77 ^b
57.0	10.20	1.361	6.022	41.88	11.27	0.97	0.56	9.74	24.30	23.99 ^b

Table XXXII (continued)

Temp (°C)	Time (min)	[Azo] x10 ⁶ mole/cc	[(CH ₃) ₃ SiH] mole/cc	Rate x10 ¹² mole/cc s						$\frac{k_{14}}{k_3^{1/2}}$	
				N ₂	Methane (total)	CH ₄ R ₂	CH ₄ R ₁₅	CH ₄ R ₁₄	C ₂ H ₆ (total) R ₃		C ₂ H ₆ R ₃
183.0	10.30	1.427	1.557	48.24	37.90	8.87	2.49	26.54	2.36	2.05	11.91 ^b
213.0	7.00	2.124	1.350	72.63	60.28	20.16	3.66	36.46	2.11	1.66	20.96 ^b

^a Cell volume 218 cc. Illuminated volume 192 cc.

^b Cell volume 186.5 cc. Illuminated volume 158 cc.

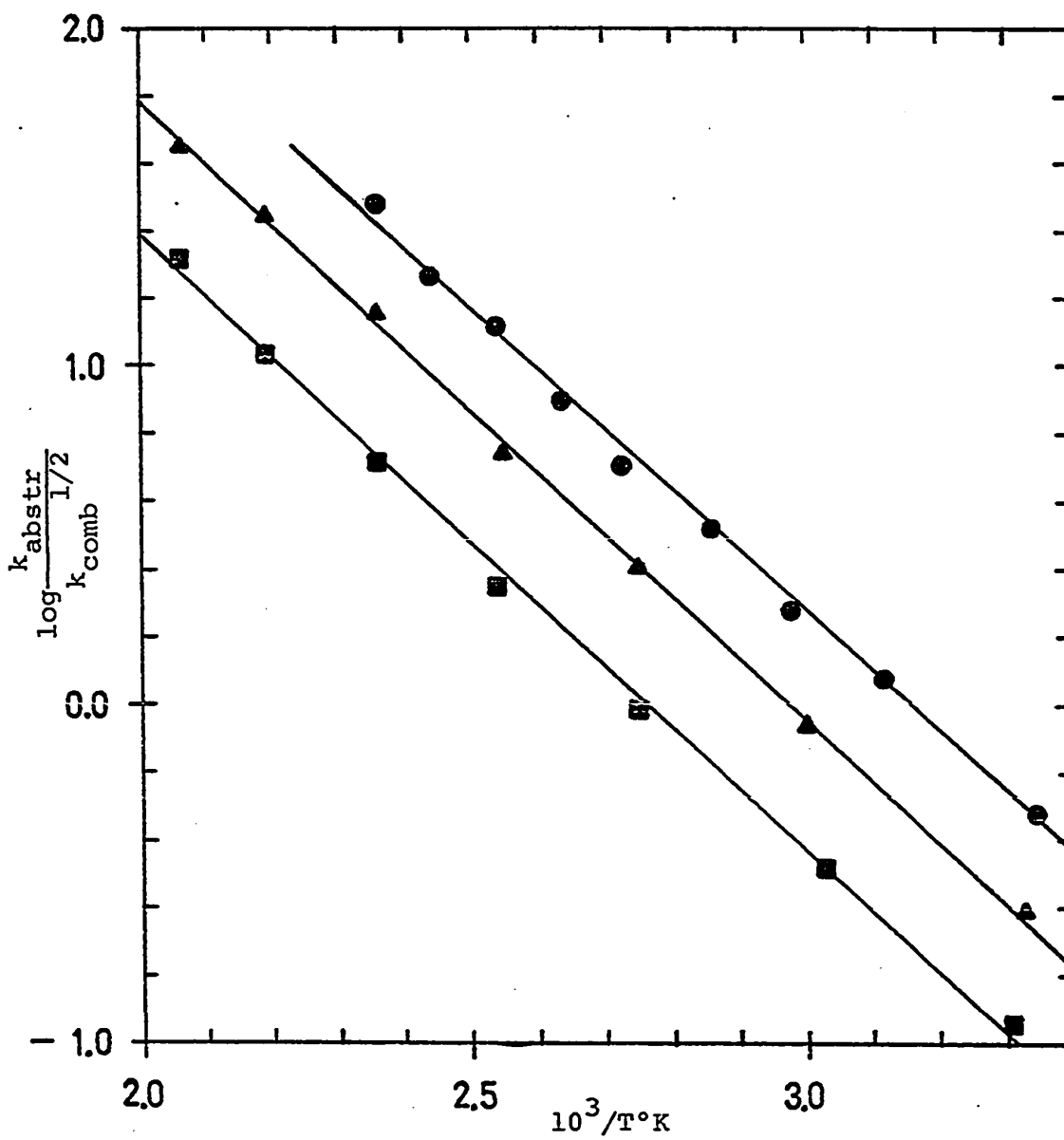


Figure 32. Arrhenius plots for reaction of methyl radicals with methylsilane ●, dimethylsilane ▲, and trimethylsilane ■.

DISCUSSION

1) Comparison of Arrhenius Parameters with Previous Values for Silanes and for Hydrocarbons:

The Arrhenius parameters determined in this study are contrasted in Table XXXIII with those found by previous authors for silane and hydrocarbon compounds. The activation energies obtained for methyl radical abstraction from silane, trimethylsilane, tetramethylsilane, and neopentane are substantially in agreement with the results of Kerr (73,116) and Thynne (118), while the value for tetramethylsilane is lower than that reported by Gowenlock (122). However, Gowenlock's value for the A factor was also quite high, and it seems possible that his results may be slightly in error. The higher activation energy for neopentane than for tetramethylsilane reported here and by Kerr is in keeping with the trend in activation energies for the Group IV tetramethyls established by Gowenlock, however.

The A factors for methyl radicals abstracting hydrogen from the methyl substituted silanes are all about the same and are similar to the values found for hydrocarbons and unsubstituted silanes. The activation energies for abstraction of the hydrogen bound to silicon are usually lower than for hydrocarbons. There is an increase in activation energy with substitution of silane by one methyl

Table XXXIII
Arrhenius Parameters for Hydrogen Atom Abstraction
by Methyl Radicals

Reaction	log A $\frac{\text{cm}^3}{\text{mole sec}}$	E $\frac{\text{kcal}}{\text{mole}}$	Refer- ence
SiH_4	12.26	7.47	a
SiH_4	11.80	6.99	115
SiH_4	11.82	6.89	118
CH_3SiH_3	12.28 ± 0.24	8.13 ± 0.39	a
CH_3SiD_3	12.25 ± 0.09	9.22 ± 0.15	a
$\text{CH}_3\text{SiD}_3^b$	12.49 ± 0.34	9.20 ± 0.55	a
$(\text{CH}_3)_2\text{SiH}_2$	12.07 ± 0.18	8.30 ± 0.31	a
$(\text{CH}_3)_2\text{SiD}_2^b$	11.92 ± 0.24	8.82 ± 0.39	a
$(\text{CH}_3)_3\text{SiH}$	11.69 ± 0.27	8.31 ± 0.47	a
$(\text{CH}_3)_3\text{SiD}^b$	11.78 ± 0.19	9.21 ± 0.33	a
$(\text{CH}_3)_3\text{SiD}^b$	10.98 ± 0.53	9.07 ± 0.92	a
$(\text{CH}_3)_3\text{SiH}$	11.34	7.83	118
$(\text{CH}_3)_3\text{SiH}$	11.1	7.0	113
$(\text{CH}_3)_4\text{Si}$	11.34 ± 0.23	9.66 ± 0.41	a
$(\text{CH}_3)_4\text{Si}$	11.53	10.30	118
$(\text{CH}_3)_4\text{Si}$	12.6	11.0	122
CH_4	11.83	14.65	141
C_2H_6^b	12.21	11.8	143
C_3H_8^b	11.87	10.2	76

Table XXXIII (continued)

Reaction	$\log A$ $\frac{\text{cm}^3}{\text{mole sec}}$	E $\frac{\text{kcal}}{\text{mole}}$	Refer- ence
$(\text{CH}_3)_3\text{CH}^b$	11.43	8.1	76
$(\text{CH}_3)_4\text{C}$	11.92 ± 0.48	11.72 ± 0.92	a
$(\text{CH}_3)_4\text{C}$	12.33	12.01	73
$(\text{CH}_3)_4\text{C}$	11.17	10.0	75

^a This work

^b CD_3 radicals

group, but additional methyl substitution does not result in further significant increase.

Abstraction from the methyl groups is insignificant compared with abstraction from the silyl group for methylsilane and dimethylsilane, but measurable abstraction of methyl group protons occurs in the case of trimethylsilane.

2) Kinetic Isotope Effect:

Kinetic isotope effects as a function of temperature have been calculated from the Arrhenius parameters and are plotted in Figures 33 and 34. The isotope effects at 300°K are also listed in Table XXXIV. In general, they tend to be smaller for the heavier molecules. This is to be expected, since the difference in zero point energies should decrease with increasing size of the molecule. The isotope effect for dimethylsilane does not fit the trend established by the results for methylsilane and trimethylsilane, and this appears to be due to a small error in the activation energy found for dimethylsilane-d₂. For monosilane the isotope effect is smaller than for methylsilane, and this is in keeping with its lower activation energy for reaction with methyl radicals. The isotope effects obtained in this work are reasonably consistent with those obtained by Jakubowski (115), and they appear to be consistent with the assumed mechanism and with the exothermicities of the reactions.

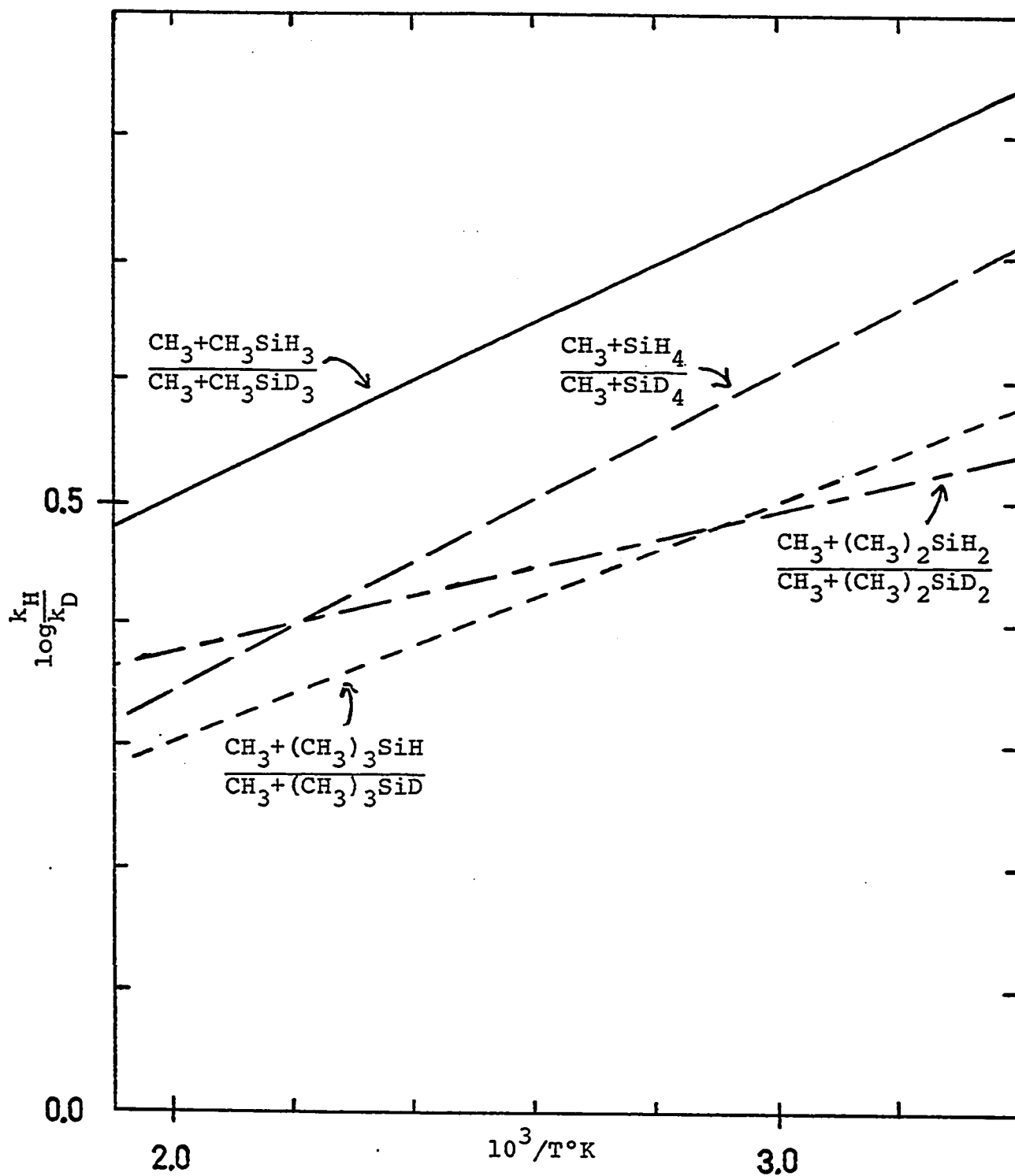


Figure 33. Kinetic isotope effect calculated from experimental data for methyl radicals reacting with
 silane — — — (115) dimethylsilane — — — —
 methylsilane — — — — trimethylsilane — — — —

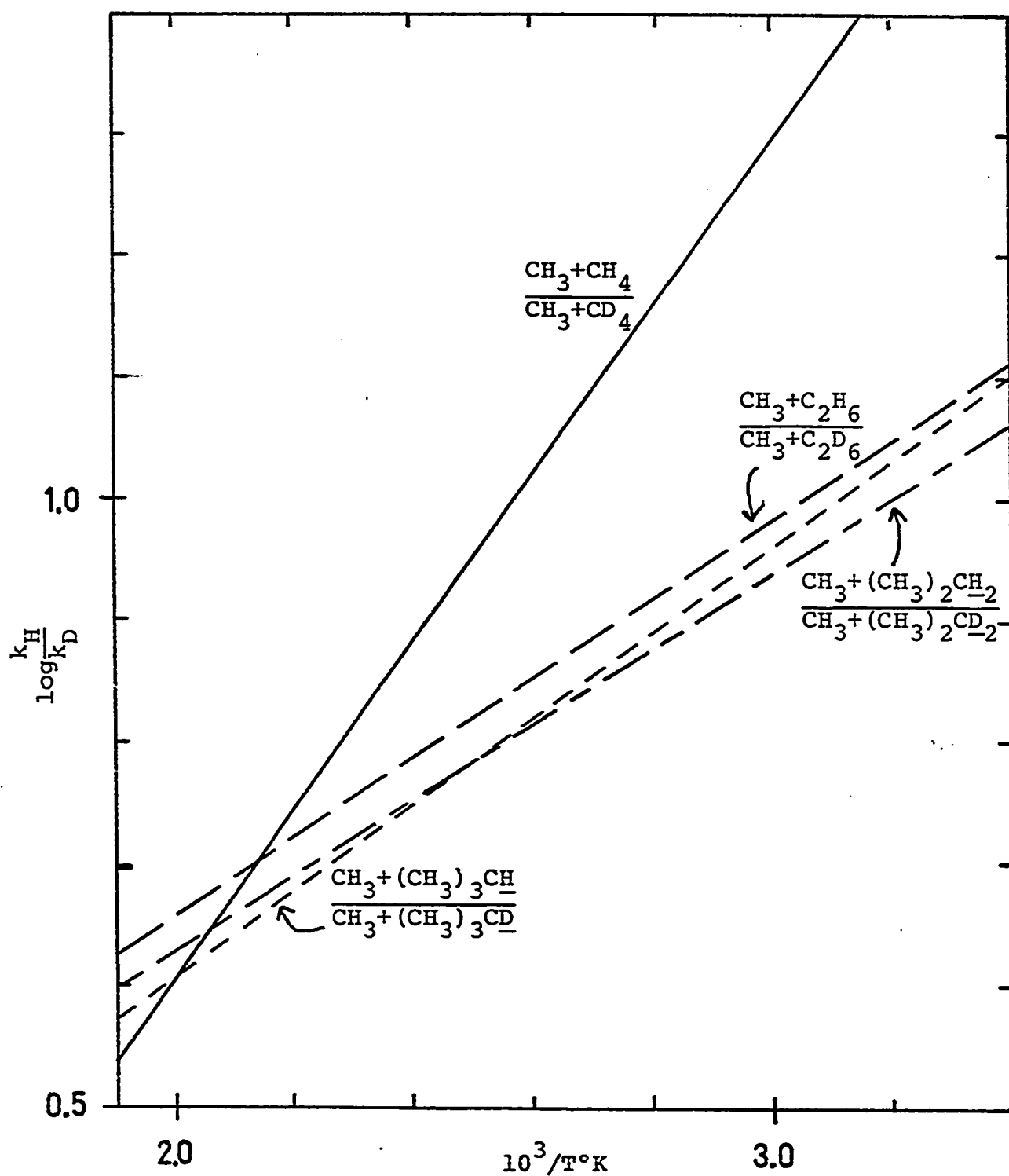


Figure 34. Kinetic isotope effect calculated from experimental data for methyl radicals reacting with methane——(141,142) propane — — — (76) ethane — — — (143) iso-butane - - - (76)

Table XXXIV

Experimental Kinetic Isotope Effects for Methyl Radicals

Reactions	$\frac{k_H}{k_D}$ 300°K	References
Monosilane	4.9	115
Methylsilane	6.7	a
Dimethylsilane	3.4	a
Trimethylsilane	3.7	a
Methane	33.5	141, 142
Ethane	12.4	143
Propane (secondary H)	11.0	76
iso-Butane (tertiary H)	11.9	76

^a This work

3) Correlation of Kinetic Data and Magnetic Shielding:

Szwarc (124), Gowenlock (122), and Bell (120) have demonstrated the existence of correlations between electronic shielding of the protons in the Group IV methyl compounds and the activation energy for their abstraction by methyl and trifluoromethyl radicals. Szwarc and Bell have both suggested that the results obtained with trifluoromethyl radicals were due to polar effects and that similar effects do not occur with methyl radicals. Gowenlock has observed an inverse relationship between activation energy for methyl radical abstraction from Group IV tetramethyls and the $^{13}\text{C-H}$ coupling constants, which he suggests may be related to the fraction of s character in C-H bonds.

Activation energies for methyl radical abstraction are contrasted with NMR chemical shifts and Hg $6(^3\text{P}_1)$ quenching cross sections in Table XXXV. The activation energies for methyl radical abstraction of hydrogen from silicon are seen to increase upon methyl substitution, while the opposite trend is observed for methyl substitution of carbon. The tau values of the methyl group protons change very little with increasing methyl substitution of silane, but there is a substantial decrease in tau value for the silyl group protons with addition of the first methyl group, and relatively smaller decreases with each succeeding methyl group. A parallel trend in tau values is seen for the corresponding hydrocarbon compounds. It is clear from

Table XXXV

Comparison of Activation Energies for Methyl Radical
Abstraction Reactions with NMR Chemical Shifts and with
Quenching Cross-Sections for $\text{Hg6}(^3\text{P}_1)$ Atoms

Compound	τ SiH	τ CH	$J(^{29}\text{Si-H})$	σ_Q^2/A^2	E
SiH_4	6.80 ^a	-	202.5 ^b	26 ⁱ	7.4 ^e
CH_3SiH_3	6.42 ^c	9.81 ^c	194.4 ^c	32 ⁱ	8.1 ^e
$(\text{CH}_3)_2\text{SiH}_2$	6.18 ^c	9.86 ^c	190.0 ^c	33 ⁱ	8.3 ^e
$(\text{CH}_3)_3\text{SiH}$	6.00 ^c	9.93 ^c	190.0 ^c	30 ⁱ	8.3 ^e
$(\text{CH}_3)_4\text{Si}$		10.00		5.0 ⁱ	9.7 ^e
CH_4		9.6 ^d		0.06 ⁱ	14.7 ^f
C_2H_6		8.9 ^d		0.10 ⁱ	11.8 ^g
$(\text{CH}_3)_2\text{CH}_2$		8.5 ^d		1.5 ⁱ	10.2 ^h
$(\text{CH}_3)_3\text{CH}$		8.3 ^d		6.8 ⁱ	8.1 ^h
$(\text{CH}_3)_4\text{C}$		9.06 ^j		1.4 ⁱ	11.7 ^e

^a Ref. 146

^b Ref. 147

^c Ref. 148

^d Ref. 149

^e This work

^f Ref. 141

^g Ref. 143

^h Ref. 76

ⁱ Ref. 92

^j Ref. 150

examination of the data that the Hg $6(3P_1)$ quenching cross sections for silane compounds are due mostly to interaction of the excited mercury atoms with the protons attached to the silicon atom. Similarly, the cross sections found with increasing methyl substitution of methane are mostly attributable to interaction with protons bound to the central carbon atom. It is seen that there is a pronounced increase in the quenching cross section per hydrogen atom both for increasing methyl substitution of silane and for increasing methyl substitution of methane. This trend is probably due to progressive weakening of bonds between hydrogen and the central atom. The pattern of the tau values suggests that the trend is probably not based on the electrophilicity of triplet mercury atoms.

The available information on bond dissociation energies for silane, trimethylsilane, methane, and isobutane are contrasted in Table XXXVI. The bond dissociation energy for the Si-H bond in trimethylsilane is undoubtedly lower than that for the Si-H bond in silane, and the trend in activation energies found by Thynne (118) and substantiated in this work is rather puzzling. It is true that the difference in bond dissociation energy between silane and trimethylsilane might be less than the corresponding difference for methane and iso-butane, and it is also true that silane bond dissociation energies are not established with great certainty, but it is hardly likely that they

Table XXXVI
 Comparison of Activation Energies
 for Hydrogen Atom Abstraction by Methyl Radicals
 with Bond Dissociation Energies

Substrate	Activation Energy kcal/mole	Bond Dissociation Energy
CH ₄	14.7 ^a	104 ^g
SiH ₄	7.5 ^b , 7.0 ^c , 6.9 ^d	94 ^h , 95 ⁱ
(CH ₃) ₃ CH	8.1 ^e	91 ^g
(CH ₃) ₃ SiH	8.3 ^b , 7.8 ^d , 7.0 ^f	74 ^j , 79 ^k , 81 ^f , 88 ^l

^a Ref. 141

^g Ref. 2

^b This work

^h Ref. 95

^c Ref. 115

ⁱ Ref. 100

^d Ref. 118

^j Ref. 99

^e Ref. 76

^k Ref. 102

^f Ref. 113

^l Ref. 98

could be sufficiently in error to explain the trend in activation energies.

The trend of decreasing bond dissociation energy with increasing methyl substitution of both methane and silane can be rationalized in terms of an increase in capacity for hyperconjugation of the resulting radical. One consequence of this hyperconjugation must be delocalization of the electron left behind in homolysis of the bond to the central atom. Perhaps this increase in delocalization with methyl substitution results in an increase in the distance at which triplet interaction with another radical would become important. If so, the lesser electronegativity of silicon, the availability of its empty d orbitals, and its greater covalent radius make it likely that such an increase in triplet repulsion would be much greater for the methyl substituted silanes than for the corresponding methyl substituted methanes. Thus the effect of the bond dissociation energy difference between trimethylsilane and monosilane might be obscured by a difference in triplet repulsion energy. In any case, it is clear that the reactivities of the methyl substituted silanes with methyl radicals cannot be explained on the basis of the measured bond dissociation energies.

BIBLIOGRAPHY

- 1) S. W. Benson. Thermochemical Kinetics. John Wiley & Sons, Inc., New York (1968).
- 2) J. A. Kerr. Chem. Rev. 66, 465 (1966).
- 3) S. W. Benson. J. Chem. Educ. 42, 502 (1965).
- 4) L. Pauling. The Nature of the Chemical Bond. 3rd Ed. Cornell U. Press, Ithica, N.Y. (1960).
- 5) G. Herzberg. Molecular Spectra and Molecular Structure. III. Electronic Spectra and Electronic Structure of Polyatomic Molecules. D. Van Nostrand Co., Inc., Princeton, N.J. (1966).
- 6) M. Karplus. J. Chem. Phys. 30, 15 (1959). K. Morokuma, L. Pedersen, M. Karplus. J. Chem. Phys. 48, 4801 (1968).
- 7) M. Karplus, G. K. Fraenkel. J. Chem. Phys. 35, 1312 (1961).
- 8) R. W. Fessenden, R. H. Schuler. J. Chem. Phys. 39, 2147 (1963).
- 9) M. C. R. Symons. Nature 222, 1123 (1969).
- 10) M. S. Kharasch, F. Engelmann, and W. H. Urry. J. Am. Chem. Soc. 65, 2428 (1943).
- 11) A. Shepp. J. Chem. Phys. 24, 939 (1956).
- 12) R. Gomer. J. Chem. Phys. 18, 998 (1950).
- 13) R. Gomer and G. B. Kistiakowsky. J. Chem. Phys. 19, 85 (1951).
- 14) E. I. Metcalfe, A. F. Trotman-Dickenson. J. Chem. Soc. 1962, 4620.
- 15) E. I. Metcalfe. J. Chem. Soc. B, 1963, 3560.
- 16) A. Shepp and K. O. Kutschke. J. Chem. Phys. 26, 1020 (1957).
- 17) R. K. Brinton and E. W. R. Steacie. Can. J. Chem. 33, 1840 (1955).

- 18) S. Toby and B. H. Weiss. J. Phys. Chem. 68, 2492 (1964).
- 19) J. Grotewold, E. A. Lissi, and M. G. Neumann. Chem. Commun. 1966, 1.
- 20) J. Grotewold, E. A. Lissi, and M. G. Neumann. J. Chem. Soc. A, 1968, 375.
- 21) F. Casas, C. Previtali, J. Grotewold, and E. A. Lissi. J. Chem. Soc. A, 1970, 1001.
- 22) M. Matsuoka, P. S. Dixon, A. P. Stefani, and M. Szwarc. Proc. Chem. Soc. 1962, 304.
- 23) J. A. Kerr, A. F. Trotman-Dickenson. Progr. in React. Kinetics 1, 105 (1961).
- 24) A. D. Stepukhovich, V. A. Ulitskii, and A. P. Sharaevskii. Zh. Fiz. Khim. 42, 1276 (1968). A. D. Stepukhovich and V. A. Ulitskii. Usp. Khim. 35, 487 (1966) and references therein.
- 25) S. W. Benson. Advan. Photochem 2, 1 (1964).
- 26) R. L. Thommarson. J. Phys. Chem. 74, 938 (1970).
- 27) J. A. Kerr and A. C. Lloyd. Quart. Rev. (London) 22, 549 (1968).
- 28) F. Paneth and W. Hofeditz. Chem. Ber. 62B, 1335 (1929).
- 29) F. Paneth and W. Lautsch. Chem. Ber. 64B, 2702 (1931).
- 30) W. A. Pryor. Free Radicals. McGraw-Hill Book Co., New York (1966).
- 31) J. G. Calvert and J. N. Pitts, Jr. Photochemistry. John Wiley & Sons, Inc., New York (1966).
- 32) S. S. Collier, D. H. Slater, J. G. Calvert. Photochem. Photobiol. 7, 737 (1968) and references therein.
- 33) V. Meyer and E. J. Constan. Ann. 214, 328 (1882).
- 34) J. Thiele. Chem. Ber. 42, 2575 (1909).
- 35) J. A. Leermakers. J. Am. Chem. Soc. 55, 3499 (1933).

- 36) F. O. Rice and B. L. Evering. J. Am. Chem. Soc. 55, 3898 (1933).
- 37) M. Burton, T. W. Davis, and H. A. Taylor. J. Am. Chem. Soc. 59, 1038 (1937).
- 38) H. L. Lochte, W. A. Noyes, and J. R. Bailey. J. Am. Chem. Soc. 44, 2556 (1922).
- 39) F. P. Jahn. J. Am. Chem. Soc. 59, 1761 (1937).
- 40) R. Renand and L. C. Leitch. Can. J. Chem. 32, 545 (1954).
- 41) R. Ohme and E. Schmitz. Angew. Chem. 77, 429 (1965).
- 42) L. Spialter, D. H. O'Brien, G. L. Untereiner, and W. A. Rush. J. Org. Chem. 30, 3278 (1965).
- 43) M. B. Robin, R. R. Hart, and N. A. Kuebler. J. Am. Chem. Soc. 89, 1564 (1967).
- 44) W. C. Sleppy and J. G. Calvert. J. Am. Chem. Soc. 81, 769 (1959).
- 45) H. Cerfontain, K. O. Kutschke. Can. J. Chem. 36, 344 (1958).
- 46) R. H. Riem and K. O. Kutschke. Can. J. Chem. 38, 2332 (1960).
- 47) R. F. Hutton and C. Steel. J. Amer. Chem. Soc. 86, 745 (1964).
- 48) C. Steel and T. F. Thomas. Chem. Commun. 1966, 900.
- 49) R. E. Rebbert and P. Ausloos. J. Am. Chem. Soc. 87, 1847 (1965).
- 50) W. E. Morganroth and J. G. Calvert. J. Am. Chem. Soc. 88, 5387 (1966).
- 51) D. H. Slater, S. S. Collier, and J. G. Calvert. J. Amer. Chem. Soc. 90, 268 (1968).
- 52) J. L. Weininger and O. K. Rice. J. Am. Chem. Soc. 74, 6216 (1952).
- 53) W. C. Worsham and O. K. Rice. J. Chem. Phys. 46, 2021 (1967).
- 54) S. Toby and J. Nimoy. J. Phys. Chem. 70, 867 (1966).

- 55) S. Toby and B. H. Weiss. J. Phys. Chem. 66, 2681 (1962).
- 56) R. E. Rebbert and P. J. Ausloos. J. Phys. Chem. 67, 1925 (1963).
- 57) S-L. Cheng, J. Nimoy, and S. Toby. J. Phys. Chem. 71, 3075 (1967).
- 58) I. I. Abram, G. S. Milne, B. S. Solomon, C. Steel. J. Amer. Chem. Soc. 91, 1220 (1969).
- 59) T. Mill, R. S. Stringham. Tetrahedron Lett. 1969, 1853.
- 60) J. A. Kerr, D. H. Slater, and J. C. Young. J. Chem. Soc. A, 1966, 104.
- 61) P. Gray and J. C. J. Thynne. Trans. Faraday Soc. 59, 2275 (1963).
- 62) P. Gray, A. Jones, J. C. J. Thynne. Trans. Faraday Soc. 61, 474 (1965).
- 63) J. C. J. Thynne. Trans. Faraday Soc. 60, 2207 (1964).
- 64) P. Ausloos and E. W. R. Steacie. Bull. Soc. Chim. Belges 63, 87 (1954).
- 65) R. W. Durham and E. W. R. Steacie. Can. J. Chem. 31, 377 (1953).
- 66) J. A. Kerr and J. G. Calvert. J. Am. Chem. Soc. 83, 3391 (1961).
- 67) M. H. Jones and E. W. R. Steacie. J. Chem. Phys. 21, 1018 (1953).
- 68) M. E. Wacks. J. Phys. Chem. 68, 2725 (1964).
- 69) S. G. Cohen and R. Zand. J. Amer. Chem. Soc. 84, 586 (1962).
- 70) H. S. Sandhu. J. Phys. Chem. 72, 1857 (1968).
- 71) A. F. Trotman-Dickenson. Advances in Free-Radical Chemistry 1, 1 (1965).
- 72) A. F. Trotman-Dickenson. Chem. & Ind. 1965, 379.
- 73) J. A. Kerr and D. Timlin. J. Chem. Soc. A 1969, 1241.

- 74) P. J. Boddy and E. W. R. Steacie. *Can. J. Chem.* 38, 1576 (1960).
- 75) A. F. Trotman-Dickenson, J. R. Birchard, and E. W. R. Steacie. *J. Chem. Phys.* 19, 163 (1951).
- 76) W. M. Jackson, J. R. McNesby, and B. de B. Darwent. *J. Chem. Phys.* 37, 1610 (1962).
- 77) J. R. McNesby and A. S. Gordon. *J. Am. Chem. Soc.* 78, 3570 (1956).
- 78) A. S. Gordon and S. R. Smith. *J. Phys. Chem.* 66, 521 (1962).
- 79) P. J. Boddy and E. W. R. Steacie. *Can. J. Chem.* 39, 13 (1961).
- 80) R. N. Birrell, A. F. Trotman-Dickenson. *J. Chem. Soc.* 1960, 2059.
- 81) J. T. Gruver and J. G. Calvert. *J. Am. Chem. Soc.* 78, 5208 (1956).
- 82) E. L. Metcalfe and A. F. Trotman-Dickenson. *J. Chem. Soc.* 1960, 5072.
- 83) J. A. Kerr and A. F. Trotman-Dickenson. *J. Chem. Soc.* 1960, 1602.
- 84) L. Pauling. *J. Chem. Phys.* 51, 2767 (1969).
- 85) R. L. Morehouse, J. J. Christiansen, and W. Gordy. *J. Chem. Phys.* 45, 1751 (1966).
- 86) G. S. Jackel and W. Gordy. *Phys. Rev.* 176, 443 (1968).
- 87) S. W. Bennett, C. Eaborn, A. Hudson, R. A. Jackson, and K. D. J. Root. *J. Chem. Soc. A* 1970, 348.
- 88) N J. Friswell and B. G. Gowenlock. *Advances in Free-Radical Chemistry* 1, 39 (1965).
- 89) D. E. Milligan and M. E. Jacox. *J. Chem. Phys.* 52, 2594 (1970).
- 90) E. Jakubowski, H. S. Sandhu, H. E. Gunning, and O. P. Strausz. *J. Chem. Phys.* 52, 4242 (1970).
- 91) J. H. Purnell and R. Walsh. *Proc. Roy. Soc. A* 293, 543 (1966).

- 92) H. E. Gunning, O. P. Strausz, M. A. Nay, and G. N. C. Woodall. *J. Amer. Chem. Soc.* 87, 179 (1965).
- 93) H. Niki and G. J. Mains. *J. Phys. Chem.* 68, 304 (1964).
- 94) W. C. Steele and F. G. A. Stone. *J. Amer. Chem. Soc.* 84, 3599 (1962).
- 95) W. C. Steele, L. D. Nichols, and F. G. A. Stone. *J. Amer. Chem. Soc.* 84, 4441 (1962).
- 96) G. G. Hess, F. W. Lampe, and L. H. Sommer. *J. Amer. Chem. Soc.* 86, 3174 (1964).
- 97) G. P. van der Kelen, O. Volders, H. van Onckelen, and Z. Eeckhaut. *Z. Anorg. Allgem. Chem.* 338, 106 (1965).
- 98) G. G. Hess, F. W. Lampe, and L. H. Sommer. *J. Amer. Chem. Soc.* 87, 5327 (1965).
- 99) J. A. Connor, G. Finney, G. J. Leigh, R. N. Haszeldine, P. J. Robinson, R. D. Sedgwick, and R. F. Simmons. *Chem. Commun.* 1966, 178.
- 100) F. E. Saalfeld and H. J. Svec. *J. Phys. Chem.* 70, 1753 (1966).
- 101) B. G. Gowenlock and J. Stevenson. *J. Organometal. Chem.* 15, 503 (1968).
- 102) P. Potzinger and F. W. Lampe. *J. Phys. Chem.* 74, 719 (1970).
- 103) B. J. Aylett. *Advan. Inorg. Chem. Radiochem.* 11, 249 (1968).
- 104) C. Eaborn. *Organosilicon Compounds*. Butterworths, London (1960).
- 105) F. G. A. Stone. *Hydrogen Compounds of the Group IV Elements*. Prentice-Hall, Inc., Englewood Cliffs, N.J. (1962).
- 106) E. A. V. Ebsworth. *Volatile Silicon Compounds*. Pergamon Press, New York (1963).
- 107) C. H. Van Dyke. *Silanes*. Kirk-Othmer *Encycl. Chem. Technol.* 2nd Ed. 18, 172 (1969).
- 108) J. J. Kohanek, P. Estacio, M. A. Ring. *Inorg. Chem.* 8, 2516 (1969).

- 109) I. M. Davidson, C. A. Lambert. J. Chem. Soc. D 1969, 1276.
- 110) O. P. Strausz, K. Obi, and W. K. Duholke. J. Amer. Chem. Soc. 90, 1359 (1968).
- 111) K. Obi, A. Clement, H. E. Gunning, and O. P. Strausz. J. Amer. Chem. Soc. 91, 1622 (1969).
- 112) M. A. Ring, G. D. Beverly, F. H. Koester, and R. P. Hollandsworth. Inorg. Chem. 8, 2033 (1969).
- 113) J. A. Kerr, D. H. Slater, and J. C. Young. J. Chem. Soc. A 1967, 134.
- 114) T. N. Bell and B. B. Johnson. Aust. J. Chem. 20, 1545 (1967).
- 115) O. P. Strausz, E. Jakubowski, H. S. Sandhu, and H. E. Gunning. J. Chem. Phys. 51, 552 (1969).
- 116) J. A. Kerr, A. Stephens, and J. C. Young. Int. J. Chem. Kinet. 1, 339 (1969).
- 117) J. A. Kerr, A. Stephens, and J. C. Young. Int. J. Chem. Kinet. 1, 371 (1969).
- 118) E. R. Morris and J. C. J. Thynne. J. Phys. Chem. 73, 3294 (1969).
- 119) E. R. Morris and J. C. J. Thynne. Trans. Faraday Soc. 66, 183 (1970).
- 120) T. N. Bell and U. F. Zucker. J. Phys. Chem. 74, 979 (1970).
- 121) H. S. Johnston. Gas Phase Reaction Rate Theory. Ronald Press, New York (1966).
- 122) A. U. Chaudhry and B. G. Gowenlock. J. Organometal. Chem. 16, 221 (1969).
- 123) E. R. Morris and J. C. J. Thynne. J. Organometal. Chem. 17, P3 (1969).
- 124) W. J. Cheng and M. Szwarc. J. Phys. Chem. 72, 494 (1968).
- 125) O. P. Strausz, R. E. Berkley, and H. E. Gunning. Can. J. Chem. 47, 3470 (1969).
- 126) E. Bamberger and W. Pemsel. Chem. Ber. 36, 56 (1903).

- 127) E. Müller and W. Rundel. Chem. Ber. 90, 1307 (1957).
- 128) V. S. Stopskii, V. B. Lebedev, B. V. Ioffe, and A. A. Petrov. Dokl. Akad. Nauk SSSR 166, 399 (1966).
- 129) B. V. Ioffe, Z. I. Sergeeva, and V. S. Stopskii. Dokl. Akad. Nauk SSSR 167, 831 (1966).
- 130) L. Spialter and G. L. Untereiner. U. S. 3, 350, 385 (1967).
- 131) B. V. Ioffe and V. S. Stopskii. Tetrahedron Lett. 1968, 1333.
- 132) B. V. Ioffe, V. S. Stopskii, and Z. I. Sergeeva. Zh. Org. Khim. 4, 986 (1968).
- 133) B. V. Ioffe and V. S. Stopskii. Zh. Org. Khim. 4, 1504 (1968).
- 134) D. M. Lemal, F. Menger, and E. Coats. J. Am. Chem. Soc. 86, 2395 (1964).
- 135) R. E. Berkley, G. N. C. Woodall, O. P. Strausz, and H. E. Gunning. Can. J. Chem. 47, 3305 (1969).
- 136) J. O. Terry and J. H. Futrell. Can. J. Chem. 45, 2327 (1967).
- 137) J. O. Terry and J. H. Futrell. Can. J. Chem. 46, 664 (1968).
- 138) S. G. Whiteway and C. R. Masson. J. Chem. Phys. 25, 233 (1956).
- 139) G. Geiseler and J. Hoffmann. Z. Phys. Chem. (Frankfurt am Main) 57, 318 (1968).
- 140) J. M. Campbell, H. E. Gunning, and O. P. Strausz. Can. J. Chem. 47, 3763 (1969).
- 141) F. S. Dainton, K. J. Ivin, and F. Wilkinson. Trans. Faraday Soc. 55, 929 (1959).
- 142) G. A. Creak, F. S. Dainton, and K. J. Ivin. Trans. Faraday Soc. 58, 326 (1962).
- 143) J. R. McNesby. J. Phys. Chem. 64, 1671 (1960).
- 144) R. E. Wilde. J. Mol. Spectry. 8, 427 (1962).
- 145) D. G. L. James and R. D. Suart. Trans. Faraday Soc. 64, 2735 (1968).

- 146) E. A. V. Ebsworth and J. J. Turner. J. Phys. Chem. 67, 805 (1963).
- 147) E. A. V. Ebsworth and J. J. Turner. J. Chem. Phys. 36, 2628 (1962).
- 148) H. Schmidbaur. Chem. Ber. 97, 1639 (1964).
- 149) J. A. Pople, W. G. Schneider, and H. J. Bernstein. High Resolution Nuclear Magnetic Resonance. McGraw-Hill Book Co., New York (1959).
- 150) G. V. Tiers. Characteristic Nuclear Magnetic Resonance (NMR) "Shielding Values" (Spectral Positions) for Hydrogen in Organic Structures. Part I. Tables of τ -Values for a Variety of Organic Compounds. Central Research Department, Minnesota Mining and Manufacturing Co., St. Paul (1958).
- 151) G. M. Barrow. Introduction to Molecular Spectroscopy. McGraw-Hill Book Co., Inc., New York (1962).

APPENDIX A

Derivation of the Expression for $k_1/k_{3a}^{1/2}$

(Reaction of n-Propyl Radicals with Propane, Chapter IV).

Combining the rate expression for Reaction 1 with the steady state assumption for iso-propyl radicals

$$R_1 = k_1 [n\text{-Pr}] [C_3H_8] = R_{1a} + R_{2a} + R_{2b} + 2R_{4a} + 2R_{4b} + R_6$$

$$R_{2a} + R_{2b} = 1.35 R_{2a}$$

$$2(R_{4a} + R_{4b}) = 3.10 R_{4a}$$

The relationship between k_1 and k_{1a} is

$$k_{1a} = k_1 \exp(0.91 - 3500/RT)$$

Therefore

$$k_1 [n\text{-Pr}] [C_3H_8] = k_1 \exp(0.91 - 3500/RT) [i\text{-Pr}] [C_3H_8] + 1.35 R_{2a} + 3.10 R_{4a} + R_6$$

Since

$$r = \frac{[i\text{-Pr}]}{[n\text{-Pr}]}$$

$$k_1 = \frac{1.35 R_{2a} + 3.10 R_{4a} + R_6}{[C_3H_8] \{1 - r \exp(0.91 - 3500/RT)\} [n\text{-Pr}]}$$

R_6 can be expressed in terms of r , R_0 , and q . Since

$$R_5 + R_6 = 2R_0$$

and

$$R_5 = \frac{q}{r} R_6$$

then

$$R_6 = \frac{2rR_0}{r + q}$$

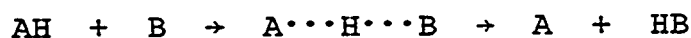
Expressing the value of $k_{3a}^{1/2}$ as $R_{3a}^{1/2}/[n-Pr]$, we obtain

$$\frac{k_1}{k_{3a}^{1/2}} = \frac{1.35 R_{2a} + 3.10 R_{4a} + \frac{2rR_0}{r + q}}{R_{3a}^{1/2} [C_3H_8] \{1 - r \exp(0.91 - 3500/RT)\}}$$

APPENDIX B

The Bond Energy Bond Order BEBO Method of Calculating
Potential Energy of Activation
for a Three-Atom Model of Reaction (121).

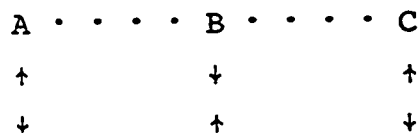
For the reaction



the following model and notation are used:

	A H B		
Bond length in stable molecule	R_1	R_2	$R_3 = R_1 + R_2$
Bond order	n	m	
Bond energy index	p	q	
Single bond length in stable molecule	R_{1s}	R_{2s}	
Single bond energy	E_{1s}	E_{2s}	E_{3s}
$R - R_s$	r_{1s}	r_{2s}	r_{3s}

The electron spins on adjacent atoms in the transition state must be antiparallel,



which requires that the electron spin functions of the two radicals must be parallel, so there will be a triplet repulsion between them.

When a homolytic hydrogen transfer reaction takes place, the energy released by the bond being formed supplies part of the energy required to break the other bond. It is assumed that the path of lowest energy is that along which the sum of the bond orders is unity.

$$n + m = 1$$

The energy of the linear complex along the locus of unit total bond order is given by

$$V = E_{1s} - E_1 - E_2 + V_{tr}$$

where V_{tr} is the triplet repulsion energy. The relationship between bond length and bond order is taken to be

$$R = R_s - 0.26 \ln(n)$$

and the relationship between bond energy and bond order is taken to be

$$E = E_s n^p$$

where p is the bond energy index.

The bond energy indexes are given by

$$p = \frac{0.26 \ln(E_s/e_x)}{R_x - R_s}$$

where R_x is the equilibrium internuclear distance (A) in the corresponding noble gas diatomic cluster or "molecule" and

e_x is the depth of its Lennard-Jones potential (cal/mole).

(See Ref. 121, page 81).

Thus the potential energy along the reaction path is given by the equation

$$V = E_{1s} - E_{1s}n^p - E_{2s}(1-n)^q + V_{tr}$$

The triplet repulsion energy is obtained from the function

$$V_{tr} = E_{3s}^{1/2} \exp(-\beta_3 r_3) \left[1 + \frac{1}{2} \exp(-\beta_3 r_3) \right]$$

where β_3 is the Morse parameter, which is calculated from the relation (151):

$$\beta_3 = 0.12177 \omega_3 \sqrt{\frac{\mu}{0.3499 E_3}}$$

ω_3 is the stretching frequency of A-B in cm^{-1} , and μ is the reduced mass of A-B in atomic mass units.

The potential energy of the system along the locus of constant bond order is then given by the equation

$$V = E_{1s}(1-n^p) - E_{2s}(1-n)^q + E_{3s} B(n-n^2)^\gamma [1 + B(n-n^2)^\gamma]$$

where

$$\gamma = 0.26_3$$

$$B = \frac{1}{2} \exp(-\beta_3 \Delta R_s)$$

$$\Delta R_s = R_{1s} + R_{2s} - R_{3s}$$

are defined for convenience.